รายงานวิจัยฉบับสมบูรณ์

โครงการ

การศึกษาบทบาทของโปรตีนที่มีผลต่อการเคลื่อนย้าย โปรตีนแอนไอออน เอ็กเชนเจอร์-วันในเซลล์ไตของมนุษย์

โดย

ดร. มุทิตา จุลกิ่ง

พฤษภาคม 2555

สัญญาเลขที่ TRG5380010

รายงานวิจัยฉบับสมบูรณ์

โครงการ

การศึกษาบทบาทของโปรตีนที่มีผลต่อการเคลื่อนย้าย โปรตีนแอนไอออน เอ็กเชนเจอร์-วันในเซลล์ไตของมนุษย์

ดร. มุทิตา จุลกิ่ง มหาวิทยาลัยมหิดล

สนับสนุนโดยสำนักงานกองทุนสนับสนุนการวิจัย
และมหาวิทยาลัยมหิดล

กิตติกรรมประกาศ

โครงการวิจัยนี้ได้รับความร่วมมือจากนักวิจัย ผู้ช่วยวิจัย และนักศึกษาหลายท่าน ซึ่งเป็นทั้งผู้ร่วมวิจัยและผู้สนับสนุน ผู้วิจัยขอขอบคุณ ศาสตราจารย์เพทาย เย็นจิตโสมนัส นักวิจัยที่ปรึกษาที่ให้คำแนะนำและสนับสนุนการทำวิจัยในโครงการวิจัยนี้ทุกๆด้าน ขอขอบคุณ รองศาสตราจารย์ นพ. บุณยฤทธิ์ ชื่นสุชน ภาควิชาพยาธิวิทยา คณะแพทยศาสตร์ศิริราชพยาบาล มหาวิทยาลัยมหิดล สำหรับการจัดหาและเตรียมชิ้นเนื้อไตมนุษย์เพื่อใช้ในงานวิจัย ขอขอบคุณ Dr. Masato Enari จาก National Cancer Center Research Institute, Division of Refractory Cancer Research เมืองโตเกียว ประเทศญี่ปุ่น ที่ให้การสนับสนุน pcCHC-FL พลาสมิดที่มีค่ายิ่งสำหรับการทำวิจัยครั้งนี้ ขอขอบคุณ คุณหนึ่งหทัย สวัสดี นักวิทยาศาสตร์ คุณดวงพร อังศุประเวศ ผู้ช่วยวิจัย และคุณณฐพล ดวงธรรม นักศึกษาปริญญาเอก ในความช่วยเหลือตลอดการทำโครงการวิจัยนี้ ขอขอบคุณเจ้าหน้าที่เพื่อนร่วมงานในหน่วยอณูชีววิทยาการแพทย์ สถานส่งเสริมการวิจัย คณะแพทยศาสตร์ศิริราชพยาบาล มหาวิทยาลัยมหิดล ทุกท่านในการสนับสนุนการทำวิจัยทั้งทางตรงและทางอ้อม ขอขอบคุณหน่วยอณูชีววิทยาการแพทย์ สถานส่งเสริมการวิจัย คณะแพทยศาสตร์ศิริราชพยาบาล มหาวิทยาลัยมหิดล ในการสนับสนุนเครื่องมือและสถานที่ทำวิจัย ท้ายสุดนี้ขอขอบคุณทุนส่งเสริมนักวิจัยรุ่นใหม่ จากสำนักงานกองทุนสนับสนุนการวิจัย ที่เอื้อให้การดำเนินการวิจัยสำเร็จลุล่วงตามเป้าหมาย ผู้วิจัยหวังเป็นอย่างยิ่งว่าองค์ความรู้จากงานวิจัยนี้ จะเป็นงานชิ้นหนึ่งในการพัฒนางานวิจัยของประเทศในอนาคต

ดร. มุทิตา จุลกิ่ง

พฤษภาคม 2555

ABSTRACT

Project Code : TRG5380010

Project Title : Roles of proteins involving in anion exchanger 1 trafficking in human kidney cells

Investigator : Dr. Mutita Junking Mahidol University

E-mail Address : mjunking@yahoo.com, mutita.jun@mahidol.ac.th

Project Period : June 2010 – May 2012

Distal renal tubular acidosis (dRTA) is a kidney disease characterized by defect of acid secretion by the α-intercalated cells of the cortical collecting duct of the distal nephron. Development of dRTA is result from impaired trafficking of kidney anion exchanger 1 (kAE1), a Cl^-/HCO_3^- exchanger at the basolateral membrane of α-intercalated cells. The trafficking route of kAE1 from its biosynthesis site to the basolateral membrane has not been well characterized. We have recently reported that AP-1 mu1A, a subunit of AP-1A adaptor complex involving in sorting of the cargo proteins, interacts with the C-terminus of kAE1. In this study, role of basolateral-related sorting proteins including adaptor protein complexes, clathrin, and protein kinase D on kAE1 localization were determined using RNA interference (RNAi) in polarized MDCK cells. Suppression of AP-1A, AP-3, AP-4, and clathrin reduced membranous kAE1. The interaction between kAE1 and sorting proteins was observed by co-immunoprecipitation and yellow fluorescent protein-based protein fragment complementation assay (YFP-PCA) in HEK 293T cells. Moreover, co-localization between kAE1 and sorting proteins was investigated by immunofluorescence staining in human kidney tissues. To gain a better understanding into normal kAE1 trafficking, further studies would be carries out in polarized kidney cell lines to examine next steps of trafficking involving transportation along cytoplasm, tethering, and fusion of kAE1 to membrane. The investigation of normal trafficking of human kAE1 will provide a new perception into a molecular mechanism associated with the pathogenesis of dRTA.

Keywords : kidney anion exchanger 1, distal renal tubular acidosis, protein trafficking, sorting protein

บทคัดย่อ

รหัสโครงการ : TRG5380010

ชื่อโครงการ : การศึกษาบทบาทของโปรตีนที่มีผลต่อการเคลื่อนย้ายโปรตีนแอนไอออนเอ็กเชนเจอร์-วัน ในเซลล์ไตของมนุษย์

ชื่อนักวิจัย : ดร. มุทิตา จุลกิ่ง มหาวิทยาลัยมหิดล

E-mail Address : mjunking@yahoo.com, mutita.jun@mahidol.ac.th

ระยะเวลาโครงการ : มิถุนายน 2553 - พฤษภาคม 2555

โรคไตผิดปกติในการขับกรด (distal renal tubular acidosis) ที่ทำให้ผู้ป่วยโรคนี้มีสภาวะเป็นกรดในร่างกาย เนื่องจากไตไม่สามารถขับกรดออกทางปัสสาวะได้ เกิดจากการขนส่งหรือการเคลื่อนย้ายโปรตีนแอนไอออนเอ็กเชนเจอร์-วันชนิดที่พบในไต (kidney anion exchanger 1; kAE1) ที่ปกติจะเคลื่อนย้ายไปอยู่ที่ส่วนฐานของเยื่อหุ้มของเซลล์ (basolateral membrane) เกิดความผิดปกติโดยเคลื่อนไปยังบริเวณอื่นของเซลล์ ทำให้โปรตีน kAE1 ซึ่งทำหน้าที่สำคัญในการแลกเปลี่ยนคลอไรด์และไบคาร์บอเนต (Cl^-/HCO_3^-) เข้าออกผ่านเยื่อหุ้มเซลล์ไตมนุษย์ ไม่สามารถทำหน้าที่ได้ตามปกติ และเป็นสาเหตุหนึ่งที่สำคัญของโรคไตผิดปกติในการขับกรด ปัจจุบันกลไกการเคลื่อนย้ายของโปรตีน kAE1 ในภาวะปกติที่จะเคลื่อนย้ายไปอยู่ที่ส่วนฐานของเยื่อหุ้มของเซลล์หลังจากที่มีการสังเคราะห์โปรตีนออกมาแล้วนั้น ยังไม่มีคำอธิบายหรือการศึกษาที่ชัดเจนว่าใช้กลไกใด และมีโปรตีนที่ทำหน้าที่ขนส่งชนิดใดบ้างที่เกี่ยวข้อง ในช่วงที่ผ่านมาคณะผู้วิจัย ได้มีการรายงานพบโปรตีนที่ทำหน้าที่ในการขนส่งโปรตีนอื่นไปยังส่วนฐานของเยื่อหุ้มเซลล์คือ Adaptor-related protein complex 1 μ1A (AP-1 mu1A) สามารถจับได้กับบริเวณปลายคาร์บอกซีของโปรตีน kAE1 และมีบทบาทสำคัญในการเคลื่อนย้ายโปรตีน kAE1 ไปยังบริเวณที่ถูกต้อง อย่างไรก็ตามโปรตีน AP-1 mu1A ไม่ได้เป็นโปรตีนเพียงชนิดเดียวที่ขนส่งโปรตีน kAE1 ไปเยื่อหุ้มเซลล์ เนื่องจากเมื่อลดการแสดงออกของโปรตีน AP-1 mu1A แล้ว ยังมีโปรตีน kAE1 บางส่วนที่ยังสามารถเคลื่อนย้ายไปยังเยื่อหุ้มเซลล์ได้ ในการศึกษาครั้งนี้คณะผู้วิจัยมีวัตถุประสงค์ที่จะทดสอบบทบาทของโปรตีนที่ทำหน้าที่ขนส่งชนิดอื่นๆ นอกจากโปรตีน AP-1 mu1A ที่มีการรายงานว่าสามารถขนส่งโปรตีนอื่นไปยังส่วนฐานของเยื่อหุ้มเซลล์ได้ โดยผู้วิจัยได้ลดการแสดงออกของโปรตีนกลุ่มดังกล่าวด้วยเทคนิค RNA interference และพบว่า มีโปรตีนอีก 3 ชนิด นอกจาก AP-1 mu1A มีผลต่อการเคลื่อนย้ายโปรตีน kAE1 ไปยังส่วนฐานของเยื่อหุ้มเซลล์เพาะเลี้ยงไตสุนัขที่ทำให้เกิดขั้ว (polarized MDCK cells) ได้แก่ โปรตีน AP-3, AP-4 และ Clathrin ซึ่งโปรตีนเหล่านี้ได้มีการศึกษาปฏิสัมพันธ์กับระหว่างโปรตีนเหล่านี้กับโปรตีน kAE1 ในเซลล์เพาะเลี้ยงไตมนุษย์ (HEK 293T cells) ด้วยเทคนิค co-immunoprecipitation และ yellow fluorescent protein-based protein fragment complementation assay (YFP-PCA) ผลการทดลองแสดงให้เห็นว่า AP-3, AP-4 และ Clathrin มีปฏิสัมพันธ์กับโปรตีน kAE1 และยังพบว่า

โปรตีนเหล่านี้มีการแสดงออกที่ตำแหน่งหรือบริเวณเดียวกันกับโปรตีน kAE1 ภายในเซลล์ของตัวอย่างชิ้นเนื้อจากไตมนุษย์จากการศึกษาด้วยเทคนิควิธีอิมมูโนฟลูออเรสเซนซ์ (immunofluorescence) ข้อมูลที่ได้เป็นการยืนยันผลที่ได้จากการวิจัยแบบ *in vitro* study และจะเป็นข้อมูลเพื่อใช้ศึกษาให้ทราบถึงบทบาทของโปรตีนที่มีปฏิสัมพันธ์กับโปรตีน kAE1 และทราบถึงกลไกหรือกระบวนการในการเคลื่อนย้ายโปรตีน kAE1 ในเซลล์ไตของมนุษย์ ซึ่งจะเป็นประโยชน์ทำให้เข้าใจกลไกการเกิดโรค การพัฒนาเทคโนโลยีในการศึกษาการเคลื่อนย้ายและหน้าที่ของโปรตีน ซึ่งจะนำไปสู่การพัฒนาวิธีการรักษาใหม่ๆ ต่อไปในอนาคต

คำหลัก : โปรตีนแอนไอออนเอ็กเซนเจอร์-วัน โรคไตผิดปกติในการขับกรด กระบวนการเคลื่อนย้ายโปรตีน โปรตีนขนส่ง

สารบัญ

LIST OF FIGURES

LIST OF TABLES

EXECUTIVE SUMMARY

Kidney anion exchanger 1 (kAE1) is a bicarbonate transporter involved in maintaining acid-base homeostasis in the human body. kAE1 is the basolateral Cl^-/HCO_3^- exchanger of the acid-secreting type A intercalated cells of the kidney. Several mutations in the *AE1 (SLC4A1)* gene have been found and associated with both autosomal dominant and autosomal recessive distal renal tubular acidosis (dRTA) which characterized by an inability of the kidney to secrete H^+ into urine resulting in systemic metabolic acidosis often accompanied by several clinical manifestations including muscle weakness, growth retardation, metabolic bone disease, nephrocalcinosis, nephrolithiasis, chronic pyelonephritis, and renal failure. The *AE1* mutations associated with dRTA do not cause defect of the protein in Cl^-/HCO_3^- exchange function but result in impaired trafficking or mistargeting of the mutant kAE1 proteins. Characterization of dRTA-associated *AE1* mutations using transfected cell systems demonstrated that AE1 mutations affect the intracellular trafficking of kAE1 protein to the basolateral surface, either mistargeting kAE1 protein to inappropriate destinations or accumulating within intracellular compartment. However, it has yet been unknown how the protein trafficking fails or why mistargeting of kAE1 protein occurs.

Protein transport along the secretory pathway is a tightly regulated process and requires specific protein-protein interactions and recognitions between cargo molecules and trafficking machinery to achieve correct targeting of cargo proteins to their destinations. Mutations that disrupt such interactions or cause protein misfolding often impair the transport process. To understand the pathogenesis of dRTA caused by *AE1* mutations, it is necessary to investigate the transport and targeting process of kAE1 protein from its biosynthesis site to the cell surface in both normal and abnormal conditions.

To investigate the trafficking process of kAE1 and why mutant kAE1 fail to transport, our group has identified interacting proteins of kAE1 in human kidney using yeast two hybrid (Y2H) screening. Proteins that specifically interact with kAE1 (either N- or C-terminus) have been screened and isolated from a human kidney cDNA library. The partial sequences of prey-cDNAs obtained from the screening and sequencing were analyzed with homology BLAST search for full-length cDNA and proteins in the NCBI GenBank and EMBL databases.

We have recently reported that AP-1 mu1A, a subunit of AP-1A adaptor complex involving in sorting of the cargo proteins, interacts with the C-terminus of kAE1. However, it is not known whether or not kAE1 trafficking depend on other sorting proteins, such as other members of adaptor complex (AP-1B, AP-3, and AP-4), Clathrin, Protein kinase D1, and Protein kinase D2 as well as motor proteins, such as kinesins which are also important in the basolateral trafficking process.

In this study, the roles of basolateral trafficking-related proteins have been characterized. Members of adaptor complex (AP-1B, AP-3, and AP-4), Clathrin, and Protein kinases (PKD1 and PKD2) were knocked down and examined for their effect on cell surface transport of kAE1 in Madin-Darby canine kidney cell lines (MDCK). Interactions between kAE1 and effected proteins were observed human kidney cell lines (HEK 293T). Moreover, localization of kAE1 and trafficking-related proteins were investigated human kidney tissues. This study provide a new insight into molecular mechanisms of kAE1 trafficking associated with adaptor-related protein complexes and motor proteins in normal conditions in human α-intercalated cells.

INTRODUCTION

Distal renal tubular acidosis (dRTA) is a kidney disease characterized by a failure of acid secretion by the α-intercalated cells of the cortical collecting duct of the distal nephron. This failure of acid secretion it leads to an inability to acidify the urine to a pH of less than 5.5. Because renal excretion is the primary means of eliminating acid from the body, the decrease net acid excretion into urine results in positive acid balance and hyperchloremic metabolic acidosis, which often associate with several clinical manifestations including muscle weakness, growth retardation, metabolic bone disease, nephrocalcinosis, nephrolithiasis, chronic pyelonephritis, and renal failure[1, 2]. Familial dRTA can be inherited in both autosomal dominant (AD) and autosomal recessive (AR) patterns with a broad spectrum of clinical severity. Patients with AD dRTA sometimes remain asymptomatic until reaching adolescence or adulthood, whereas others with AR dRTA may be severity affected since young ages accompanied with failure to thrive, growth retardation and rickets. Development of dRTA can result from mutations in any genes of several ion transporters and enzymes required for acid secretion and bicarbonate reabsorption across the α-intercalated cell membrane[3, 4]. A common hereditary cause is mutations of *solute carrier family 4, anion exchanger, member 1* (*SLC4A1*) or *AE1* gene encoding anion exchanger 1 (AE1, band 3)[5], the basolateral bicarbonate transporter of the intercalated cell, which may transmit in an autosomal dominant fashion in western European cases, or in an autosomal recessive fashion in Southeast Asian cases. The Southeast Asian cases are associated with more severe hypokalemia[5].

Human AE1 is a prototype member of bicarbonate transporter superfamily involving in maintenance of acid-base homeostasis in human body. The human *AE1* gene located on chromosome 17q21-22. The *AE1* gene comprises 20 exons and 19 introns ranging to approximately 20 kb[6, 7]. It encodes erythroid AE1 (eAE1), the major integral protein that serves the dual roles of Cl^-/HCO_3^- exchange and cytoskeletal anchorage of red cell membrane, and kidney AE1 (kAE1), which is the basolateral Cl^-/HCO_3^- exchanger of the acid-secreting α-intercalated cell of the kidney. Transcription of the eAE1 in erythroid precursors is under the control of an erythroid-specific promoter upstream of exon 1, while the renal transcription arises from a distinct promoter within intron 3 of the *AE1* gene. Thus the resultant kidney transcripts encode kidney-specific kAE1 polypeptides lacking 65 amino acids at the N-terminus[8].

The function of kAE1 is important in the process of bicarbonate reabsorption across the basolateral membrane of the α-intercalated cells of the renal collecting duct, which occurs in association with net acid excretion mediated by H^+-ATPase pump in the apical membrane of these cells. Failure of either acid excretion or bicarbonate reabsorption by these cells leads to intracellular accumulation of H^+ and HCO_3^- and inhibit further dissociation of carbonic acid, leading to an electro neutral imbalance and failure of the α-intercalated cells in acid

secretion or dRTA[8-10]. Despite the importance of kAE1 for acid-base homeostasis, very little is known about its trafficking or regulation in the kidney. Animal studies suggest that the α-intercalated cells might increase kAE1 levels at the basolateral membrane during chronic metabolic acidosis and reduce kAE1 levels during acute metabolic alkalosis[11-14] but the mechanism for how this occurs is unknown.

AE1 is a 911 amino acid multispanning membrane protein, with both N-terminal (residues 1-359) and C-terminal (residues 881-911) domains located in the cytoplasm. Both the N- and C-termini are essential for basolateral trafficking of kAE1[15]. Several motifs located within the cytosolic domains of integral membrane proteins are involved in the targeting of basolateral proteins, including tyrosine motifs and di-leucine motifs[16]. The study of a natural C-terminal truncation mutant kAE1R901stop[17, 18] showed that the C-terminus contains a nonclassical tyrosine motif, Y904 (using erythrocyte AE1 numbering) that is critical for basolateral trafficking[15, 18, 19]. The identity of the N-terminal trafficking determinant is unknown, but one suggestion is that the N-terminal tyrosine residue Y359 might be important[15, 20]. This is because both Y359 and Y904 are known to be phosphorylated in eAE1[21] and Y359 and Y904 in kAE1 are phosphorylated under specific conditions and that tyrosine phosphorylation can influence kAE1 localization[22].

Several mutations in *AE1* gene have been found to be associated with both autosomal dominant and autosomal recessive dRTA[23-25]. The mutations associated with autosomal dominant dRTA such as missense mutations in codon 589 (R589H, R589S, R589C), S613F, and R901X still maintaining anion exchange activity, are defective in AE1 traffic to the basolateral surface, causing either intracellular retention of AE1 in non-polarized human embryonic kidney 293 (HEK 293) or mistargeting of AE1 to apical membrane in polarized Madin-Darby canine kidney (MDCK) cells[18, 19, 26, 27]. The *AE1* mutations linked to autosomal recessive dRTA are G701D, ΔV850 and A858D[28]. A current hypothesis is that these mutations caused dRTA either by preventing the movement of mutant and normal proteins to the cell surface (impaired trafficking) or sending the mutant proteins to inappropriate site (mis-targeting), which resulted in impairing bicarbonate movement across the basolateral membrane[26, 29].

The trafficking itinerary of kAE1 from its biosynthesis site to specialized subdomains on the basolateral membrane surface has not been well characterized. So far, beyond observations that some mutations caused defects in trafficking to basolateral membrane of kAE1, it has yet been unknown how the protein trafficking fails and what checkpoint is present in normal trafficking of kAE1. Thus, to understand kAE1 transport, targeting, and regulation, it is necessary to identify kAE1 binding proteins (kAE1-BPs). The possibility is that different binding protein(s) that interact with either C-terminal or N-terminal cytoplasmic domain of kAE1 may contribute kAE1 trafficking or targeting to basolateral membrane in human kidney. The yeast-two hybrid (Y2H) system is among a few methods to demonstrate protein-protein

interaction *in vivo* [30]. This can be carried out by a selection or screening for novel proteins from cDNA library that specifically interacts with a target protein of interest. The principle of this system is based on transcription readout taking place within living yeast cells. Y2H screening has been conducted to isolate protein from cDNA library derived from human kidney cells that interacts with the large N-terminal and C-terminal region of kAE1. To gain a better insight into kAE1 trafficking, we recently reported for proteins binding to the C-terminal region of kAE1 (Ct-kAE1) containing motifs crucial for intracellular trafficking by a yeast two-hybrid (Y2H) screen[31]. An adaptor-related protein complex 1 μ1A (AP-1 mu1A) subunit was found to interact with Ct-kAE1 by the Y2H screen. The interaction between Ct-kAE1 or full-length kAE1 with AP-1 mu1A was confirmed by *in vitro* and *in situ* studies, including GST pull-down assay, co-immunoprecipitation, affinity co-purification, co-localization, and yellow fluorescent protein (YFP)-based protein fragment complementation assay (PCA). Interestingly, suppression of endogenous AP-1 mu1A in human embryonic kidney (HEK) 293T by small interfering RNA (siRNA) decreased membrane localization of kAE1 and increased its intracellular accumulation, suggesting a role of AP-1 mu1A in the kAE1 trafficking in kidney α-intercalated cells[31].

The adaptor protein complexes play crucial roles in cargo selection and vesicle formation in post-Golgi trafficking pathways. So far, four types of adaptor protein complexes have been described: AP-1, AP-2, AP-3 and AP-4. Three of them (AP-1, AP-3 and AP-4) function in protein sorting at the trans-Golgi network (TGN) or endosomes, while one (AP-2) mediates endocytosis at the plasma membrane. In mammalian, two forms of AP-1 complexes, AP-1A and AP-1B, exist. Both share the same subunits except the medium chain, which is a central subunit that mediates cargo selection via direct binding with tyrosine-based sorting motifs on the cytoplasmic domain of cargo proteins[32-34]. AP-1A contains an ubiquitiously expressed mu1A whereas AP-1B contains an epithelial-specific mu1B subunit[35]. Functionally, the ubiquitous AP-1A facilitates vesicle transport between the TGN and early endosomes, and the epithelial-specific AP-1B is required for polarized trafficking of many basolateral membrane proteins[36]. The AP-3 adaptor protein regulates the exit of exogenous vesicular stomatitis virus glycoprotein (VSVG) that contains basolateral sorting signal, from the Golgi complex in HeLa cells [37]. Simmen *et al.* [38] have proposed a role for AP-4 in basolateral sorting of receptors for LDL, transferrin and mannose-6-phosphate in MDCK cells, but their study did not fully clarify the organelle location of this sorting event. Clathrin is expected to be involved in basolateral protein sorting, as adaptor protein complexes have binding sites for clathrin[39]. All four adaptor protein complexes bind directly to both YXXΦ motifs (in which X represents any amino acid and Φ represents a large hydrophobic residue) and [D/E]XXXL[L/I] 'acidic dileucine' motifs, at least one of which is contained in many clathrin-coated vesicles cargo proteins. Clathrin-coated vesicles (CCV) are vehicles for intracellular trafficking in all nucleated cells. Many

studies have demonstrated their essential roles in endocytosis and cellular signaling processes at the plasma membrane. Clathrin is also required for polarity of the basolateral plasma membrane proteins in the MDCK cells. Suppression of clathrin expression by RNA interference depolarized most basolateral proteins and slowed down the exit of basolateral proteins from the Golgi complex and promoted their mis-sorting into apical carrier vesicles while clathrin knockdown did not affect the polarity of apical proteins. These results demonstrate necessity for clathrin in basolateral protein trafficking in epithelial cells[40].

In polarized epithelial cells, protein transport from the TGN is directed towards two different plasma membrane domains, apical and basolateral. For basolateral proteins, adaptor protein complexes and clathrin-coated vesicles might be involved in sorting proteins in the TGN. Protein kinase D1 (PKD1) is a serine/threonine kinase that binds to the TGN through its first cysteine-rich domain in a DAG-dependent process[41, 42]. Expression of a kinase-inactive form of PKD inhibited protein transport from the TGN to the cell surface[43]. Two additional isoforms of PKD, PKD2 and PKD3, have been identified. In polarized MDCK cells, PKD1 was required to transport proteins that contained basolateral sorting signals. Inactivation of PKD1 arrested basolateral cargo molecules in the TGN. Proteins containing apical sorting signals were not found arrested in the TGN when the kinase activity of PKD1 was compromised in the MDCK cells[43]. Similarly, PKD2 and PKD3 are also necessary for the transport of basolateral proteins from the TGN. Interestingly, PKD1 and PKD2 are responsible for transporting different basolateral cargo molecules from the TGN. In cells deficient in PKD1 kinase activity, the basolateral protein Sec6 was found arrested in the TGN[43]. Transport of E-cadherin and β-integrin to the basolateral surface was unaffected under these conditions. Conversely, expression of a kinase-inactive form of PKD2 resulted in retardation of β-integrin and E-cadherin transport, but not of Sec6p transport, in the TGN. PKD3 was found to inhibit the trafficking of the VSV-G protein (a protein containing the basolateral sorting signals) but did not affect the transport of apical cargo or of the basolateral proteins Sec6p, β-integrin, and E-cadherin[43]. Thus, PKD3 is also involved in the transport of basolateral cargo. However, the identities of the intracellular molecules that require the activity of PKD3 are not known.

RNA interference (RNAi) is a powerful technology for investigation of protein expression or function. RNA interference is a process by which gene is post-transcriptional suppressed using double stranded RNA (dsRNA) duplexes as guide to target and destroy their homologous mRNA in a sequence specific manner[44, 45]. The most important characteristics of RNAi is that it is triggered by dsRNA, which is cleaved into 21-23 bp so called small interfering RNA (siRNA) by RNase III-like enzyme inducer[46]. The siRNA is subsequently loaded onto multicomponent nuclease to form a complex known as RNA-induced silencing complex (RISC). The RISC hybridizes to target mRNA with a complementary region leading to

cleavage of its target in the middle of 21-23 bp of the complementary without affecting the unrelated RNA.

In this study, the role of basolateral-related sorting proteins including adaptor protein complexes, clathrin, and protein kinase D on kAE1 localization were determined using RNAi in polarized MDCK cells permanently expressing kAE1-HA. The interaction between kAE1 and sorting proteins was observed *in vitro* by co-immunoprecipitation and *in situ* by yellow fluorescent protein-based protein fragment complementation assay (YFP-PCA) in human kidney cell lines (HEK 293T). Moreover, co-localization between kAE1 and sorting proteins was investigated in human kidney tissues by using immunofluorescence staining. To gain a better insight into normal kAE1 trafficking, further studies would be carries out in polarized kidney cell lines to examine next steps of trafficking involving transportation along cytoplasm, tethering, and fusion to membrane. The investigation of the normal trafficking of human kAE1 will provide a new perception into a molecular mechanism associated with the pathogenesis of dRTA.

OBJECTIVES

1. To study the role of basolateral trafficking-related proteins on kAE1 localization in MDCK and HEK 293T cells.
2. To examine the interaction between kAE1 and basolateral trafficking-related proteins in HEK 293T cells.
3. To observe the expression and localization of kAE1 and basolateral trafficking-related proteins in human kidney tissues.

RESEARCH METHODOLOGY

1. Establishment of MDCK cells permanently expressing kAE1 (MDCK-kAE1-HA)

1.1 Cell culture and viral preparation

HEK 293T cells were maintained in complete medium [Dulbecco's Modified Eagle Medium (DMEM) supplemented with 10% fetal bovine serum (PERBIO), 100 Units/ml penicillin and 100 μg/ml streptomycin]. The cells were cultured in 25-cm^2 flask at 37ºC with 5% CO_2 and sub-cultured twice per week following a standard trypsinization protocol. The day before transfection, the cells were cultured in 25-cm^2 flask with 50% confluent then cells will be co-transfected with pVpack-GP, pVpack-VSVG, and pFB Neo-WT kAE1 HA557 (1.5 μg each) using FuGENE® 6 Transfection Reagent (Roche). After incubate for 24-36 h, culture medium was collected and filtered.

1.2 Viral transfection

The day before transfection, MDCK cells were cultured in 25-cm^2 flask with 50-70% confluent. In order to make cells susceptible to virus, 1:1000 of Polybrene (Sigma) was added for 2 h. Then culture medium containing virus prepared as above was added to Polybrene treated MDCK cells for 24-36 h. Then culture medium was removed and replaced with medium containing G418 (Sigma). The cells were cultured in G418 medium for 1 week, and colonies resistant to G418 were screened. kAE1-HA was detected by rabbit anti-HA (Invitrogen), or mouse anti-β-actin antibody (Sigma) as an internal control followed by probing with either swine anti-rabbit antibody conjugated-horseradish peroxidase (HRP) (DakoCytomation) or rabbit anti-mouse antibody conjugated-HRP (DakoCytomation) respectively. Chemiluminescent signals generated by SuperSignal West Pico Chemiluminescent Substrate (Thermo Scientific) were detected using a G:BOX chemiluminescence imaging system (Syngene).

1.3 Immunofluorescent staining in polarized MDCK cells

MDCK-kAE1-HA cells or wild type MDCK cells were grown on 24 mm polyester Transwell filter supports (Corning Costar), with a diameter of 12 mm and a pore size of 0.4 μm for 4 days. Filters were rinsed twice with cold PBS and fixed in ice-cold methanol for 10 min. After two washes with PBS, cells were permeabilized with 0.2% (v/v) Triton X-100 in PBS for 15 min, washed 3 times in PBS, and blocked with 3% (w/v) BSA/PBS for 30 min prior to incubation with rabbit anti-HA (Invitrogen) for 60 min at room temperature. Cells were then washed three times with PBS and incubated with donkey anti-rabbit IgG conjugated with Cy3 fluoresceine (Jackson Immunoresearch Laboratories) for 30 min at room temperature. The filters were incubate with PBS containing Hoechst 33342 (Molecular Probes) and then washed with PBS and mounted with Fluorosave (Invitrogen). Cellular localization of kAE1-HA was observed by using a laser scanning confocal Zeiss LSM 510 microscope (Carl Zeiss).

2. Conventional PCR

To examine mRNA expression of sorting proteins from MDCK-kAE1-HA cells, total RNA was prepared by Trizol reagent (Invitrogen) and chloroform extraction. mRNA was quantified by conventional PCR using a pair of specific primers for each sorting proteins consisting of forward primer and reverse primer (Table 1). The assay was performed by using GoTaq® DNA polymerase (Promega) and thermocycler (Biometra). Briefly, RNA samples (1 μg) were reverse transcribed using the SuperScript ^{III} First-Strand Synthesis System (Invitrogen) as specified by the manufacturer. The PCR amplification of the cDNA products was carried out in a reaction that contained 1 μl of cDNA, 5x colorless GoTaq® reaction buffer (Promega), 10 mM dNTP mix (Promega), 10 pmol of each primer and 0.25U GoTaq® DNA polymerase (Promega). cDNA samples were heated at 95°C for 5 minutes and then subjected to 30 amplification cycles of denaturation at 95°C for 30 seconds, primer annealing at 58°C for 30 seconds, and extension at 72°C for 30 seconds, followed by a final extension at 72°C for 10 minutes. DNA fragments were visualized after agarose gel electrophoresis by staining with ethidium bromide. The following negative controls were included water instead of cDNA.

Table 1 Sequences of primers for candidate sorting proteins

Sorting protein	Forward primer	Reverse primer
Adaptor-related protein complex 1A (AP-1A)	CTAGTGTGGAGGCCGAAGAC	CGGAGCTGGTAATCTCCATT
Adaptor-related protein complex 1B (AP-1B)	CAATGCCTCCCTGGTGTACT	GACACAGCGTTGGTGACAGT
Adaptor-related protein complex 3 (AP-3)	ATGAACCTGACACCCACACA	GGCTCGGATTCTCTTCTGGT
Adaptor-related protein complex 4 (AP-4)	GGCTCAAGAGCTTCCTTCCT	TACCGCATCACAGTCAGCTC
Clathrin heavy chain (CTLC)	TGAAGTTGGCACACCACCTA	TGGCTTCATGAGGTGCAGTA
Protein kinase D1 (PKD1)	TGCACCGAAAGTACCAAACA	ACTCTGCCATTGCCATCTCT
Protein kinase D2 (PKD2)	CAACAAGGACACGCTGAGAA	GCAGTGACGATCTCAAAGCA

3. RNA interference

Small interfering RNA (siRNA) directed against each sorting proteins was designed using BLOCK-iT^{TM} RNAi Designer (Invitrogen). The target sequences for siRNA of each sorting protein are shown in Table 2. Transfection of each siRNA or siControl was performed using Lipofectamine 2000 (Invitrogen) as detailed by the manufacturer. MDCK-kAE1-HA cells (10^4 cells) were grown on 24 mm polyester Transwell filter supports for 2 days before transfection. The double-stranded siRNA were transfected. Then the cells were harvested 3 days after transfection for further study by immunofluorescence staining and flow cytometry.

To examine knockdown efficiency by siRNA, total RNA was prepared from the transfected cells by Trizol reagent (Invitrogen) and chloroform extraction. The mRNA was quantified by real-time RT-PCR using a pair of specific primers as showed in Table 1. The assay was performed by using LightCycler® 480 SYBR Green I Master (Roche) and a LightCycler® 480 Instrument equipped with a 96-well thermal cycler (Roche). Briefly, RNA

samples (1 μg) were reverse transcribed using the SuperScript ^{III} First-Strand Synthesis System (Invitrogen) as specified by the manufacturer. cDNA templates were then subjected to a 10-minute initial denaturation at 95°C prior to 50 cycles of PCR (95°C for 15 seconds, 58°C for 15 seconds, and 72°C for 30 seconds, per cycle) in the presence of *Taq* DNA polymerase and the primer pairs. The mRNA levels were normalized against human beta-actin (forward primer 5'-AGAAAATCTGGCACCACACC-3' and reverse primer 5'-CTCCTTAATGTCACGCACGA–3') using the comparative Ct (delta delta Ct) method. The experiment to generate each data set was performed in triplicate, which was expressed as an average value (mean ± SE) and the significant of differences was addressed by Student's *t*-test. A P-value < 0.05 was considered statistically different.

Table 2 Accession number and target sequence for siRNAs

Sorting proteins	Accession number	Target sequence
Adaptor-related protein complex 1A (AP-1A)	NM_032493.3	TCCGAAGGCATCAAGTATCGGAAGA
Adaptor-related protein complex 1B (AP-1B)	NM_005498.4	AATTCCACCAGTGCGTGCGGC
Adaptor-related protein complex 3 (AP-3)	NM_012095.4	AAGGCAGCTATACATTTGATC
Adaptor-related protein complex 4 (AP-4)	NM_004722.3	AAGTGCTGGACTATGGCTATG
Clathrin heavy chain (CTLC)	NM_004859.3	AAGCCACAGCTGGAATAATTG
Protein kinase D1 (PKD1)	NM_002742.2	AAGTGACCATTAATGGAGATT
Protein kinase D2 (PKD2)	NM_016457.4	AACAACACGACCAACAGATAC

4. Flow cytometry

HA epitope inserted at the third extracellular loop of kAE1 would be expressed extracellularly. Thus, expression of kAE1-HA on the cell surface could be determined by fluorescence staining and flow cytometry. MDCK-kAE1-HA cells were transfected with siRNA against each of sorting protein or siControl. Three days after transfections, the cells were collected by trypsinization then centrifugation at 4°C. They were re-suspended in chilled DMEM containing with 2% fetal bovine serum, 1% BSA, and 10 mM NaN_3, before incubated with rabbit anti-HA antibody (Invitrogen) for 1 hour at 4°C. After incubation, the cells were washed twice with chilled DMEM containing with 2% fetal bovine serum, 1% BSA, and 10 mM NaN_3. Then, donkey anti-rabbit IgG conjugated with Cy3 fluoresceine (Jackson Immunoresearch Laboratories) was used for 1 hour at 4°C. The cells were washed again and analyzed by using FACSort™ flow cytometer (Becton–Dickinson).

5. Co-immunoprecipitation

HEK 293T cells were transfected with kAE1-Myc for 48 hours. Then the HEK 293T cells were lysed in RIPA buffer containing 1% NP-40, 0.5% sodium deoxycholate, 0.1% SDS, 150 mM NaCl, 20 mM Tris–HCl; pH 7.4, 5 mM EDTA, and protease inhibitor cocktail. Five μg of mouse anti-AP-1A (Abnova), mouse anti-AP-1B (Abnova), goat anti-AP-3 (Santa Cruz

Biotechnology), mouse anti-AP-4 (Santa Cruz Biotechnology), or goat anti-Clathrin (Santa Cruz Biotechnology) were added to lysates. The mixture was incubated with gentle rotation at 4°C for 6 hours. The incubation was continued 24 hours after addition of Protein G Sepharose (Amersham Pharmacia Biosciences). Subsequently, Protein G Sepharose was collected by centrifugation at 13,000 x g for 5 min and washed twice with 0.1% Triton X-100, 150 mM NaCl, 20 mM Tris–HCl; pH 7.4, 5 mM EDTA. The bound proteins were eluted by boiling in SDS-PAGE loading buffer, separated by SDS-PAGE, and transferred to nitrocellulose membrane. After blocking with 5% skim milk, the membranes were incubated with mouse anti-Myc (Santa Cruz Biotechnology) followed by probing with either a rabbit anti-mouse antibody conjugated-horseradish peroxidase (HRP) (DakoCytomation). Chemiluminescent signals generated by SuperSignal West Pico Chemiluminescent Substrate (Thermo Scientific) were detected using a G:BOX chemiluminescence imaging system (Syngene).

6. **Construction of sorting proteins-expressed vectors**

pcDNA3.1/Zeo-YFP[1]-Zip and pcDNA3.1/Zeo-YFP[2]-Zip, encoding two separate fragments of yellow fluorescent protein (YFP) fused with leucine zipper protein inserted between the *Not*I/*Xba*I sites of the pcDNA3.1/Zeo vectors (Invitrogen), were the gifts from Professor Stephen W. Michnick, University of Montreal, Canada. These constructs were consisted of the sequences encoding YFP fragments (either YFP[1] – amino acids 1 to 158, or YFP[2] – amino acids 159 to 240) and *Zip* cDNA encoding leucine zipper. A sequence encoding flexible 10 amino-acid linker $(GGGGS)_2$ was inserted between the sequences encoding YFP fragment and leucine zipper. The full-length cDNAs encoding kAE1 wild type (WT) were amplified by PCR and subcloned into the *Bsp*EI/*Xba*I sites of the pcDNA3.1/Zeo-YFP[1]-Zip by replacing the Zip sequence. AP-1A, AP-1B, AP-3, and AP-4 were also amplified by PCR and subcloned into the *Bsp*EI/*Xba*I, *Not*I/*Xba*I, *BamH*I/*Xho*I, and *Not*I/*Xba*I of the pcDNA3.1/Zeo-YFP[2]-Zip, respectively. pcDNA3.1-CHC-FL constructs for full-length clathrin heavy chain were the gifts from Dr. Masato Enari, National Cancer Center Research Institute, Division of Refractory Cancer Research, Tokyo, JAPAN. The construct was subcloned into the *Hind*III/*Not*I site of pcDNA3.1/Zeo-YFP[2]-Zip by replacing the Zip sequence. Plasmid constructs, including pcDNA3.1/Zeo-YFP[1]-kAE1, pcDNA3.1/Zeo-YFP[2]-AP-1A, pcDNA3.1/Zeo-YFP[2]-AP-1B, pcDNA3.1/Zeo-YFP[2]-AP-3, pcDNA3.1/Zeo-YFP[2]-AP-4, and pcDNA3.1/Zeo-YFP[2]-CLTC were generated. These constructs could express YFP[1]-kAE1, YFP[2]-AP-1A, YFP[2]-AP-1B, YFP[2]-AP-3, YFP[2]-AP-4 and YFP[2]-CLTC fusion proteins, respectively. The insert sequences in all constructs and their in-frame junctions were confirmed by DNA sequencing.

7. Yellow fluorescent protein-based protein fragment complementation assay (YFP-PCA)

Two days before transfection, the HEK 293T cells were collected by trypsinization and seeded in 6-well plates. The cultured cells were individually transfected with 1 μg each of the following constructs: pcDNA3.1/Zeo-YFP[1]-kAE1, pcDNA3.1/Zeo-YFP[2]-AP-1A, pcDNA3.1/Zeo-YFP[2]-AP-1B, pcDNA3.1/Zeo-YFP[2]-AP-3, pcDNA3.1/Zeo-YFP[2]-AP-4, and pcDNA3.1/Zeo-YFP[2]-CLTC by using Lipofectamine 2000 (Invitrogen) according to the manufacture's protocol. The cells were also co-transfected with different pairs of the constructs including: pcDNA3.1/Zeo-YFP[1] and pcDNA3.1/Zeo-YFP[2] (as a negative control), pcDNA3.1/Zeo-YFP[1]-kAE1 and pcDNA3.1/Zeo-YFP[2]-kAE1 (as a positive control due to kAE1 dimerization), pcDNA3.1/Zeo-YFP[1]-kAE1 and pcDNA3.1/Zeo-YFP[2]-AP-1A, pcDNA3.1/Zeo-YFP[1]-kAE1 and pcDNA3.1/Zeo-YFP[2]-AP-1B, pcDNA3.1/Zeo-YFP[1]-kAE1 and pcDNA3.1/Zeo-YFP[2]-AP-3, pcDNA3.1/Zeo-YFP[1]-kAE1 and pcDNA3.1/Zeo-YFP[2]-AP-4 and pcDNA3.1/Zeo-YFP[1]-kAE1 and pcDNA3.1/Zeo-YFP[2]-CLTC. Two days after transfection, the cells were fixed *in situ* in 3% formaldehyde, rinsed, permeabilized with 0.1% Triton X-100 in PBS and blocked with 1% BSA. Then the cells were reacted with rabbit anti-TGN46 (Abcam), followed by donkey anti-rabbit IgG conjugated with Cy3 fluoresceine (Jackson Immunoresearch Laboratories). The coverslips were incubate with PBS containing Hoechst 33342 (Molecular Probes) and then washed with PBS and mounted with Fluorosave (Invitrogen). Cell fluorescence images were observed by using a laser scanning confocal Zeiss LSM 510 microscope (Carl Zeiss).

8. Double immunofluorescence staining

Human fresh frozen tissues were obtained from leftover specimens of the Department of Pathology, Faculty of Medicine Siriraj Hospital, Mahidol University, Thailand. The protocol was approved by the Human Research Ethics Committee, Siriraj Institutional Review Board, Mahidol University (#*Si*128/2011). Sections were fixed by acetone for 10 minutes before immunostaining with the rabbit anti-human band3 (kAE1) (Santa Cruz Biotechnology) and mouse anti-AP-1A (Abnova), mouse anti-AP-1B (Abnova), goat anti-AP-3 (Santa Cruz Biotechnology), mouse anti-AP-4 (Santa Cruz Biotechnology), or goat anti-Clathrin (Santa Cruz Biotechnology) as the primary antibodies, followed by donkey anti-rabbit IgG conjugated with Cy3 fluoresceine (Jackson Immunoresearch Laboratories) and goat anti-mouse IgG or donkey anti-goat coupled to Alexa 488 (Invitrogen) as the secondary antibodies. The sections were then were incubate with PBS containing Hoechst 33342 (Molecular Probes) and then washed with PBS and mounted with Fluorosave (Invitrogen). The sections were examined under the LSM 510 META confocal microscope (Carl Ziess).

RESULTS

1. MDCK cells permanently expressing kAE1 was established as MDCK-kAE1-HA cells.

MDCK cells that permanently expressed HA-tagged kAE1 (kAE1-HA) were constructed as MDCK-kAE1-HA using retroviral system. kAE1-HA in MDCK cells was determined by immunoblotting and immunofluorescence staining. kAE1-HA could be detected in protein lysate (Figure 1A) and localized at basolateral membrane of polarized MDCK-kAE1-HA cells (Figure 1B).

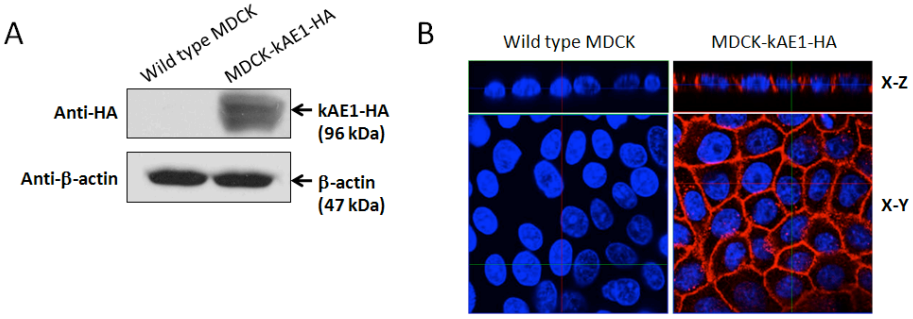

Figure 1 Expression of kAE1-HA in MDCK cells. (A) Immunoblotting using anti-HA antibody. (B) Localization of kAE1 in polarized MDCK-kAE1-HA cells by confocal microscopy using anti-Ct-kAE1 antibody.

2. The endogenous expression of basolateral sorting proteins were detected in MDCK-kAE1-HA cells.

The expression of AP-1 mu1A (AP-1A) and other six candidate sorting proteins, which may affect kAE1 trafficking, were determined in MDCK-kAE1-HA cells. Total RNA was extracted and reverse transcribed. Then mRNA was quantified by conventional PCR using primers as shown in Table 1. All selected sorting proteins were detected in MDCK-kAE1-HA cells (Figure 2).

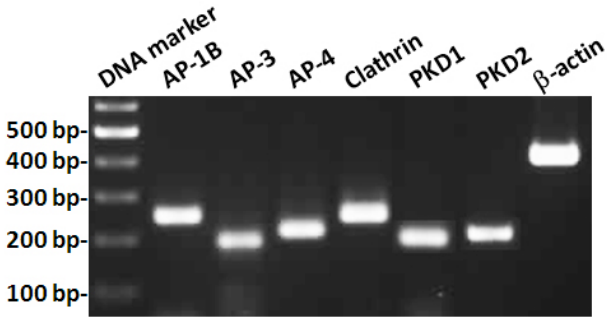

Figure 2 Gene expressions of candidate sorting proteins in MDCK-kAE1-HA cells were determined by conventional PCR.

3. Suppression of AP-1A, AP-3, AP-4, and CLTC but not AP-1B, PKD1, and PKD2 reduced basolateral kAE1 in MDCK-kAE1-HA cells

To address the effect of selected sorting proteins on kAE1 localization, we employed siRNA to transiently deplete the expression of each sorting proteins in MDCK-kAE1-HA cells. siRNAs targeting sorting proteins were designed (Table 2) and the efficiency of siRNAs in suppression of endogenous sorting proteins is shown in Figure 3. As shown by real-time PCR analysis, transfection of MDCK-kAE1-HA cells with 10, 20, and 40 pmol of siRNA against each of sorting protein reduced transcription within 24 h. Moreover, siRNA treatment efficiency suppressed the level of sorting proteins in a time-dependent manner, and the suppression effects were detected until 72 h after transfection (Figure 3A). Neither siRNA-scramble (siControl), nor Lipofectamine 2000 (data not show) affected the level of sorting proteins expression. Protein expression was also determined by Western blot analysis. Transfection of MDCK-kAE1-HA cells with 40 pmol of each siRNA clearly decreased adaptor protein complexes and clathrin proteins while expression of kAE1-HA was not changed (Figure 3B).

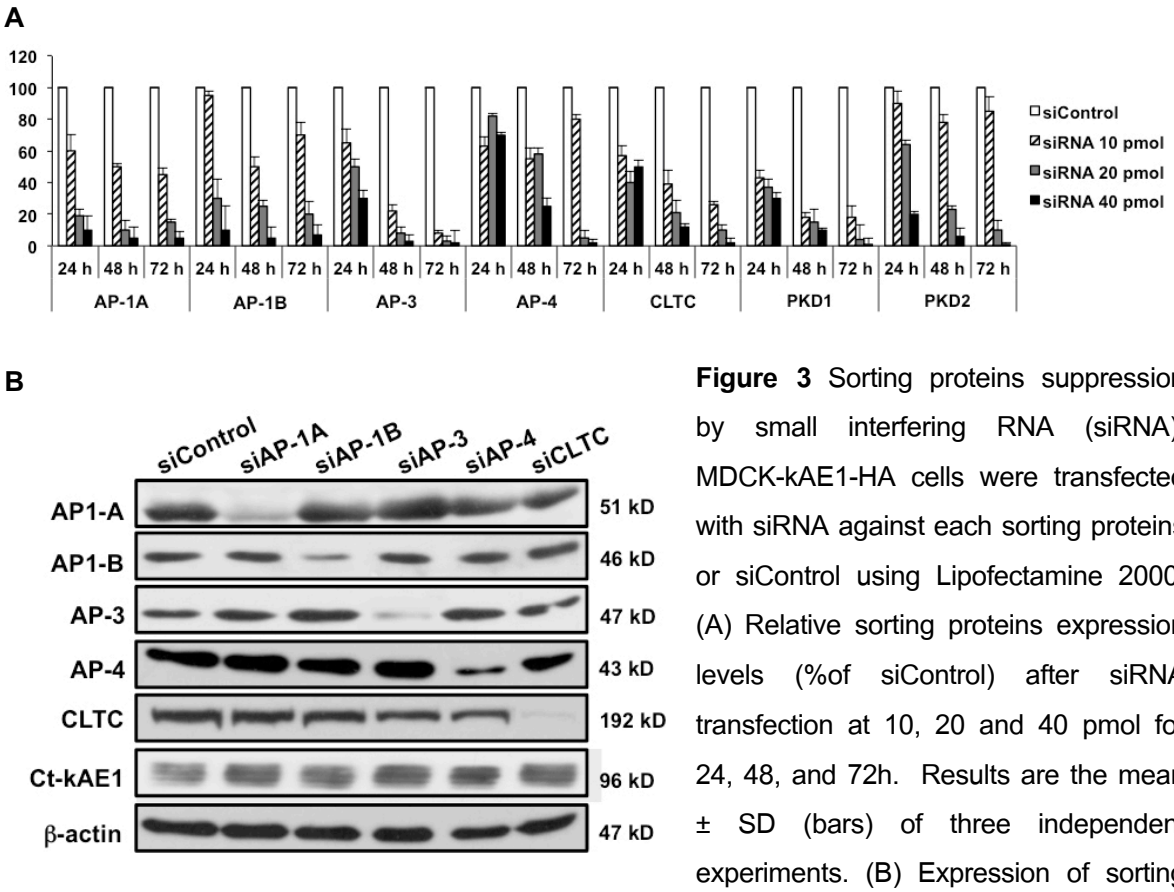

Figure 3 Sorting proteins suppression by small interfering RNA (siRNA). MDCK-kAE1-HA cells were transfected with siRNA against each sorting proteins or siControl using Lipofectamine 2000. (A) Relative sorting proteins expression levels (%of siControl) after siRNA transfection at 10, 20 and 40 pmol for 24, 48, and 72h. Results are the mean ± SD (bars) of three independent experiments. (B) Expression of sorting proteins by immunoblotting after 40 pmol of siRNA transfection for 72 h.

The effects of siRNA against each sorting protein on kAE1 localization were observed. HA epitope inserted at the third extracellular loop of kAE1 would be expressed extracellularly. Thus, expression of kAE1-HA on the cell surface could be determined by flow cytometry and immunofluorescence staining. Non-polarized and polarized MDCK-kAE1-HA cells were transfected with 40 pmol of siRNA against each sorting protein for 72 h then non-polarized MDCK-kAE1-HA cells were collected and determined by flow cytometry using anti-HA antibody. The results showed that siRNA targeting AP-1A, AP-3, AP-4, and clathrin decreased membranous kAE1 expression >30% while siRNA against AP-1B, PKD1, and PKD2 did not (Figure 4). siRNA transfected polarized MDCK-kAE1-HA cells were immunofluorescence stained using anti-HA antibody. Reduction of basolateral kAE1 was observed in polarized MDCK-kAE1-HA cells transfected with siRNA targeting AP-1A, AP-3, AP-4, and clathrin, but suppression of AP-1B, PKD1, and PKD2 did not affect kAE1 localization (Figure 5).

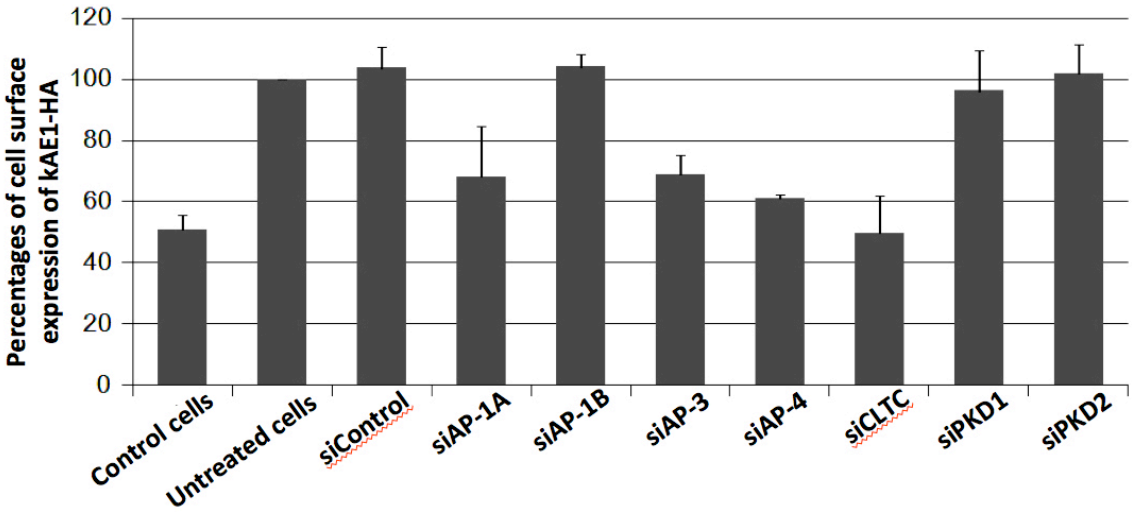

Figure 4 Percentage of cell surface expression of kAE1. MDCK-kAE1-HA cells were transfected with 40 pmol of siRNA against each sorting proteins or siControl for 72 h. Cells were collected and determined by flow cytometry using anti-HA antibody. Control cells are wild type MDCK cells. Untreated cells are untransfected MDCK-kAE1-HA cells. Results are the mean ± SD (bars) of three independent experiments.

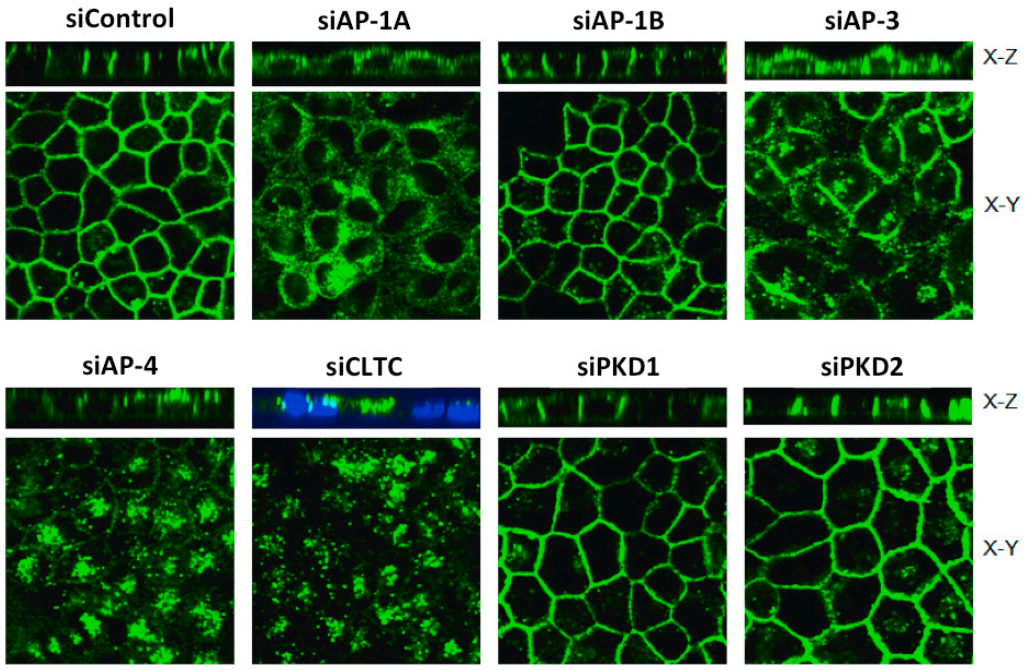

Figure 5 Localization of kAE1 in polarized cells. MDCK-kAE1-HA cells were grown on polyester Transwell filter supports for 2 days then cells were transfected with 40 pmol of siRNA for 72 h. Immunofluorescence staining was done using anti-HA antibody. Localization of kAE1 was observed by laser scanning confocal microscope.

4. kAE1 interacts with sorting proteins: AP-1A, AP-3, and AP-4 and clathrin but not AP-1B in HEK 293T cells by co-immunoprecipitation and YFP-PCA

To establish whether kAE1 interacts with adaptor proteins complexes and clathrin, full-length kAE1 cDNA sequences were previously sub-cloned into mammalian expression vectors with Myc epitope inserted at the third extracellular loop of kAE1 and transfected in to HEK 293T cells. Proteins interaction was observed by co-immunoprecipitated kAE1-Myc with adaptor proteins complexes (AP-1A, AP-1B, AP-3, and AP-4) or clathrin using antibody against each of adaptor proteins complexes or clathrin, the co-immunoprecipitated kAE1 was detected by Western blot method using anti-Myc antibody.

Figure 6 showed co-immunoprecipitation of kAE1-Myc with AP-1A, AP-3, AP-4, and clathrin which indicate the interaction of kAE1 and these sorting proteins. However, co-immunoprecipitaion of kAE1-Myc with AP-1B using anti-AP-1B antibody; the co-immunoprecipitated kAE1 could not be detected. This suggests that another adaptor complexes other than AP-1B could interact with kAE1 and are responsible for the basolateral sorting of kAE1.

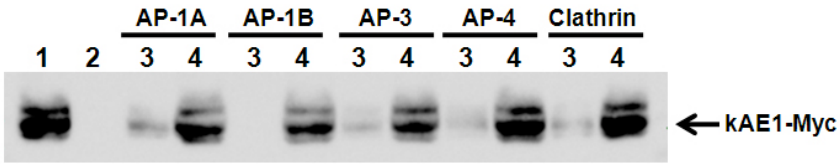

Figure 6 Co-immunoprecipitation study using HEK 293T cells demonstrated interaction between kAE1 and sorting proteins. HEK 293T cells expressing kAE1-Myc were lysed and proteins were either directly run on SDS-PAGE or immunoprecipitated with antibody against adaptor-related proteins or clathrin as indicated prior to the SDS-PAGE. After transferring proteins on nitrocellulose membrane, samples were blotted with anti-Myc antibody. Lane 1: input; lane 2: immunoprecipitation with no antibody, lane 3: immunoprecipitation with antibody against adaptor-related proteins or clathrin, and lane 4: unbound.

The interaction between kAE1 and sorting proteins within HEK 293T cells were next examined by yellow fluorescent protein (YFP)-based protein fragment complementation assay (PCA). The YFP fusion proteins were individually expressed (data not shown) or co-expressed in HEK 293T cells and their interactions demonstrated by intracellular green fluorescent signals that were captured by confocal microscopy. HEK 293T cells were co-transfected to express YFP[1] and YFP[2] as a negative control, no fluorescent signal was detected (Figure 7A). As a positive control, the HEK 293T cells were co-transfected to express YFP[1]-kAE1 and YFP[2]-kAE1; dimerization of kAE1 fusion proteins resulted in YFP[1] and YFP[2] complementation (Figure 7B) showing intracellular green-fluorescent signals. Similarly, when they were co-transfected to express either YFP[1]-kAE1 and YFP[2]-AP-1A (Figure 7C) or YFP[2]-AP-3, YFP[2]-AP-4, and YFP[2]-CLTC (Figure 7E, 7F, and 7G), intracellular green-fluorescent signals were captured. However, intracellular green-fluorescent signals were not detected in HEK 293T cells with co-expression of YFP[1]-kAE1 and YFP[2]-AP-1B (Figure 7D). These confirmed the co-immunoprecipitation results that kAE1 could interact with AP-1A, AP-3, AP-4, and Clathrin but not AP-1B.

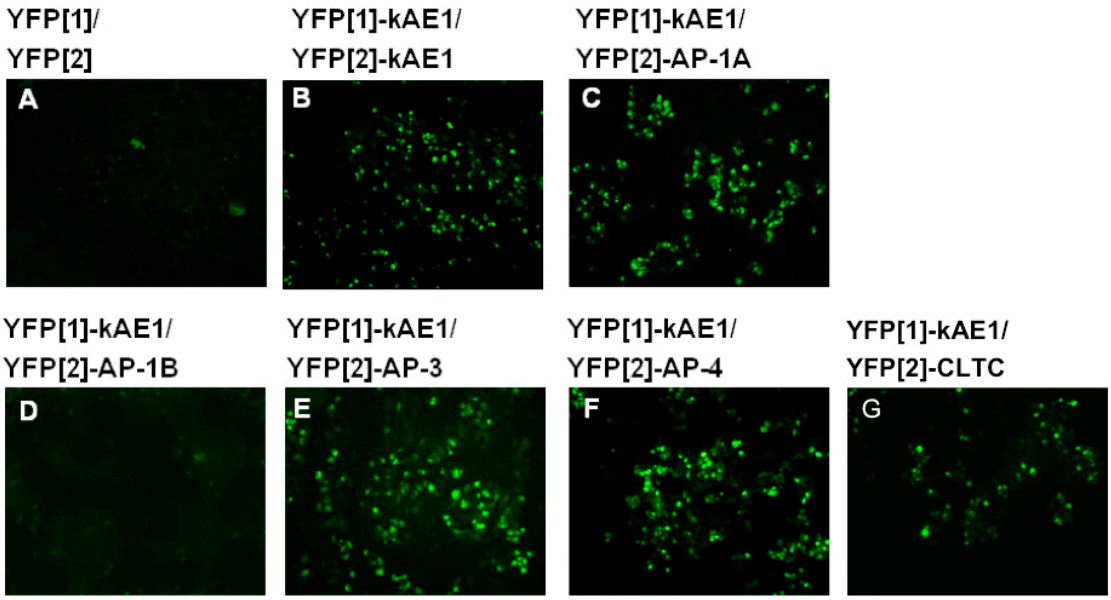

Figure 7 Investigation of *in situ* interaction between kAE1 and sorting proteins in HEK 293T cells by yellow fluorescent protein (YFP)-based protein fragment complementation assay (PCA). (A) The cells were co-transfected to express YFP[1] and YFP[2] as negative control, showing no fluorescent signal. (B) The cells were co-transfected to express YFP[1]-kAE1 and YFP[2]-kAE1 as positive control generating intracellular green fluorescent signals. (C) The cells were co-transfected to express YFP[1]-kAE1 and YFP[2]-AP-1A, (E) YFP[1]-kAE1 and YFP[2]-AP-3, (F) YFP[1]-kAE1 and YFP[2]-AP-4, (G) YFP[1]-kAE1 and YFP[2]-CLTC showing intracellular green fluorescent signals indicating their interaction. (D) The cells were co-transfected to express YFP[1]-kAE1 and YFP[2]-AP-1B showing no fluorescent signal indicating no interaction between kAE1 and AP-1B.

5. kAE1 co-localizes with AP-1A, AP-3, AP-4, and clathrin but not AP-1B in human kidney tissues as determined by double immunofluorescence staining

According to the *in vitro* interaction between kAE1 and basolateral-sorting proteins, we suppose that kAE1 and those basolateral-sorting proteins co-localized in cells of kidney tissues. We further determined the expression and localization of these proteins in human kidney tissues. Human fresh frozen tissues were obtained from leftover specimens of the Department of Pathology, Faculty of Medicine Siriraj Hospital, Mahidol University, Thailand. The protocol was approved by the Human Research Ethics Committee, Siriraj Institutional Review Board, Mahidol University (#*Si*128/2011). Sections were fixed and immunostained with the anti-Ct-kAE1 antibody and the antibodies against each of sorting proteins as the primary antibodies, followed by the secondary antibodies coupled to Cy3 or Alexa 488. The sections were then examined under the LSM 510 META confocal microscope (Carl Ziess). The antibody against kAE1

detected both a clear predominant basolateral staining and a discrete vesicular intracellular staining. In a high intensity, AP-1A, AP-3, AP-4, and clathrin were stained similarly as that of kAE1 at basolateral membrane. In the insets, a higher magnification of the intracellular red and green staining showed co-localization of both endogenous kAE1 and endogenous sorting proteins with the exception of AP-1B, supporting that kAE1 interacts with AP-1A, AP-3, AP-4, and clathrin in the human kidney tissue (Figure 8)

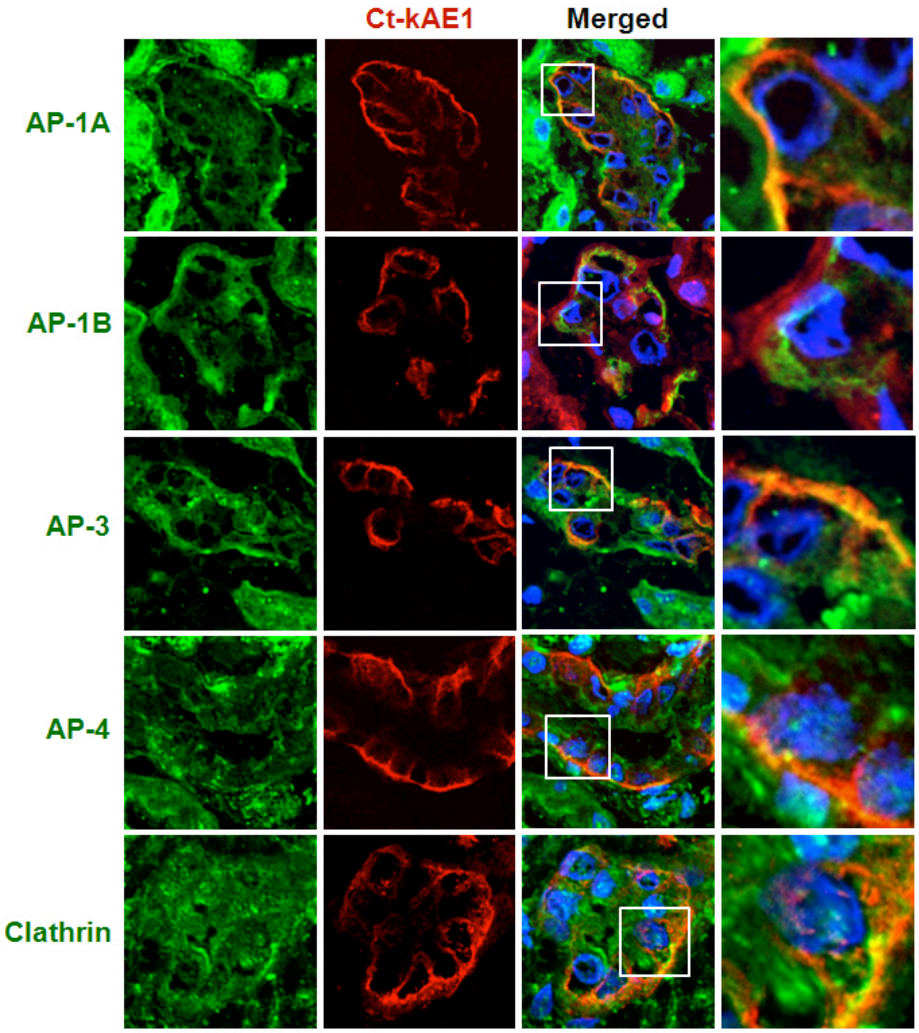

Figure 8 kAE1 protein co-localizes with endogenous KIF3B in human kidney tissues. Fresh frozen human kidney sections were incubated with the rabbit anti-kAE1 antibody and the goat or mouse antibodies against each of sorting protein (first column). Slides were then incubated with the anti-rabbit antibody coupled to Cy3 (red) and the anti-goat or anti-mouse antibodies coupled to Alexa 488 (green), followed by nuclear staining with Hoechst 33258 (blue). The samples were examined using confocal microscope and a 100 X lens.

DISCUSSION AND CONCLUSION

Trafficking defect of kAE1 has been revealed as a potential molecular basis of dRTA caused by *SLC4A1* mutations since almost all mutant kAE1 showed normal level or modest reduction of anion-transport activities[5, 18, 24, 26, 47]. However, to date, the trafficking pathway of kAE1 to the polarized basolateral cell surface and its defect associated with dRTA have not been clearly described. To solve defective steps in kAE1 trafficking process, identification of proteins involved in kAE1 intracellular trafficking is essential. We previously reported the effect of AP-1 mu1A, a medium subunit of an adaptor protein complex AP-1A – clathrin-associated adaptor proteins, on kAE1 trafficking[31]. Suppression of endogenous AP-1 mu1A in human embryonic kidney (HEK) 293T by small interfering RNA (siRNA) decreased membrane localization of kAE1, suggesting a role of AP-1 mu1A in the kAE1 trafficking in kidney α-intercalated cells[31]. In this study, we proposed to identify the molecular mechanisms of kAE1 protein trafficking to basolateral membrane of kidney cells. Role of basolateral sorting proteins including four adaptor protein complexes (AP-1A, AP-1B, AP-3, and AP-4), clathrin heavy chain, and two protein kinases D (PKD1 and PKD2), were identified using siRNA. Suppression of AP-1A, AP-3, AP-4, and Clathrin heavy chain in MDCK-kAE1-HA cells decreased basolateral membrane localization (Figure 4 and 5). While reduction of AP-1B, PKD1, and PKD2 did not affect kAE1 localization (Figure 4 and 5). The role of the AP-1B complex in kAE1 basolateral sorting was previously examined by expression of wild-type C-terminal kAE1 or kAE1Δ11(with 11-amino acid deletion) in LLC-PK1 cells, which lack the mu1B subunit[19]. Although the AP-1B complex cannot form in these cells, wild-type kAE1 was correctly targeted to the basolateral membrane[19]. The role of PKD1 and PKD2 were previously reported to involved in the transport of basolateral cargo in MDCK cells[43]. However, recruitment and activation of PKD at the TGN need activation of a not-yet-identified G protein–coupled receptor (GPCR) by cargo activates a trimeric G protein[48]. kAE1 might has no G protein–coupled receptor sequence or motif that show no effect on basolateral localization of kAE1 in PKD1 and PKD2 suppressed MDCK cells.

The adaptor protein complexes play essential roles in cargo selection and vesicle formation in post-Golgi trafficking pathways. We previously reported that kAE1 interacts with AP-1 mu1A, a subunit of AP-1A adaptor complex, in a yeast two-hybrid screen[31]. The interaction was confirmed by GST pull-down assay, co-immunoprecipitation, affinity co-purification, and YFP-based protein fragmentation complementation assay (YFP-PCA)[31]. In this study, we investigated whether kAE1 interacts with AP-1B, AP-3, AP-4, and clathrin, *in vitro* co-immunoprecipitation and *in situ* YFP-PCA in HEK 293T cells were conducted. The results showed kAE1 interacts with AP-1A, which confirm our previous report. Here, we found kAE1 also interacts with AP-3, AP-4 and clathrin (Figure 6 and 7). kAE1 do not

interact with AP-1B by both assays. In general, various membrane proteins are sorted to the basolateral membrane through the interaction of tyrosine-based targeting motifs in their cytoplasmic domains with adaptor protein complexes, one of which is AP-1B. The study in LLC-PK1 cells demonstrated that full length kAE1, which contain a tyrosine-based basolateral-sorting signal, did not recognize the AP-1B complex[15]. Moreover, LLC-PK1 cells, which the AP-1B complex cannot form, wild-type kAE1 was correctly targeted to the basolateral membrane[19]. These studies reveal that another adaptor complex other than AP-1B is responsible for the basolateral sorting of kAE1 in LLC-PK1 cells. In addition with our finding, these data supported the concept that AP-1B is not involved in kAE1 impaired trafficking associated with dRTA.

The kAE1 protein predominantly localizes at basolateral membrane but it also co-localizes with AP-1A at TGN of HEK 293T[31]. In this study, we observed co-localization of endogenous kAE1 and basolateral-sorting proteins, unless AP-1B, in intracellular of human kidney tissue sections (Figure 8). The kAE1 is a chloride/bicarbonate exchanger located at the basolateral membrane of α-intercalated cells. The interaction between kAE1 and basolateral-sorting proteins is may be transient and necessary for targeting newly synthesized kAE1 protein from TGN. The defective protein trafficking due to mutations of the kAE1, which cause dRTA, has been attributed to impaired acid secretion secondary to a loss of Cl^-/HCO_3^- transport[15, 17, 19, 20, 27, 49]. However, our results show that the mechanism underlying this defect in trafficking may also involve the interaction between kAE1 and sorting proteins, which facilitates transport of vesicles from TGN (Figure 9). Several sorting signals for basolateral membranes are known, such as tyrosine and dileucine motifs[50]. Adaptor proteins are known to bind to these motifs and are involved in basolateral sorting. Motor proteins are also required for transportation of a cargo protein from TGN to the plasma membranes. KIF3B is one of the kinesin II subfamilies of the kinesin superfamily, which consists of a large family of molecular motors that transport the intracellular cargo along the microtubules using the energy derived from hydrolysis of ATP[51]. We reported that kAE1 interacts with kinesin family member 3B (KIF3B) in kidney cells[52]. Suppression of endogenous KIF3B in HEK 293T cells by small interfering RNA (siRNA) decreases membrane localization of kAE1, which suggest that KIF3B is involved in the trafficking of kAE1 to the plasma membrane of human kidney α-intercalated cells[52]. Mechanisms of kAE1 sorting and transportation are proposed as shown in figure 9.

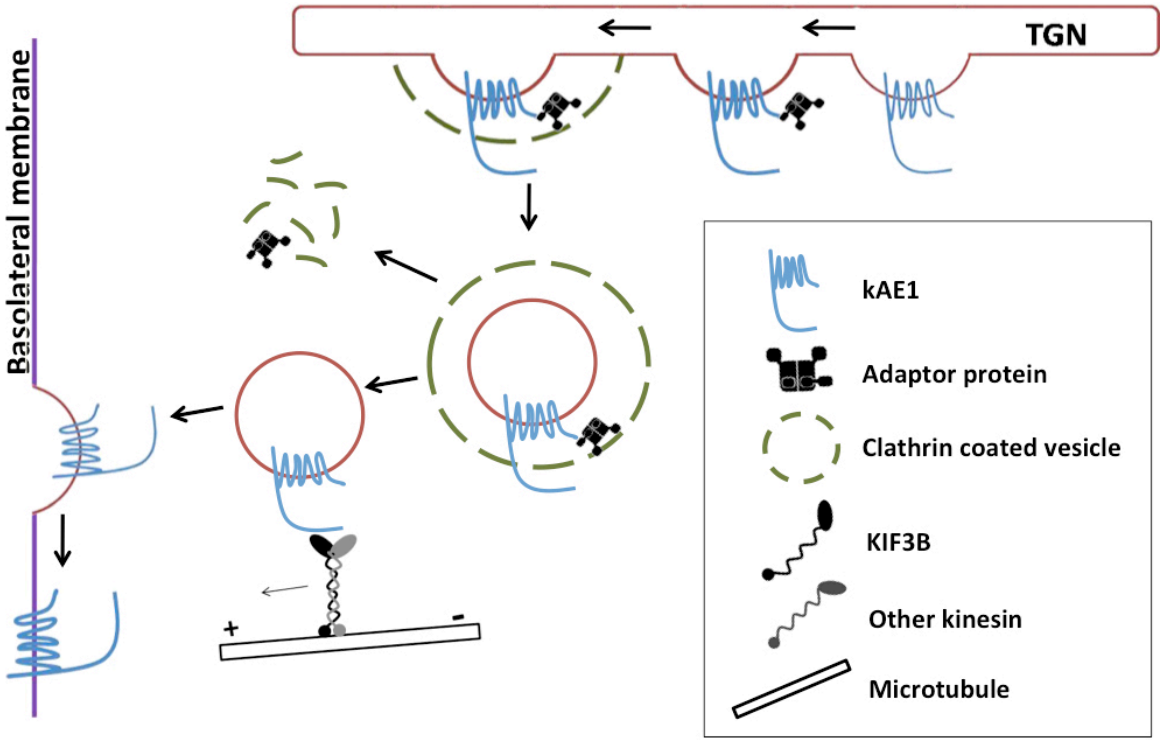

Figure 9 Schematic representation of model for basolateral trafficking of kAE1 in polarized cells. Newly synthesized kAE1 leaves the trans-Golgi network (TGN). The adaptor proteins are recruited to the TGN membrane through sorting signal at C-terminus of kAE1. Clathrin assembles onto the adaptors to form the clathrin-coated vesicle. Following detachment from the TGN membrane the clathrin and adaptor proteins are uncoated separately. The vesicle containing kAE1 is then transported along microtubules to the cell surface via the motor protein complexes (KIF3B).

In conclusion, we have demonstrated a critical role for adaptor protein complexes (AP-1A, AP-3, and AP-4) and clathrin heavy chain in kAE1 trafficking to the basolateral membrane by a knockdown study which showed a marked reduction of kAE1 on the membrane and its accumulation in the cytoplasm of polarized MDCK cells. Role of sorting proteins on kAE1 trafficking is based on their interaction. To gain a better insight into normal kAE1 trafficking, further studies would be carries out in polarized kidney cell lines to examine next steps of trafficking involving transportation along cytoplasm, tethering, and fusion to membrane. The investigation of the normal trafficking of human kAE1 will provide a new perception the molecular defect of dRTA associated with *SLC4A1* mutations.

REFERENCES

1. Alper SL. Genetic diseases of acid-base transporters. Annual review of physiology. 2002;64:899-923. Epub 2002/02/05.
2. Rodriguez-Soriano J. New insights into the pathogenesis of renal tubular acidosis--from functional to molecular studies. Pediatr Nephrol. 2000;14(12):1121-36. Epub 2000/10/25.
3. Dubose T, Alpern R. The metabolic and molecular bases of inherited disease. New York: McGraw-Hill. 1995.
4. Rodriguez-Soriano J. Pediatric kidney disease. 2nd ed Boston: Little brown. 1992.
5. Bruce LJ, Cope DL, Jones GK, Schofield AE, Burley M, Povey S, et al. Familial distal renal tubular acidosis is associated with mutations in the red cell anion exchanger (Band 3, AE1) gene. J Clin Invest. 1997;100(7):1693-707.
6. Sahr KE, Taylor WM, Daniels BP, Rubin HL, Jarolim P. The structure and organization of the human erythroid anion exchanger (AE1) gene. Genomics. 1994;24(3):491-501.
7. Schofield AE, Martin PG, Spillett D, Tanner MJ. The structure of the human red blood cell anion exchanger (EPB3, AE1, band 3) gene. Blood. 1994;84(6):2000-12.
8. Brosius FC, 3rd, Alper SL, Garcia AM, Lodish HF. The major kidney band 3 gene transcript predicts an amino-terminal truncated band 3 polypeptide. The Journal of biological chemistry. 1989;264(14):7784-7.
9. Karet FE, Finberg KE, Nelson RD, Nayir A, Mocan H, Sanjad SA, et al. Mutations in the gene encoding B1 subunit of H+-ATPase cause renal tubular acidosis with sensorineural deafness. Nature genetics. 1999;21(1):84-90.
10. Tang XB, Fujinaga J, Kopito R, Casey JR. Topology of the region surrounding Glu681 of human AE1 protein, the erythrocyte anion exchanger. The Journal of biological chemistry. 1998;273(35):22545-53.
11. Fejes-Toth G, Chen WR, Rusvai E, Moser T, Naray-Fejes-Toth A. Differential expression of AE1 in renal HCO3-secreting and -reabsorbing intercalated cells. The Journal of biological chemistry. 1994;269(43):26717-21.
12. Huber S, Asan E, Jons T, Kerscher C, Puschel B, Drenckhahn D. Expression of rat kidney anion exchanger 1 in type A intercalated cells in metabolic acidosis and alkalosis. The American journal of physiology. 1999;277(6 Pt 2):F841-9.
13. Sabolic I, Brown D, Gluck SL, Alper SL. Regulation of AE1 anion exchanger and H(+)-ATPase in rat cortex by acute metabolic acidosis and alkalosis. Kidney international. 1997;51(1):125-37.
14. Verlander JW, Madsen KM, Cannon JK, Tisher CC. Activation of acid-secreting intercalated cells in rabbit collecting duct with ammonium chloride loading. The American journal of physiology. 1994;266(4 Pt 2):F633-45.

15. Toye AM, Banting G, Tanner MJ. Regions of human kidney anion exchanger 1 (kAE1) required for basolateral targeting of kAE1 in polarised kidney cells: mis-targeting explains dominant renal tubular acidosis (dRTA). Journal of cell science. 2004;117(Pt 8):1399-410.
16. Bonifacino JS, Traub LM. Signals for sorting of transmembrane proteins to endosomes and lysosomes. Annual review of biochemistry. 2003;72:395-447.
17. Karet FE, Gainza FJ, Gyory AZ, Unwin RJ, Wrong O, Tanner MJ, et al. Mutations in the chloride-bicarbonate exchanger gene AE1 cause autosomal dominant but not autosomal recessive distal renal tubular acidosis. Proceedings of the National Academy of Sciences of the United States of America. 1998;95(11):6337-42. Epub 1998/05/30.
18. Toye AM, Bruce LJ, Unwin RJ, Wrong O, Tanner MJ. Band 3 Walton, a C-terminal deletion associated with distal renal tubular acidosis, is expressed in the red cell membrane but retained internally in kidney cells. Blood. 2002;99(1):342-7.
19. Devonald MA, Smith AN, Poon JP, Ihrke G, Karet FE. Non-polarized targeting of AE1 causes autosomal dominant distal renal tubular acidosis. Nature genetics. 2003;33(2):125-7. Epub 2003/01/23.
20. Toye AM. Defective kidney anion-exchanger 1 (AE1, Band 3) trafficking in dominant distal renal tubular acidosis (dRTA). Biochemical Society symposium. 2005(72):47-63. Epub 2005/01/15.
21. Yannoukakos D, Meyer HE, Vasseur C, Driancourt C, Wajcman H, Bursaux E. Three regions of erythrocyte band 3 protein are phosphorylated on tyrosines: characterization of the phosphorylation sites by solid phase sequencing combined with capillary electrophoresis. Biochimica et biophysica acta. 1991;1066(1):70-6.
22. Williamson RC, Brown AC, Mawby WJ, Toye AM. Human kidney anion exchanger 1 localisation in MDCK cells is controlled by the phosphorylation status of two critical tyrosines. Journal of cell science. 2008;121(Pt 20):3422-32.
23. Bruce LJ, Unwin RJ, Wrong O, Tanner MJ. The association between familial distal renal tubular acidosis and mutations in the red cell anion exchanger (band 3, AE1) gene. Biochemistry and cell biology = Biochimie et biologie cellulaire. 1998;76(5):723-8.
24. Sawasdee N, Udomchaiprasertkul W, Noisakran S, Rungroj N, Akkarapatumwong V, Yenchitsomanus PT. Trafficking defect of mutant kidney anion exchanger 1 (kAE1) proteins associated with distal renal tubular acidosis and Southeast Asian ovalocytosis. Biochemical and biophysical research communications. 2006;350(3):723-30.
25. Vasuvattakul S, Yenchitsomanus PT, Vachuanichsanong P, Thuwajit P, Kaitwatcharachai C, Laosombat V, et al. Autosomal recessive distal renal tubular acidosis associated with Southeast Asian ovalocytosis. Kidney international. 1999;56(5):1674-82.
26. Quilty JA, Li J, Reithmeier RA. Impaired trafficking of distal renal tubular acidosis mutants of the human kidney anion exchanger kAE1. American journal of physiology. 2002;282(5):F810-20.

27. Rungroj N, Devonald MA, Cuthbert AW, Reimann F, Akkarapatumwong V, Yenchitsomanus PT, et al. A novel missense mutation in AE1 causing autosomal dominant distal renal tubular acidosis retains normal transport function but is mistargeted in polarized epithelial cells. The Journal of biological chemistry. 2004;279(14):13833-8. Epub 2004/01/22.
28. Yenchitsomanus PT. Human anion exchanger1 mutations and distal renal tubular acidosis. The Southeast Asian journal of tropical medicine and public health. 2003;34(3):651-8.
29. Quilty JA, Cordat E, Reithmeier RA. Impaired trafficking of human kidney anion exchanger (kAE1) caused by hetero-oligomer formation with a truncated mutant associated with distal renal tubular acidosis. The Biochemical journal. 2002;368(Pt 3):895-903.
30. Ausubel F, Brent R, Kingston R, Moore D, Seidman J, Smith J, et al. Current protocols in molecular biology. United States: John Wiley and Sons Inc,New York, NY. 1998.
31. Sawasdee N, Junking M, Ngaojanlar P, Sukomon N, Ungsupravate D, Limjindaporn T, et al. Human kidney anion exchanger 1 interacts with adaptor-related protein complex 1 mu1A (AP-1 mu1A). Biochemical and biophysical research communications. 2010;401(1):85-91. Epub 2010/09/14.
32. Ohno H, Fournier MC, Poy G, Bonifacino JS. Structural determinants of interaction of tyrosine-based sorting signals with the adaptor medium chains. J Biol Chem. 1996;271(46):29009-15.
33. Ohno H, Stewart J, Fournier MC, Bosshart H, Rhee I, Miyatake S, et al. Interaction of tyrosine-based sorting signals with clathrin-associated proteins. Science. 1995;269(5232):1872-5.
34. Owen DJ, Evans PR. A structural explanation for the recognition of tyrosine-based endocytotic signals. Science. 1998;282(5392):1327-32.
35. Aguilar RC, Ohno H, Roche KW, Bonifacino JS. Functional domain mapping of the clathrin-associated adaptor medium chains mu1 and mu2. J Biol Chem. 1997;272(43):27160-6.
36. Folsch H. The building blocks for basolateral vesicles in polarized epithelial cells. Trends Cell Biol. 2005;15(4):222-8.
37. Nishimura N, Plutner H, Hahn K, Balch WE. The delta subunit of AP-3 is required for efficient transport of VSV-G from the trans-Golgi network to the cell surface. Proceedings of the National Academy of Sciences of the United States of America. 2002;99(10):6755-60. Epub 2002/05/09.
38. Simmen T, Honing S, Icking A, Tikkanen R, Hunziker W. AP-4 binds basolateral signals and participates in basolateral sorting in epithelial MDCK cells. Nature cell biology. 2002;4(2):154-9. Epub 2002/01/22.

39. Bonifacino JS, Lippincott-Schwartz J. Coat proteins: shaping membrane transport. Nature reviews Molecular cell biology. 2003;4(5):409-14. Epub 2003/05/03.
40. Deborde S, Perret E, Gravotta D, Deora A, Salvarezza S, Schreiner R, et al. Clathrin is a key regulator of basolateral polarity. Nature. 2008;452(7188):719-23. Epub 2008/04/11.
41. Maeda Y, Beznoussenko GV, Van Lint J, Mironov AA, Malhotra V. Recruitment of protein kinase D to the trans-Golgi network via the first cysteine-rich domain. The EMBO journal. 2001;20(21):5982-90. Epub 2001/11/02.
42. Baron CL, Malhotra V. Role of diacylglycerol in PKD recruitment to the TGN and protein transport to the plasma membrane. Science. 2002;295(5553):325-8. Epub 2001/12/01.
43. Yeaman C, Ayala MI, Wright JR, Bard F, Bossard C, Ang A, et al. Protein kinase D regulates basolateral membrane protein exit from trans-Golgi network. Nature cell biology. 2004;6(2):106-12. Epub 2004/01/27.
44. Tuschl T, Zamore PD, Lehmann R, Bartel DP, Sharp PA. Targeted mRNA degradation by double-stranded RNA in vitro. Genes & development. 1999;13(24):3191-7.
45. Hannon GJ. RNA interference. Nature. 2002;418(6894):244-51.
46. Hamilton AJ, Baulcombe DC. A species of small antisense RNA in posttranscriptional gene silencing in plants. Science (New York, NY. 1999;286(5441):950-2.
47. Jarolim P, Shayakul C, Prabakaran D, Jiang L, Stuart-Tilley A, Rubin HL, et al. Autosomal dominant distal renal tubular acidosis is associated in three families with heterozygosity for the R589H mutation in the AE1 (band 3) Cl-/HCO3- exchanger. J Biol Chem. 1998;273(11):6380-8.
48. Bard F, Malhotra V. The formation of TGN-to-plasma-membrane transport carriers. Annual review of cell and developmental biology. 2006;22:439-55. Epub 2006/07/11.
49. Cheidde L, Vieira TC, Lima PR, Saad ST, Heilberg IP. A novel mutation in the anion exchanger 1 gene is associated with familial distal renal tubular acidosis and nephrocalcinosis. Pediatrics. 2003;112(6 Pt 1):1361-7. Epub 2003/12/05.
50. Folsch H, Ohno H, Bonifacino JS, Mellman I. A novel clathrin adaptor complex mediates basolateral targeting in polarized epithelial cells. Cell. 1999;99(2):189-98. Epub 1999/10/27.
51. Zhang Y, Hancock WO. The two motor domains of KIF3A/B coordinate for processive motility and move at different speeds. Biophysical journal. 2004;87(3):1795-804. Epub 2004/09/04.
52. Duangtum N, Junking M, Sawasdee N, Cheunsuchon B, Limjindaporn T, Yenchitsomanus PT. Human kidney anion exchanger 1 interacts with kinesin family member 3B (KIF3B). Biochemical and biophysical research communications. 2011;413(1):69-74. Epub 2011/08/30.

OUTPUT

1. ผลงานตีพิมพ์ในวารสารวิชาการนานาชาติ
   1.1 Sawasdee N[±], Junking M[±], Ngaojanlar P, Sukomon N, Ungsupavate D, Limjindaporn T, Akkarapatumwong V, Noisakran S, Yenchitsomanus PT. *Human kidney anion exchanger 1 interacts with adaptor-related protein complex 1 m1A (AP-1 mu1A).* Biochemical and Biophysical Research Communications **2010**; 401: 85-91. [±]These two authors contributed equally.
   1.2 Duangtum N[±], Junking M[±], Sawasdee N, Cheunsuchon B, Limjindaporn T, Yenchitsomanus PT. *Human kidney anion exchanger 1 interacts with kinesin family member 3B (KIF3B).* Biochemical and Biophysical Research Communications **2011**; 413: 69-74. [±]These two authors contributed equally.
2. ผลงานที่อยู่ในระหว่างการเตรียม manuscript เพื่อตีพิมพ์ในวารสารวิชาการนานาชาติ
   2.1 Mutita Junking[a], Nunghathai Sawasdee[a], Duangporn Ungsupravate[a], Natapol Duangtum[b], Boonyarit Cheunsuchon[c], Thawornchai Limjindaporn[d], Pa-thai Yenchitsomanus[a]. *Molecular mechanisms of human kidney anion exchanger 1 (kAE1) sorting in kidney cells.* คาดว่าจะตีพิมพ์ในวารสาร PLoS Biology (IF2011=11.452)
3. การนำผลงานวิจัยไปใช้ประโยชน์เชิงวิชาการ (มีการพัฒนาการเรียนการสอน/สร้างนักวิจัยใหม่)
   3.1 งานบางส่วนที่ได้รับการตีพิมพ์ในข้อ 1.2 เป็นส่วนหนึ่งในวิทยานิพนธ์ระดับปริญญาโทของ นายณฐพล ดวงธรรม นักศึกษาปริญญาโท ภาควิชากายวิภาคศาสตร์ คณะแพทยศาสตร์ศิริราชพยาบาล มหาวิทยาลัยมหิดล

ภาคผนวก

Biochemical and Biophysical Research Communications 401 (2010) 85–91

Contents lists available at ScienceDirect

Biochemical and Biophysical Research Communications

journal homepage: www.elsevier.com/locate/ybbrc

Human kidney anion exchanger 1 interacts with adaptor-related protein complex 1 μ1A (AP-1 mu1A)

Nunghathai Sawasdee [a,1], Mutita Junking [a,1], Piengpaga Ngaojanlar [a,b], Nattakan Sukomon [a], Duangporn Ungsupravate [a], Thawornchai Limjindaporn [a,c], Varaporn Akkarapatumwong [d], Sansanee Noisakran [a], Pa-thai Yenchitsomanus [a,*]

[a] Division of Medical Molecular Biology and BIOTEC-Medical Biotechnology Unit, Department of Research and Development, Faculty of Medicine Siriraj Hospital, Mahidol University, Bangkok 10700, Thailand
[b] Department of Immunology and Graduate Program in Immunology, Faculty of Medicine Siriraj Hospital, Mahidol University, Bangkok 10700, Thailand
[c] Department of Anatomy, Faculty of Medicine Siriraj Hospital, Mahidol University, Bangkok 10700, Thailand
[d] Institute of Molecular Biosciences, Mahidol University at Salaya Campus, Nakorn Pathom 73170, Thailand

ARTICLE INFO

Article history:
Received 31 August 2010
Available online 15 September 2010

Keywords:
Kidney anion exchanger 1
Band 3
Adaptor-related protein complex 1 mu1A
Distal renal tubular acidosis
Protein–protein interaction
Protein trafficking

ABSTRACT

Kidney anion exchanger 1 (kAE1) mediates chloride (Cl^-) and bicarbonate (HCO_3^-) exchange at the basolateral membrane of kidney α-intercalated cells. Impaired trafficking of kAE1 leads to defect of the Cl^-/HCO_3^- exchange at the basolateral membrane and failure of proton (H^+) secretion at the apical membrane, causing a kidney disease – distal renal tubular acidosis (dRTA). To gain a better insight into kAE1 trafficking, we searched for proteins physically interacting with the C-terminal region of kAE1 (Ct-kAE1), which contains motifs crucial for intracellular trafficking, by a yeast two-hybrid (Y2H) system. An adaptor-related protein complex 1 μ1A (AP-1 mu1A) subunit was found to interact with Ct-kAE1. The interaction between either Ct-kAE1 or full-length kAE1 and AP-1 mu1A were confirmed in human embryonic kidney (HEK) 293T by co-immunoprecipitation, affinity co-purification, co-localization, yellow fluorescent protein (YFP)-based protein fragment complementation assay (PCA) and GST pull-down assay. The interacting site for AP-1 mu1A on Ct-kAE1 was found to be Y904DEV907, a subset of YXXØ motif. Interestingly, suppression of endogenous AP-1 mu1A in HEK 293T by small interfering RNA (siRNA) decreased membrane localization of kAE1 and increased its intracellular accumulation, suggesting for the first time that AP-1 mu1A is involved in the kAE1 trafficking of kidney α-intercalated cells.

1. Introduction

Human anion exchanger 1 (AE1 or band 3), encoded by *solute carrier family 4, anion exchanger, member 1 (SLC4A1)* gene, is a plasma membrane transporter functioning in Cl^-/HCO_3^- exchange to regulate intracellular pH and acid–base homeostasis in the human [1]. Two AE1 isoforms, erythroid AE1 (eAE1) and kidney AE1 (kAE1), have been characterized [2]. eAE1 is a major protein on red cell membrane, functioning in both electroneutral anion (Cl^-/HCO_3^-) exchange and cytoskeletal anchorage. It contains 911 amino acids which organize into three structurally and functionally distinct domains: a cytoskeleton-associated amino-terminal domain, a central anion-transporting transmembrane segment, and short cytoplasmic carboxyl-terminal domain [3]. kAE1, which lacks the first 65 amino acids, is expressed at the basolateral membrane of acid-secreting α-intercalated cells of kidney and mediates Cl^-/HCO_3^- transport across the basolateral membrane to balance H^+ secretion across the apical surface into urine [4].

Failure of either acid excretion or bicarbonate reabsorption due to mutations in the gene encoding H^+-ATPase or kAE1, respectively, leads to distal renal tubular acidosis (dRTA), a kidney disorder characterized by an inability to acidify urine resulting in systemic metabolic acidosis and several clinical manifestations such as muscle weakness, failure to thrive, hypokalemia, hypercalciuria, hypocitraturia, and nephrolithiasis or nephrocalcinosis [5]. Genetic studies revealed two modes of inheritance of dRTA attributable to *SLC4A1* mutations: autosomal dominant (AD) and autosomal recessive (AR) dRTA [6], in which molecular mechanisms have been unveiled. The *SLC4A1* mutations causing both forms of dRTA generate mutant kAE1 that almost maintains functional anion-exchange activity but exhibits basolateral trafficking defect and intracellular retention in human embryonic kidney 293 (HEK 293) [7–10] cells and several mutations showed either intracellular retention or apical mis-targeting of kAE1 in polarized Madin–Darby canine kidney (MDCK) cells [11–13].

* Corresponding author. Fax: +66 2 4184793.
E-mail address: grpye@mahidol.ac.th (P.-t. Yenchitsomanus).
[1] These two authors contributed equally.

0006-291X/$ - see front matter © 2010 Elsevier Inc. All rights reserved.
doi:10.1016/j.bbrc.2010.09.015

The involvement of the C-terminal portion of kAE1 in proper basolateral trafficking was reported [13,14]. A 20-bp deletion in exon 20 of *SLC4A1* leading to a mutation that changes alanine to leucine (A > L) at position 888 and a premature termination codon at position 889 (A888L + 889X), which truncates the protein by 23 amino acids, was identified in two affected brothers with dRTA [15]. R901X (band3 Walton) mutation, a deletion of the last 11 amino acids of AE1, was found to be associated with dominant dRTA in two affected brothers of one family [11,13,16]. Furthermore, tyrosine residue at position 904 (Tyr904) is critical for polarized transport of kAE1 as Y904A or Y904A + V907A mutation caused non-polarized distribution of kAE1 in polarized MDCK cells [11,13]. Removal of the last five amino acids was sufficient to retard kAE1 trafficking in HEK 293 and LLC-PK1 cells [17]. Despite many pieces of evidence suggesting that C-terminal portion of kAE1 is involved in basolateral membrane trafficking, very little information is known for proteins that physically interact with the C-terminal tail of kAE1 [18]. We reported here that kAE1 interacts with AP-1 mu1A, a subunit of AP-1A adaptor complex, in a yeast two-hybrid screening. The interaction was further confirmed by co-immunoprecipitation, affinity co-purification, immunofluorescence staining, protein fragmentation complementation assay (PCA) [19], and GST pull-down assay . The effect of AP-1 mu1A suppression by RNA interference on kAE1 trafficking in HEK 293T cells was also identified.

2. Materials and methods

2.1. Plasmid construction

pcDNA3-kAE1 (a kind gift from Professor Reinhart Reithmeier, University of Toronto, Canada) containing full-length kAE1 cDNA was used as a template for amplification of a sequence consisting of 108 bp encoding the C-terminal 36 amino acids of AE1 (Ct-kAE1). The *EcoR*I/*Sal*I-digested Ct-kAE1 was subsequently inserted in-frame into pGBKT7 plasmid (Clontech) to generate a bait construct (pGBKT7-Ct-kAE1) expressing a fusion of GAL4-DNA binding domain and Ct-kAE1 in a yeast two-hybrid system. The details of plasmid construction for co-immunoprecipitation, affinity co-purification, double immunofluorescence staining, yellow fluorescent protein (YFP)-based protein fragment complementation assay (PCA), GST pull-down assay, and immunofluorescence staining and flow cytometry were described in the Supplementary material.

2.2. Yeast two-hybrid screening

To generate the bait strain, pGBKT7-Ct-kAE1 was transformed into the yeast AH109 strain. The bait construct was tested for correct protein expression prior to library screening. No intrinsic transcriptional activity of the bait construct was observed as measured in an autoactivation test by growing on synthetic dropout (SD)/-His-Ade medium supplemented with X-α-gal. The prey strain, Y187, pre-transformed with the prey plasmids, pACT2, which carried the GAL4-activation domain fused to fragments from a human kidney cDNA library. The yeast two-hybrid screen was performed according to the manufacturer's protocol (Clontech). Mated diploids whose cDNA-encoded products interacted with the bait protein were selected by growth on SD/-Trp-Leu-His-Ade plates and SD/-Trp-Leu-His-Ade plates supplemented with X-α-gal (Clontech) to assay for activation of reporter genes [*HIS3, ADE2, MEL1* (α-galactosidase)]. The positive colonies with strong reporter activities were selected. The prey plasmids rescued from positive colonies were transformed into *E. coli* for PCR amplification. The *Alu*I restriction patterns of PCR products were generated and the representatives from different restriction patterns were chosen for the specificity tests. Specific interactions between the bait protein and the encoded products of isolated preys were tested by re-transforming the prey plasmid into the yeast strain AH109 and then re-mated with the opposite mating strain Y187 harboring either the bait plasmid (Ct-kAE1), empty vector, or two other plasmids containing unrelated genes (p53 and laminC). The cDNA fragments of the positive clones from the specificity tests were sequenced and aligned with the database (http://www.ncbi.nlm.nih.gov) in order to obtain full-length cDNA sequences that were completely matched with the in-put sequences.

2.3. Cell culture and transfection

HEK 293T cells were maintained in complete Dulbecco's Modified Eagle Medium (DMEM, Gibco) supplemented with 10% fetal bovine serum (Perbio), 100 units/ml penicillin and 100 μg/ml streptomycin at 37 °C with 5% CO_2. Two days before transfection, the HEK 293T cells were collected and seeded in six-well plates. The cultured cells were transfected with pcDNA3.1 vector or its derivative constructs according to the designed experiments by DEAE-dextran method as previously described [20] or by Lipofectamine transfection method following the manufacture's protocol (Invitrogen). After transfection for 2 days, the cells were collected for further analyses.

2.4. Co-immunoprecipitation and affinity co-purification

Two days post-transfection, the HEK 293T cells were lyzed in lysis buffer containing protease inhibitor cocktail (Roche). Co-immunoprecipitation and affinity co-purification using Co^{2+}-chelated resins (BD Biosciences) were performed as described in our previous study [20].

2.5. Double immunofluorescence staining

HEK 293T cells were grown on coverslips for 1 day, transfected or co-transfected with plasmid constructs using Lipofectamine 2000 (Invitrogen), and cultured for another 2 days. The immunofluorescence staining was performed using rabbit anti-Ct-kAE1, mouse anti-Myc, mouse anti-AP-1 mu1A (Abnova), rabbit anti-calregulin (Santa Cruz) or rabbit anti-TGN46 (Abcam), followed by donkey anti-rabbit IgG conjugated with Cy3 fluoresceine (Jackson Immunoresearch Laboratories) and goat anti-mouse IgG conjugated with Alexa 488 fluoresceine (Molecular Probes) by protocol which was described in our previous study [20].

2.6. Yellow fluorescent protein (YFP)-based protein fragment complementation assay (PCA)

Two days before transfection, the HEK 293T cells were collected and seeded in six-well plates. The cultured cells were individually transfected with 1 μg each of the YFP construct or co-transfected with different pairs of the constructs. Two days after transfection, the cells were fixed in 3% formaldehyde, permeabilized with 0.1% Triton X-100 and blocked with 1% BSA. The coverslips were washed and mounted with Fluorosave. Cell fluorescence images were observed by using a laser scanning confocal Zeiss LSM 510 microscope (Carl Zeiss).

2.7. GST pull-down assay

The pGEX4T-2-GST, pGEX4T-2-GST-Ct-kAE1 and pGEX4T-2-GST-Ct-kAE1 mutants were transformed into *E. coli* BL21 (DE3). The pTrcHisA-AP-1 mu1A were transformed into *E. coli* DH5α. The bacterial cells were grown in Luria broth to express the recombinant proteins. The bacterial cells were lyzed in lysis buffer. The

GST or GST-fusion proteins were conjugated with Glutathione-Sepharose 4B beads (Amersham) then incubated with His-tagged AP-1 mu1A soluble lysate. The unbound proteins were eliminated by serial washing: once with PBS containing 0.1% Triton X-100, 20 mM EDTA, once with PBS containing 0.1% Triton X-100, 10 mM EDTA, and once with PBS. The binding protein complexes were eluted and subjected to analysis by Western blotting using mouse anti-His antibody (Amersham) and rabbit anti-mouse IgG-HRP conjugate (Santa Cruz). Chemiluminescent signals generated by SuperSignal West Pico Chemiluminescent Substrate (Thermo Scientific) were detected by exposure to an X-ray film.

2.8. RNA interference

Small interfering RNA (siRNA) directed against mu1A subunit of AP-1 (siAP-1 mu1A) has previously been described [21]; its sequence was 5′-TCCGAAGGCATCAAGTATCGGAAGA-3′ (Invitrogen). Transfection of either siAP-1 mu1A or siControl was performed using Lipofectamine 2000 (Invitrogen). The efficiency of AP-1 mu1A knockdown by siRNA was examined by real time RT-PCR and Western blotting (see details in Supplementary material). HEK 293T cells were seeded for 24 h before transfection. The double-stranded siRNA were transfected twice with a 24-h interval. pcDNA3.1-kAE1-HA or pcDNA3-kAE1-Myc was co-transfected with first transfection of siRNA. Cells were harvested 48 h after the second transfection for further study.

2.9. Flow cytometry

Myc epitope inserted at the third extracellular loop of kAE1 would be expressed extracellularly. Thus, expression of kAE1-Myc on the cell surface could be determined by fluorescence staining and flow cytometry. HEK 293T cells were co-transfected with the pcDNA3-kAE1-Myc and siAP-1 mu1A or siControl. Two days after transfections, the cells were collected and determined by flow cytometry as described in our previous study [20].

3. Results and discussion

Trafficking defect of kAE1 has been revealed as a potential molecular basis of dRTA caused by *SLC4A1* mutations [9,10,20,22]. However, to date, the trafficking pathway of kAE1 to cell surface have not been clearly described. In this study, we have firstly reported a novel interaction between kAE1 and AP-1 mu1A, a medium subunit of an adaptor protein complex AP-1A. The interaction of the two proteins was confirmed by *in vitro* and *in situ* studies. The interacting site for AP-1 mu1A on Ct-kAE1 was also identified by YFP-PCA and GST pull-down assay. We therefore examined whether AP-1 mu1A is necessary for kAE1 targeting to the plasma membrane by knocking down AP-1 mu1A using RNA interference.

3.1. Identification of AP-1 mu1A as a Ct-kAE1-binding protein in a yeast two-hybrid screening

To explore the molecular trafficking machineries involved in the basolateral sorting and transport of kAE1, a yeast two-hybrid screening was carried out to search for proteins that bind to the C-terminus of kAE1 (Ct-kAE1, amino-acids 876–911), which contains a putative tyrosine-based sorting signal Y904DEV907. A bait construct, pGBKT7-Ct-kAE1, was used to screen a human kidney cDNA library. One plasmid contained a partial cDNA sequence encoded C-terminal fragment of AP-1 mu1A (amino acids 306–423, Fig. 1A). It is interesting that this region is a part of the AP-1 mu1A segment which reported to directly interact with tyrosine-based sorting signals present in cargo proteins [22]. The prey plasmid containing partial AP-1 mu1A cDNA sequence isolated from the initial screen was re-transformed for re-mating. Mated diploid cells were cultured on SD/-Trp-Leu-His-Ade and SD/-Trp-Leu-His-Ade/X-α-Gal plates as shown in Fig. 1B. Only the diploid cells with both plasmids containing Ct-kAE1 and AP-1 mu1A cDNA sequences activated the expression of reporter genes; hence, they grew and turned blue on plates, respectively.

3.2. kAE1 interacted with AP-1 mu1A in HEK 293T cells as detected by co-immunoprecipitation and affinity co-purification

To establish whether kAE1 interacts with AP-1 mu1A in mammalian cells, full-length kAE1 and AP-1 mu1A cDNA sequences were sub-cloned into mammalian expression vectors and transfected or co-transfected into HEK 293T cells. Fig. 2A shows co-immunoprecipitation of kAE1 with His-AP-1 mu1A by using anti-His antibody; the co-immunoprecipitated kAE1 could be detected by Western blot using anti-Ct-kAE1 antibody (lane 3). Similarly, in the affinity co-purification assay using Co^{2+} column (Fig. 2B), kAE1 was co-purified with His-AP-1 mu1A, which was detected using anti-Ct-kAE1 antibody (lane 3). Lanes 1, 2, and 5 in both figures were lysate inputs.

3.3. Subcellular localization of kAE1 and AP-1 mu1A in HEK 293T cells

Subcellular localization of kAE1 and AP-1 mu1A in HEK 293T cells was investigated by double immunofluorescence staining and confocal microscopy. kAE1-HA and His-AP-1 mu1A showed

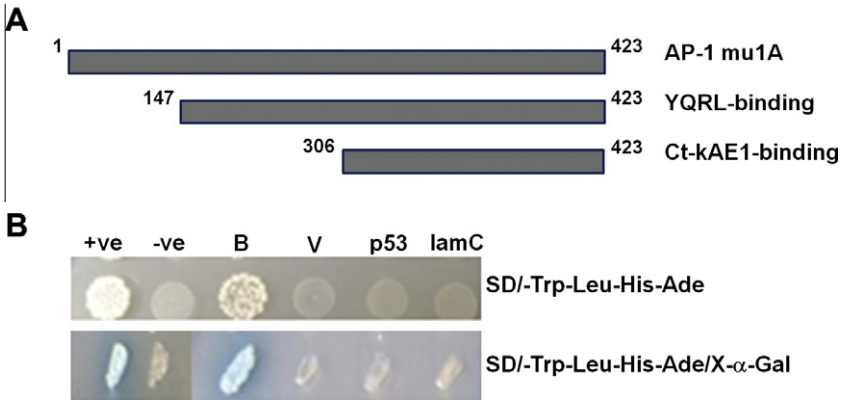

Fig. 1. Identification of AP-1 mu1A as a kAE1 interacting protein by yeast two-hybrid system. (A) Schematic diagram of the identified AP-1 mu1A fragment. (B) Specificity test of Ct-kAE1 and AP-1 mu1A interaction by growth of yeast diploids on synthetic dropout (SD)/-Trp-Leu-His-Ade medium and SD/-Trp–Leu-His-Ade/X-α-Gal agar plates.

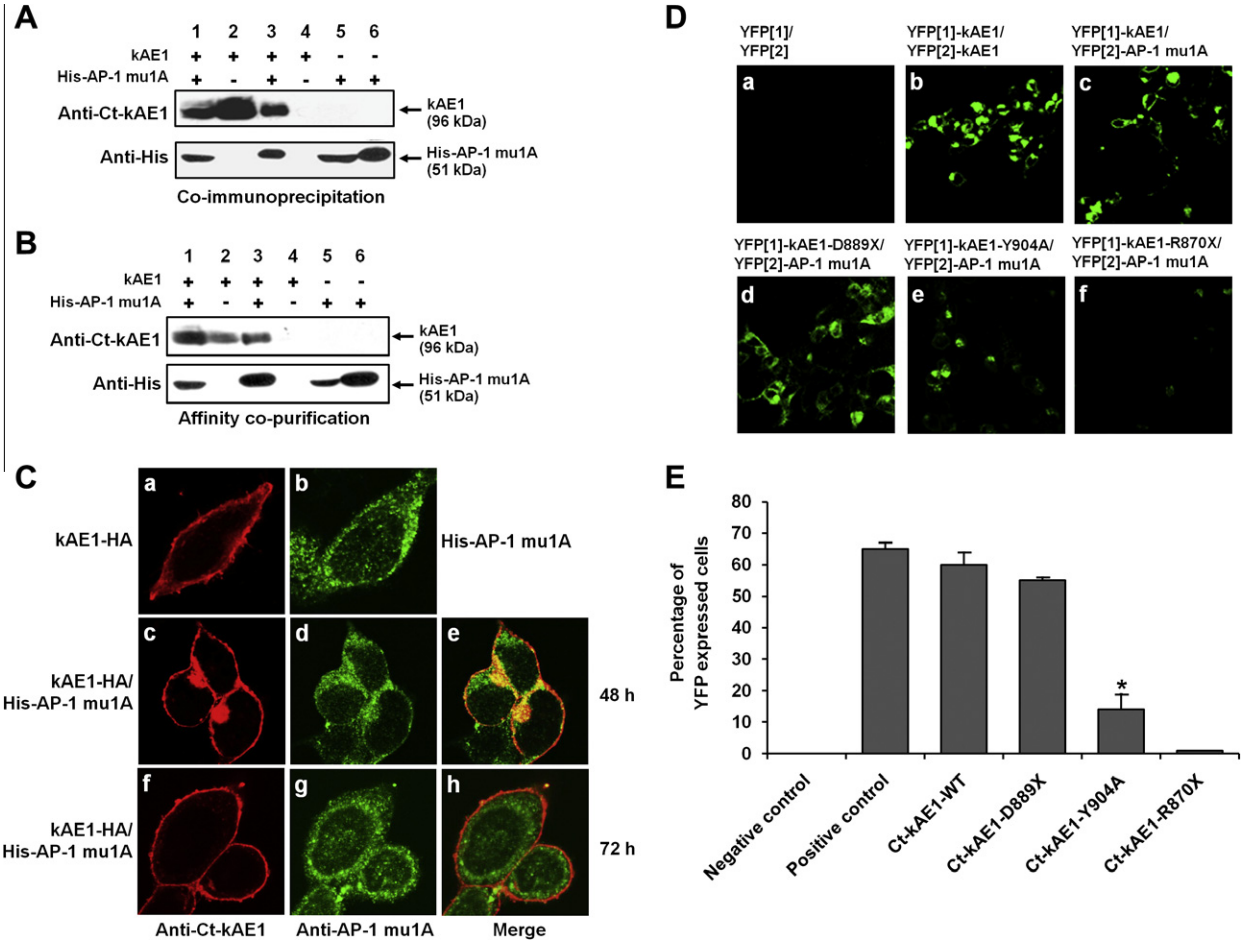

Fig. 2. Verification of kAE1 and AP-1 mu1A interaction by co-immunoprecipiation and co-purification assays and cellular localization of kAE1 and AP1-mu1A. (A) Co-immunoprecipitation of kAE1 and AP-1 mu1A expressed in HEK 293T cells. (B) Affinity co-purification of kAE1 and AP-1 mu1A expressed in HEK 293T cells. (C) Cellular localization of kAE1 and AP1-mu1A. kAE1-HA and His-AP-1 mu1A was individually transfected (a and b, respectively). kAE1-HA and His-AP-1 mu1A were co-transfected HEK 293T cells at 48 h (c–e) and 72 h (f–h). (D) Investigation of *in situ* interaction between kAE1 and AP-1 mu1A expressed in HEK 293T cells by YFP-PCA. (E) Percentage of YFP-expressed cells obtained from (D).

differential localization in the transfected HEK 293T cells in both individually (Fig. 2C(a, b)) or co-transfected to express kAE1-HA and His-AP-1 mu1A (Fig. 2C(c–h)). While His-AP-1 mu1A dispersed throughout the cytoplasm (Fig. 2C(b, d, g)), kAE1-HA showed dynamic distribution. After transfection for 48 h, kAE1-HA might saturate the sorting pathway (Fig. 2C(c)), which was co-stained with

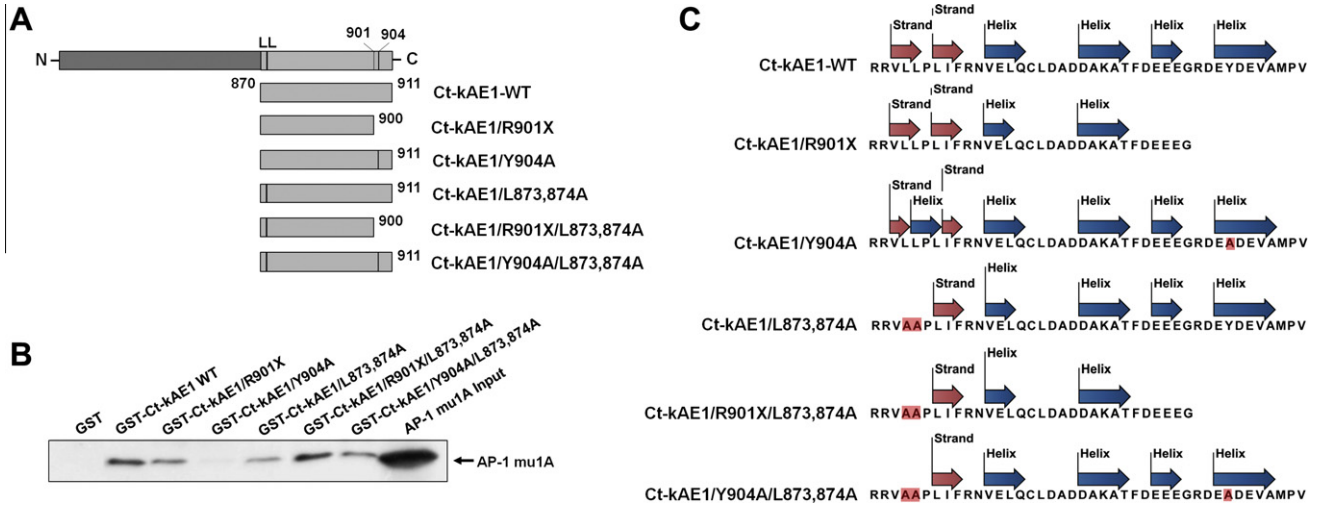

Fig. 3. (A) Illustrations of the carboxyl terminus of kAE1 (Ct-kAE1). Different GST-Ct-kAE1-mutants were generated from GST-Ct-kAE1-WT. (B) GST pull-down binding assay. (C) Prediction of secondary structures of Ct-kAE1-WT and Ct-kAE1-mutants by using CLC Main Workbench software.

His-AP-1 mu1A at Golgi/TGN like and partially stained at the cell membrane (Fig. 2C(e)). However, after transfection for 72 h, kAE1-HA was localized at cell membrane (Fig 2C(f–h)).

3.4. kAE1 interacted with AP-1 mu1A in HEK 293T cells as examined by yellow fluorescent protein (YFP)-based protein fragment complementation assay (PCA)

The interaction between kAE1 and AP-1 mu1A within HEK 293T cells was examined by YFP-PCA. Each of YFP fusion protein was co-expressed in HEK 293T cells and their interactions demonstrated by intracellular green-fluorescent signals. Percentage of YFP-expressed cells was calculated from the number of YFP-expressed cells against the number of nuclear-stained cells by using Hoechst 33258. HEK 293T cells were co-transfected to express YFP[1] and YFP[2] as a negative control (Fig. 2D(a)) and co-transfected to express YFP[1]-kAE1 and YFP[2]-kAE1 as a positive control whose dimerization of kAE1 fusion proteins resulted in YFP[1] and YFP[2] complementation (Fig. 2D(b)) showing intracellular green-fluorescent signals for >60% of the cell population (Fig. 2E). Similarly, when they were co-transfected to express either YFP[1]-kAE1 and YFP[2]-AP-1 mu1A (Fig. 2D(c)) or YFP[1]-kAE1-R889X and YFP[2]-AP-1 mu1A (Fig. 2D(d)), intracellular green-fluorescent signals were captured at >50% of the cell population (Fig. 2E). However, co-expression of YFP[1]-kAE1-Y904A with YFP[2]-AP-1 mu1A showed a reduction in intracellular green-fluorescent signals (Fig. 2D(e)) to be <20% of the cell population (Fig. 2E). Interaction of YFP[1]-kAE1-R870X which lacked C-terminus, and YFP[2]-AP-1 mu1A did not show intracellular green-fluorescent signals (Fig. 2D-f, and E)). It is surprising that deletion of in the YDEV motif did not totally diminish the interaction between kAE1 and AP-1 mu1A but it did for the whole Ct-kAE1 deletion as shown by the result of R870X mutant. These results indicate that although Tyr904 in the YDEV motif is critical for the interaction, the dileucine (Leu873Leu874) motif in Ct-kAE1 might also be used for the interaction.

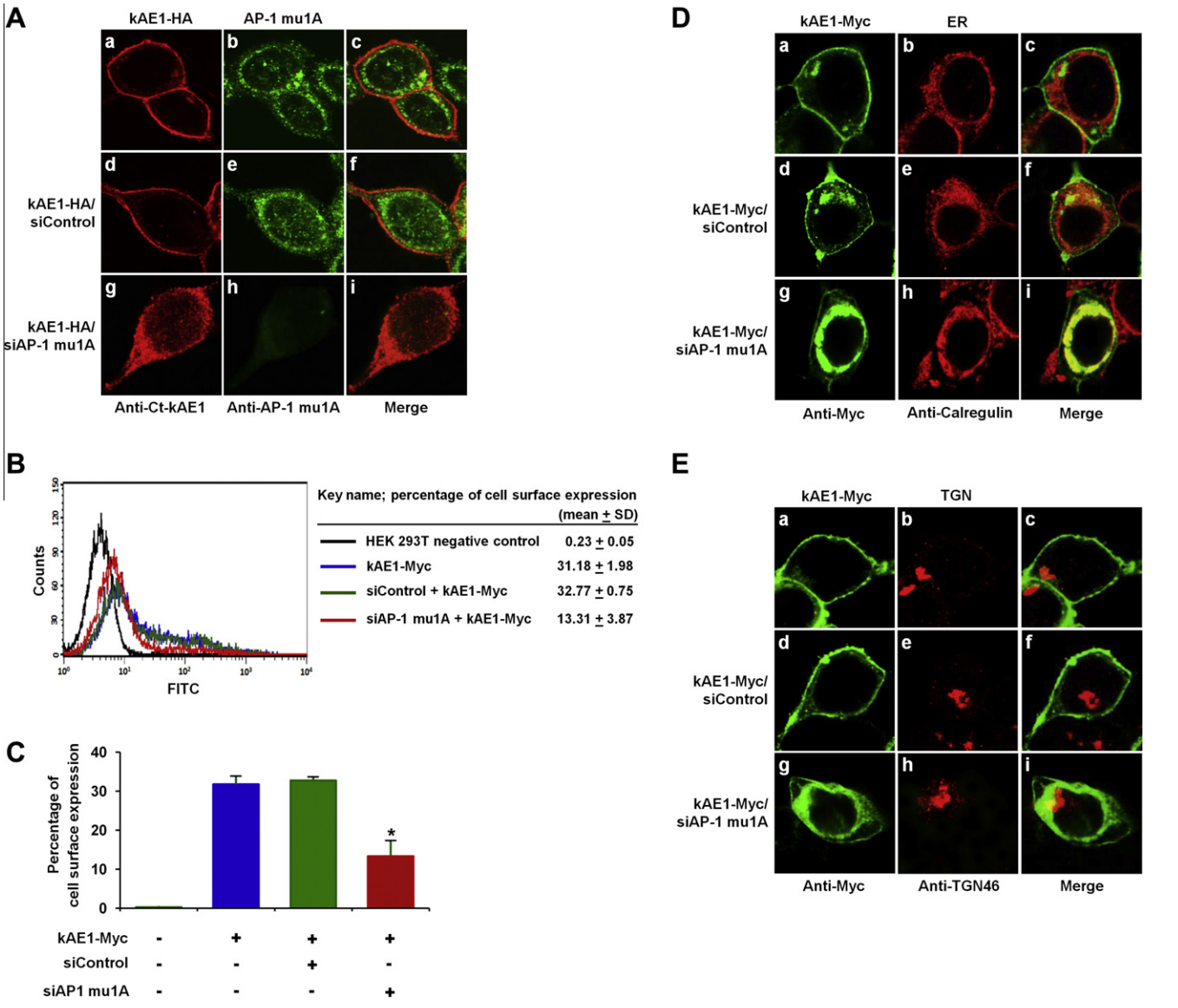

Fig. 4. Subcellular localization of kAE1 and AP-1 mu1A in HEK 293T cells. (A) HEK 293T cells were transfected to express kAE1-HA (a–c) or co-transfected with siControl (d–f) or with siAP-1 mu1A (g–i). (B) Cell-surface expression of kAE1-Myc in transfected HEK 293T cells measured by flow cytometry. Percentages of cell-surface expression of kAE1-Myc (mean ± SD) in different conditions are also indicated. (C) The bar graph showing percentages of cell-surface expression of kAE1-Myc. (D) Localizations of kAE1 and ER marker or (D) TGN marker in HEK 293T cells with suppression of AP-1 mu1A by siRNA.

3.5. Ct-kAE1 interacted with AP-1 mu1A in GST pull-down assay

To identify specific interaction site of AP-1 mu1A on Ct-kAE1, we conducted a series of GST pull-down assay using Ct-kAE1 containing individual or combinations of truncated and point mutations (Fig. 3A). His-tagged AP-1 mu1A protein was incubated with GST-Ct-kAE1-WT or GST-Ct-kAE1-mutants. All GST-Ct-kAE1-mutants could pull down His-AP-1 mu1A (Fig. 3B, lanes 3–7). However, a very faint band was observed in the binding between GST-Ct-kAE1/Y904A and His-AP-1 mu1A (Fig. 3B, lane 4). This has prompted us to suspect that there might be another potential binding motif on Ct-kAE1 that interacts with AP-1 mu1A. Therefore, we introduced a combination of deletion of the YDEV motif and substitution at the dileucine motif (Fig. 3B, lane 6) or substitutions at both Tyr904 and dileucine motif (Fig. 3B, lane 7) to Ct-kAE1, the binding to AP-1 mu1A still occurred. We then used CLC Main Workbench software (CLC bio) to predict secondary structures of Ct-kAE1-WT and Ct-kAE1-mutants. The prediction showed that Ct-kAE1-WT consists of four helices and two upstream strands (Fig. 3C). It is interesting that in substitution of tyrosine (Y) by alanine (A) at the position 904 in the YDEV motif affected the predicted secondary structure by the presence of a helix between those two upstream strands, where dileucine residues (Leu873-Leu874) and dileucine-like residues (Leu876Ile877) were located (Fig. 3C). However, this dileucine-like motif might not be affected in other Ct-kAE1-mutants. Taken together, the YDEV motif is most likely a primary interaction site of AP-1 mu1A and either dileucine residues (Leu873Leu874) or dileucine-like residues (Leu876Ile877) may also play roles. However, the role of this dileucine-like motif in binding to AP-1 mu1A needed further investigation.

3.6. Suppression of endogenous AP-1 mu1A reduced membranous kAE1 and accumulated kAE1 in the ER of HEK 293T cells

To address the functional significance of AP-1 mu1A in kAE1 trafficking, we employed siRNA-knockdown to suppress endogenous AP-1 mu1A in HEK 293T cells and examined subcellular localization of kAE1. The efficiency of siRNA was determined by real-time PCR and Western blotting (Supplementary Fig. 1).

HEK 293T cells were co-transfected with kAE1-HA and siControl or kAE1-HA and siAP-1 mu1A. Subcellular localization of kAE1 and AP-1 mu1A was examined by immunofluorescence staining using anti-Ct-kAE1 and anti AP-1 mu1A, respectively. The results showed that without AP-1 mu1A suppression, kAE1-HA was mainly located at the cell surface (Fig. 4A(a–f)) but with AP-1 mu1A suppression, kAE1-HA was accumulated in the cytoplasm (Fig. 4A(g–i)).

To quantitatively measure kAE1 expression at the cell surface, we transfected the plasmid construct to express kAE1 containing Myc epitope at the position 557 in the third extracellular loop of kAE1 to allow immunological detection at the surface of intact cells by flow cytometry. The HEK 293T cells individually expressing kAE1-Myc or co-expressing kAE1-Myc with siControl transfection had mean fluorescence intensities of 31.18 ± 1.98% and 32.77 ± 0.75%, respectively (Fig. 4B and C). However, HEK 293T cells with suppression of AP-1 mu1A showed lower levels of kAE1-Myc on the cell surface (13.31 ± 3.87%) than those of the control cells (Fig. 4B and C). The incomplete reduction of cell-surface expression of kAE1 is possibly attributable to the incomplete AP-1 mu1A knockdown. However, this confirms the result of the immunofluorescence staining in the AP-1 mu1A suppressed cells.

To address the location of kAE1-Myc with respect to intracellular organelles when AP-1 mu1A was suppressed, we co-transfected to express kAE1-Myc with siAP-1 and stained the cells with antibodies specific to cellular organelle markers, calregulin for ER and TGN46 for trans-Golgi network (TGN). In the parental and siControl cells, kAE1-Myc was predominantly expressed at the cell membrane (Fig. 4D(a–f) and E(a–f)). In the cells with AP-1 mu1A suppression by siRNA, kAE1-Myc was heavily accumulated in the cytoplasm with calregulin in ER (Fig. 4D(g–i)) but slightly co-localized with TGN46 in TGN (Fig 4E(g–i)). Thus, it is likely that the interaction between kAE1 and AP-1 mu1A normally occurs in Golgi/TGN-like compartment. However, when AP-1 mu1A is suppressed, kAE1 fails to exit from ER resulting in its accumulation in this cellular organelle.

4. Conclusion

We firstly identified and characterized the interaction between human kAE1 and AP-1 mu1A and suggested the amino acid motifs in Ct-kAE1 that are essential for this interaction. A critical role for AP-1 mu1A in kAE1 trafficking to the plasma membrane showed a marked reduction of kAE1 on the membrane and its accumulation in the cytoplasm, particularly in ER. Further studies will be toward the exploration of the role of AP-1 mu1A in kAE1 trafficking to basolateral membrane in polarized cells. The insight into the molecular mechanisms overriding the trafficking of kAE1 to the basolateral membrane will provide a better understanding of the molecular defect of dRTA associated with *SLC4A1* mutations.

Acknowledgments

M.J. is supported by post-doctoral fellowship grant from Thailand Research Fund (TRF). P.N. was supported by the Thailand Graduate Institute of Science and Technology (TGIST) Scholarship from the National Science and Technology Development Agent (NSTDA), and by the Graduate Thesis Scholarship from the Faculty of Medicine Siriraj Hospital, Mahidol University. Dr. Wanna Thongnoppakhun is thanked for assisting in AP-1 mu1A cDNA isolation and Dr. Siraprapha Sanchatjate for helping in a part of manuscript preparation. PY is supported by Charoemprakiat Grant, Faculty of Medicine Siriraj Hospital, and Senior Research Scholar Grant, Thailand Research Fund (TRF) and Commission of Higher Education (CHE).

Appendix A. Supplementary data

Supplementary data associated with this article can be found, in the online version, at doi:10.1016/j.bbrc.2010.09.015.

References

[1] M.J. Godinich, M.L. Jennings, Renal chloride-bicarbonate exchangers, Curr. Opin. Nephrol. Hypertens. 4 (1995) 398–401.
[2] P. Yenchitsomanus, N. Sawasdee, A. Paemanee, et al., Anion exchanger 1 mutations associated with distal renal tubular acidosis in the Thai population, J. Hum. Genet. 48 (2003) 451–456.
[3] M.J. Tanner, The structure and function of band 3 (AE1): Recent developments (review), Mol. Membr. Biol. 14 (1997) 155–165.
[4] A. Kollert-Jons, S. Wagner, S. Hubner, et al., Anion exchanger 1 in human kidney and oncocytoma differs from erythroid AE1 in its NH2 terminus, Am. J. Physiol. 265 (1993) F813–821.
[5] S.L. Alper, Genetic diseases of acid–base transporters, Annu. Rev. Physiol. 64 (2002) 899–923.
[6] P. Yenchitsomanus, S. Kittanakom, N. Rungroj, et al., Molecular mechanisms of autosomal dominant and recessive distal renal tubular acidosis caused by SLC4A1 (AE1) mutations, J. Mol. Genet. Med. 1 (2005) 49–62.
[7] J.A. Quilty, E. Cordat, R.A. Reithmeier, Impaired trafficking of human kidney anion exchanger (kAE1) caused by hetero-oligomer formation with a truncated mutant associated with distal renal tubular acidosis, Biochem. J. 368 (2002) 895–903.
[8] S. Kittanakom, E. Cordat, V. Akkarapatumwong, et al., Trafficking defects of a novel autosomal recessive distal renal tubular acidosis mutant (S773P) of the human kidney anion exchanger (kAE1), J. Biol. Chem. 279 (2004) 40960–40971.
[9] J.A. Quilty, J. Li, R.A. Reithmeier, Impaired trafficking of distal renal tubular acidosis mutants of the human kidney anion exchanger kAE1, Am. J. Physiol. Renal. Physiol. 282 (2002) F810–820.

[10] A.M. Toye, L.J. Bruce, R.J. Unwin, et al., Band 3 Walton, a C-terminal deletion associated with distal renal tubular acidosis, is expressed in the red cell membrane but retained internally in kidney cells, Blood 99 (2002) 342–347.
[11] M.A. Devonald, A.N. Smith, J.P. Poon, et al., Non-polarized targeting of AE1 causes autosomal dominant distal renal tubular acidosis, Nat. Genet. 33 (2003) 125–127.
[12] N. Rungroj, M.A. Devonald, A.W. Cuthbert, et al., A novel missense mutation in AE1 causing autosomal dominant distal renal tubular acidosis retains normal transport function but is mistargeted in polarized epithelial cells, J. Biol. Chem. 279 (2004) 13833–13838.
[13] A.M. Toye, G. Banting, M.J. Tanner, Regions of human kidney anion exchanger 1 (kAE1) required for basolateral targeting of kAE1 in polarised kidney cells: mis-targeting explains dominant renal tubular acidosis (dRTA), J. Cell. Sci. 117 (2004) 1399–1410.
[14] A.M. Toye, Defective kidney anion-exchanger 1 (AE1, Band 3) trafficking in dominant distal renal tubular acidosis (dRTA), Biochem. Soc. Symp. (2005) 47–63.
[15] L. Cheidde, T.C. Vieira, P.R. Lima, et al., A novel mutation in the anion exchanger 1 gene is associated with familial distal renal tubular acidosis and nephrocalcinosis, Pediatrics 112 (2003) 1361–1367.
[16] F.E. Karet, F.J. Gainza, A.Z. Gyory, et al., Mutations in the chloride-bicarbonate exchanger gene AE1 cause autosomal dominant but not autosomal recessive distal renal tubular acidosis, Proc. Natl. Acad. Sci. USA 95 (1998) 6337–6342.
[17] E. Cordat, J. Li, R.A. Reithmeier, Carboxyl-terminal truncations of human anion exchanger impair its trafficking to the plasma membrane, Traffic 4 (2003) 642–651.
[18] M.J. Tanner, Band 3 anion exchanger and its involvement in erythrocyte and kidney disorders, Curr. Opin. Hematol. 9 (2002) 133–139.
[19] S.W. Michnick, I. Remy, F.X. Campbell-Valois, et al., Detection of protein-protein interactions by protein fragment complementation strategies, Methods Enzymol. 328 (2000) 208–230.
[20] N. Sawasdee, W. Udomchaiprasertkul, S. Noisakran, et al., Trafficking defect of mutant kidney anion exchanger 1 (kAE1) proteins associated with distal renal tubular acidosis and Southeast Asian ovalocytosis, Biochem. Biophys. Res. Commun. 350 (2006) 723–730.
[21] J. Hirst, A. Motley, K. Harasaki, et al., EpsinR: an ENTH domain-containing protein that interacts with AP-1, Mol. Biol. Cell. 14 (2003) 625–641.
[22] R.C. Aguilar, H. Ohno, K.W. Roche, et al., Functional domain mapping of the clathrin-associated adaptor medium chains mu1 and mu2, J. Biol. Chem. 272 (1997) 27160–27166.

Biochemical and Biophysical Research Communications 413 (2011) 69–74

Contents lists available at SciVerse ScienceDirect

Biochemical and Biophysical Research Communications

journal homepage: www.elsevier.com/locate/ybbrc

Human kidney anion exchanger 1 interacts with kinesin family member 3B (KIF3B)

Natapol Duangtum [a,b,1], Mutita Junking [a,1], Nunghathai Sawasdee [a], Boonyarit Cheunsuchon [c], Thawornchai Limjindaporn [b,*], Pa-thai Yenchitsomanus [a,*]

[a] Medical Molecular Biology Unit, Office for Research and Development Faculty of Medicine Siriraj Hospital, Mahidol University, Bangkok 10700, Thailand
[b] Department of Anatomy, Faculty of Medicine Siriraj Hospital, Mahidol University, Bangkok 10700, Thailand
[c] Department of Pathology, Faculty of Medicine Siriraj Hospital, Mahidol University, Bangkok 10700, Thailand

ARTICLE INFO

Article history:
Received 10 August 2011
Available online 17 August 2011

Keywords:
Kidney anion exchanger 1 (kAE1)
Kinesin family member 3B (KIF3B)
Distal renal tubular acidosis
Protein–protein interaction
Protein trafficking

ABSTRACT

Impaired trafficking of human kidney anion exchanger 1 (kAE1) to the basolateral membrane of α-intercalated cells of the kidney collecting duct leads to the defect of the Cl^-/HCO_3^- exchange and the failure of proton (H^+) secretion at the apical membrane of these cells, causing distal renal tubular acidosis (dRTA). In the sorting process, kAE1 interacts with AP-1 mu1A, a subunit of AP-1A adaptor complex. However, it is not known whether kAE1 interacts with motor proteins in its trafficking process to the plasma membrane or not. We report here that kAE1 interacts with kinesin family member 3B (KIF3B) in kidney cells and a dileucine motif at the carboxyl terminus of kAE1 contributes to this interaction. We have also demonstrated that kAE1 co-localizes with KIF3B in human kidney tissues and the suppression of endogenous KIF3B in HEK293T cells by small interfering RNA (siRNA) decreases membrane localization of kAE1 but increases its intracellular accumulation. All results suggest that KIF3B is involved in the trafficking of kAE1 to the plasma membrane of human kidney α-intercalated cells.

1. Introduction

Human anion exchanger 1 (AE1 or band 3) is a chloride and bicarbonate exchanger (Cl^-/HCO_3^-) which is involved in maintaining acid–base homeostasis in the human body [1]. Two isoforms of AE1, erythroid AE1 (eAE1) and kidney AE1 (kAE1) are encoded by *solute carrier family 4, member 1* (*SLC4A1*) gene (MIM 109270). Transcription of eAE1 in the erythroid precursor is under the control of the erythroid-specific promoter upstream of exon 1, whereas the renal transcription arises from the distinct promoter within intron 3 of the *SLC4A1* gene [2]. Thus, the kAE1 polypeptide lacks 65 amino acids presented at the N-terminus of human eAE1 [3]. kAE1, which is the basolateral Cl^-/HCO_3^- exchanger of the acid-secreting α-intercalated cells of kidney distal tubule [4], comprises 846 amino acids and has three functionally distinct structural domains including a cytoplasmic amino-(N-) terminal domain (403 amino acids), a central transmembrane domain (497 amino acids) and a short cytoplasmic carboxyl-(C-) terminal domain (40 amino acids) [5,6].

Mutations of the *SLC4A1* gene can cause distal renal tubular acidosis (dRTA), which is characterized by the impaired H^+ secretion into urine leading to systemic metabolic acidosis. It has previously shown that dRTA is caused either by preventing the transport of mutant kAE1 to the cell surface or by mis-targeting the mutant kAE1 to the apical membrane instead of the correct basolateral membrane of the α-intercalated cells [7,8]. Deletion of either the N-terminal or C-terminal domain of kAE1 resulted in the apical mis-localization, suggesting that a determinant within the kAE1 N-terminus cooperates with the C-terminus for kAE1 basolateral localization [14]. Despite much evidence suggesting that the C-terminal portion of kAE1 is involved in basolateral membrane trafficking, very little information is known about proteins that physically interact with the C-terminal tail of kAE1 [9]. Our group is interested in identifying the protein that interacts with kAE1 and plays a role in its basolateral trafficking. We have recently reported that AP-1 mu1A, a subunit of AP-1A adaptor complex involving in sorting of the cargo proteins, interacts with the C-terminus of kAE1 [14]. However, it is not known whether or not kAE1 interacts with motor proteins, such as kinesins, which are also important in the trafficking process.

KIF3B is one of the kinesin II subfamilies of the kinesin superfamily, which consists of a large family of molecular motors that transport the intracellular cargo along the microtubules using the energy derived from hydrolysis of ATP [10]. Members of the kinesin II subfamily are plus end-directed motor proteins that are involved in the trafficking, assembly and maintenance of cilia and flagella, and in the transport of the endoplasmic reticulum to the Golgi membrane [11,12]. A heterotrimeric complex of KIF3B with KIF3A and KAP3 determines the functional diversity of the KIF3B complex. Transportation of matrix metalloproteinase (MT1-MMP) vesicles along microtubules is regulated by KIF5B and KIF3A/KIF3B kinesins.

* Corresponding authors.
E-mail addresses: limjindaporn@yahoo.com (T. Limjindaporn), grpye@mahidol.ac.th (P.-t. Yenchitsomanus).
[1] These authors contributed equally to this work.

0006-291X/$ - see front matter © 2011 Elsevier Inc. All rights reserved.
doi:10.1016/j.bbrc.2011.08.050

Results from siRNA-KIF3A/KIF3B knockdown studies revealed that transport by these kinesins is essential for transport of MT1-MMP to the cell surface of the primary human macrophage [13]. In addition, the interaction between KIF3B and chloride channel protein (CLC-5) was previously shown to facilitate the transport of CLC-5-containing vesicles to the cell surface of HEK 293 cells [14].

2. Materials and methods

2.1. Plasmid constructions

PCR-based amplification of KIF3B-HA was performed by using pcDNA3.1-KIF3B-His, which is available in our laboratory as a template and through using primers containing the hemagglutinin (HA) epitope sequences to add HA at the C-terminus of KIF3B. KIF3B-HA was cloned into *Eco*RV and *Xho*I sites of a pcDNA3.1/hygro plasmid. The clone was designated pcDNA3.1-KIF3B-HA. Plasmid pcDNA3/kAE1-Myc, containing a sequence of Myc epitope inserted at position 557 in the third extracellular loop of kAE1, was generated from pcDNA3-kAE1 by site-directed mutagenesis following the protocol of the QuickChange TM site-directed mutagenesis kit from Stratagene, USA. By DNA sequencing, the tag and insert sequences in the plasmid constructs were proved to be correct and in frame with the gene sequences.

2.2. Cell culture and transfection

Human embryonic kidney (HEK293T) cells were grown in DMEM/F-12 (Gibco) supplemented with 10% FBS (Gibco) and 1.2% penicillin/streptomycin in 6-well plates prior to transfection. Cells were transfected using Lipofectamine 2000 (Invitrogen) according to the manufacturer's instructions. Cells were processed for further studies at 48 h post-transfection.

2.3. Co-immunoprecipitation and immunoblotting

HEK293T cells were co-transfected with pcDNA3/kAE1-Myc and pcDNA3.1-KIF3B-HA constructs. Two days after transfection, the transfected cells were detached and collected by centrifugation. Cells were lysed in PBS containing 1% Triton X-100 and inhibitors cocktail (Roche). Aliquots of the cell lysates were saved and the remaining cell lysates were incubated with the mouse anti-Myc antibody followed by precipitation with Protein G-Sepharose (Thermo Scientific). The bound kAE1 protein was eluted with Laemmli buffer before separation by electrophoresis and detection by Western blot analysis using the rabbit anti-HA polyclonal antibody (Invitrogen) as the primary antibody and the swine anti-rabbit IgG-HRP (Santa Cruz) as the secondary antibody. Chemiluminescent signals generated by SuperSignal West Pico Chemiluminescent Substrate (Thermo Scientific) were detected by exposure to an X-ray film.

2.4. GST pull-down assay

The pGEX4T-2-GST, pGEX4T-2-GST-Nt-kAE1 and pGEX4T-2-GST-Ct-kAE1 constructs [14] were transformed into *Escherichia coli* strain BL21 (DE3). The pTrcHisA-KIF3B was transformed into *E. coli* strain DH5α. The bacterial cells were grown in Luria broth to express the recombinant proteins. The bacterial cells were lysed by lysis buffer. The GST or GST-fusion proteins were conjugated with Glutathione-Sepharose 4B beads (Amersham) and then incubated with HEK293T cell lysate. The unbound proteins were eliminated by serial washing as described previously [15]. The binding protein complexes were eluted and subjected to Western blot analysis using the rabbit polyclonal anti-KIF3B antibody (Santa Cruz) as the primary antibody and the swine anti-rabbit IgG-HRP (Santa Cruz) as the secondary antibody. Chemiluminescent signals generated by SuperSignal West Pico Chemiluminescent Substrate (Thermo Scientific) were detected by exposure to an X-ray film.

2.5. RNA interference

Small interfering RNA (siRNA) directed against KIF3B derived from the mRNA sequence (5′-CCT GCA AGG TTT CAA TGG AAC CA-3′) of human KIF3B (siKIF3B) was purchased from Invitrogen. Transfection of either siKIF3B or siControl was performed using Lipofectamine 2000 (Invitrogen). HEK293T cells (5×10^5 cells) were seeded into a six-well plate, 24 h before transfection. For the co-tranfection with knockdown experiment, pcDNA3/kAE1-Myc was transfected after 24 h of siRNA transfection. Cells were harvested 72 h after the siKIF3B transfection.

2.6. Double immunofluorescence staining

HEK293T cells were grown on coverslips for 24 h, co-transfected with plasmid constructs using Lipofectamine 2000 (Invitrogen) and cultured for 48 h. The protocol for double immunofluorescence staining was described previously [16]. Firstly, co-staining of kAE1 and KIF3B was performed by using the mouse anti-Myc and the rabbit anti-KIF3B (Santa Cruz) as the primary antibodies followed by the goat anti-mouse IgG conjugated with Alexa 488 fluoresceine (Molecular Probes) and the donkey anti-rabbit IgG conjugated with Cy3 fluoresceine (Jackson Immunoresearch Laboratories) as the secondary antibodies. Secondly, co-staining of kAE1 and calnexin was performed by using the mouse anti-Myc and the rabbit anti-calnexin (Santa Cruz) as the primary antibodies followed by the goat anti-mouse IgG conjugated with Alexa 488 fluoresceine (Molecular Probes) and the donkey anti-rabbit IgG conjugated with Cy3 fluoresceine (Jackson Immunoresearch Laboratories) as the secondary antibodies.

Human fresh frozen tissues were obtained from leftover specimens of the Department of Pathology, Faculty of Medicine Siriraj Hospital, Mahidol University, Thailand. The protocol was approved by the Human Research Ethics Committee, Siriraj Institutional Review Board, Mahidol University (#Si128/2011). Sections were fixed by acetone for 10 min before immunostaining with the rabbit anti-Ct-kAE1 and the goat anti-KIF3B (Santa Cruz) as the primary antibodies, followed by the anti-mouse antibody coupled to Cy3 and the anti-rabbit antibody coupled to Alexa 488 as the secondary antibodies. The sections were then examined under the LSM 510 META confocal microscope (Carl Ziess).

2.7. Flow cytometry

Myc epitope was inserted at the third extracellular loop of kAE1 to express extracellularly. As a result, expression of kAE1-Myc on the cell surface could be determined by fluorescence staining and flow cytometry [16]. HEK293T cells were co-transfected either with the pcDNA3/kAE1-Myc and siKIF3B or with the pcDNA3/kAE1-Myc and siControl, respectively. Two days after transfections, the cells were collected and determined by flow cytometry as previously described [16].

3. Results

3.1. kAE1 interacts with KIF3B and dileucine motif of Ct-kAE1 is critical for KIF3B binding

To establish whether kAE1 interacts with KIF3B in kidney cells or not, we performed co-immunoprecipitation and GST pull-down

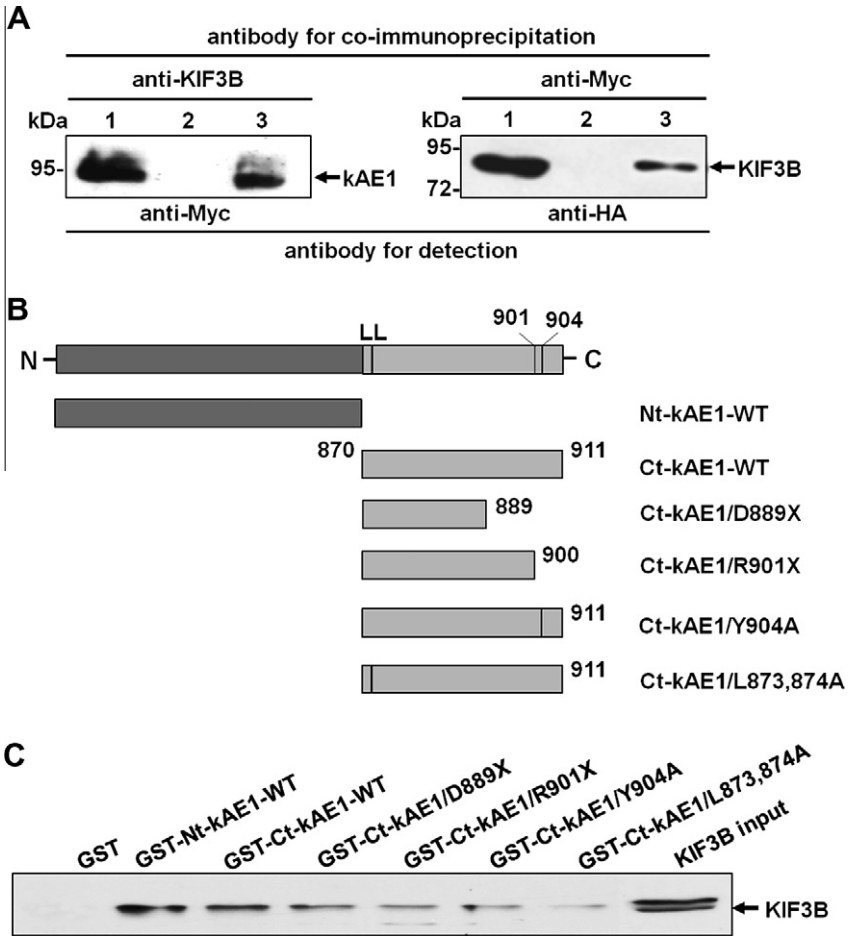

Fig. 1. Interaction of kAE1and KIF3B in HEK293T cells. (A) Co-immunoprecipiation studies using HEK293T cells demonstrated interactions between kAE1 and KIF3B. *Lane 1*: input; *Lane 2*: pull-down with no antibody; *Lane 3*: pull-down with anti-KIF3B (left panel), or anti-HA antibodies (right panel). (B) Maps of the carboxyl terminus of kAE1 (Ct-kAE1). Different GST-Ct-kAE1-mutants were generated from GST-Ct-kAE1-WT. (C) GST pull-down binding assay.

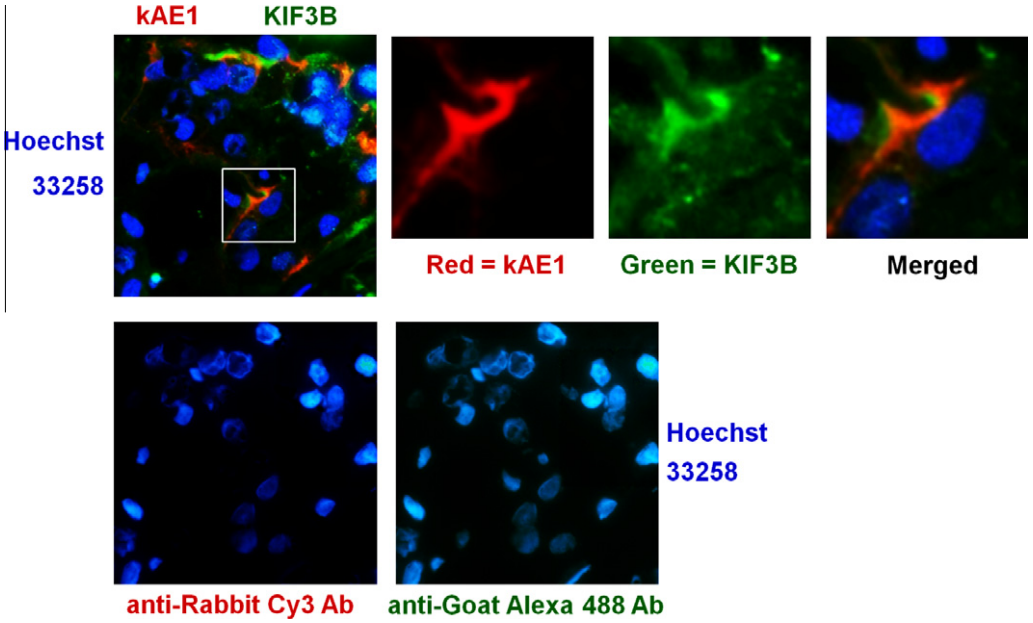

Fig. 2. kAE1 protein co-localizes with endogenous KIF3B in human kidney tissue. Fresh frozen human kidney sections were incubated with the rabbit anti-kAE1 antibody and the goat anti-KIF3B (top panels) or no primary antibody (bottom panels). Slides were then incubated with the anti-rabbit antibody coupled to Cy3 (red) and the anti-goat antibody coupled to Alexa 488 (green), followed by nuclear staining with Hoechst 33,258 (blue). The samples were examined using a LSM 510 META Carl Zeiss confocal microscope and a 100× lens. (For interpretation of the references to color in this figure legend, the reader is referred to the web version of this article.)

studies. The interaction was analyzed by co-transfection of HEK293T cells with the plasmid constructs expressing kAE1 and KIF3B tagged with Myc and HA epitopes, respectively. When KIF3B-HA was immunoprecipitated with anti-KIF3B antibody, the immunoreactive band of kAE1 was detected in the immunoprecipitate (Fig. 1A, left panel). In addition, kAE1-Myc was reciprocally co-immunoprecipitated with anti-HA antibody (Fig. 1A, right panel). The results indicated the interaction of kAE1 and KIF3B in HEK293T cells.

A series of GST pull-down assays were subsequently performed using Nt-kAE1 and Ct-kAE1 containing truncated or point mutations (Fig. 1B). GST-Nt-kAE1-WT, GST-Ct-kAE1-WT and a series of GST-Ct-kAE1-mutants interacted with KIF3B in the GST pull-down assays (Fig. 1C, lanes 2–6). In contrast, a very faint band was ob – served in the binding between GST-Ct-kAE1/L873, 874A and KIF3B from HEK293T cell lysate (Fig. 1C, lane 7) – suggesting that dileucine motif of Ct-kAE1 is critical for KIF3B binding. As a control, GST alone did not interact with KIF3B (Fig. 1C, lane 1).

3.2. kAE1 co-localizes with KIF3B in human kidney tissue

We further asked whether kAE1 interacts with KIF3B in human kidney tissue or not. Human kidney sections were stained with the rabbit anti-Ct-kAE1 and the goat anti-KIF3B as the primary antibodies followed by the anti-mouse antibody coupled to Cy3 and the anti-rabbit antibody coupled to Alexa 488 as the secondary antibodies (Fig. 2). In contrast with sections incubated with secondary antibodies only (Fig. 2, bottom sections), the antibody against kAE1 detected both a clear predominant basolateral staining and a discrete vesicular intracellular staining. In a high intensity, KIF3B was stained similarly as that of kAE1 at the basolateral membrane. In the insets (Fig. 2, top right boxes), a higher magnification of the intracellular red and green staining showed co-localization of both endogenous kAE1 and endogenous KIF3B, supporting that kAE1 interacts with KIF3B in the human kidney tissue.

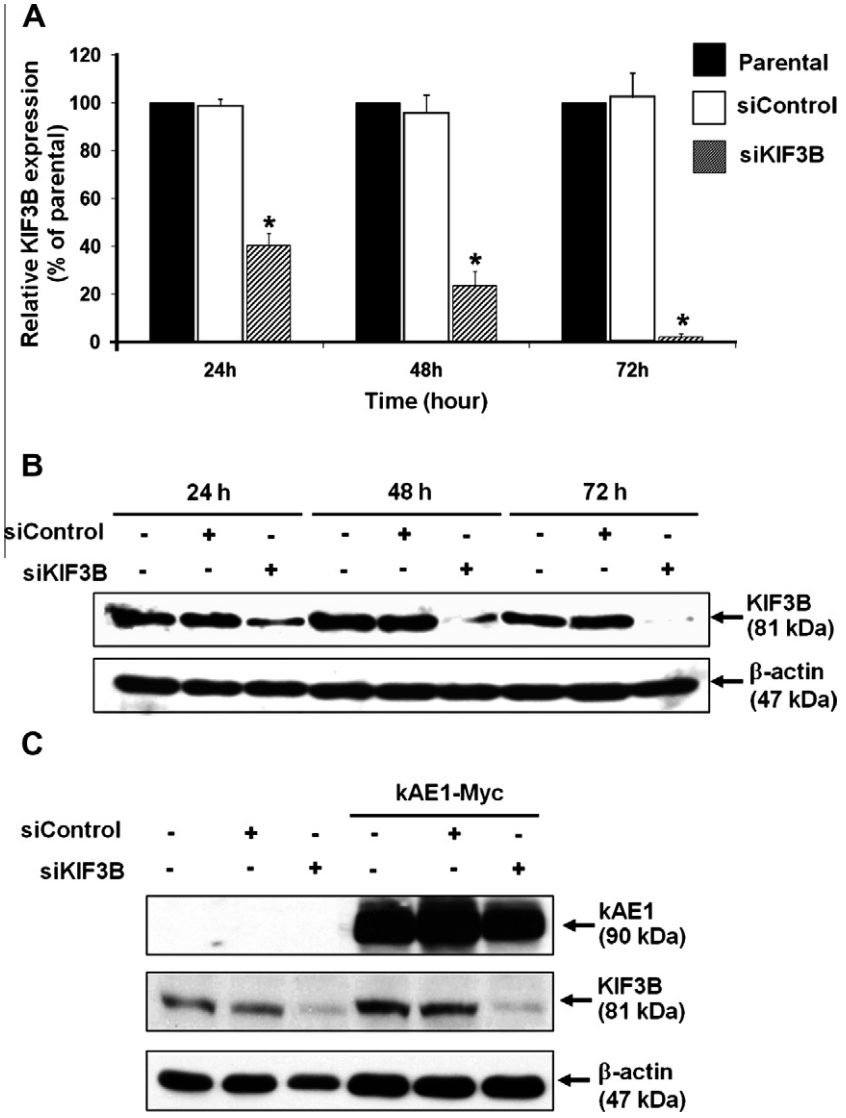

Fig. 3. Endogenous suppression of KIF3B by small interfering RNA (siRNA) in HEK293T cells. (A) Expression of KIF3B mRNA was determined by real-time PCR. Black columns represent the baseline KIF3B expression in HEK293T cells (parental expression, 100%). White columns represent the relative KIF3B expression after transfection with siControl. Strip columns represent the relative KIF3B expression after transfection with siKIF3B. Results are averaged (mean + SE) from three independent experiments. (B) Expression of KIF3B protein was detected by Western blot analysis. (C) Expression of kAE1-Myc after co-transfection with siRNA for 72 h was detected by Western blot analysis.

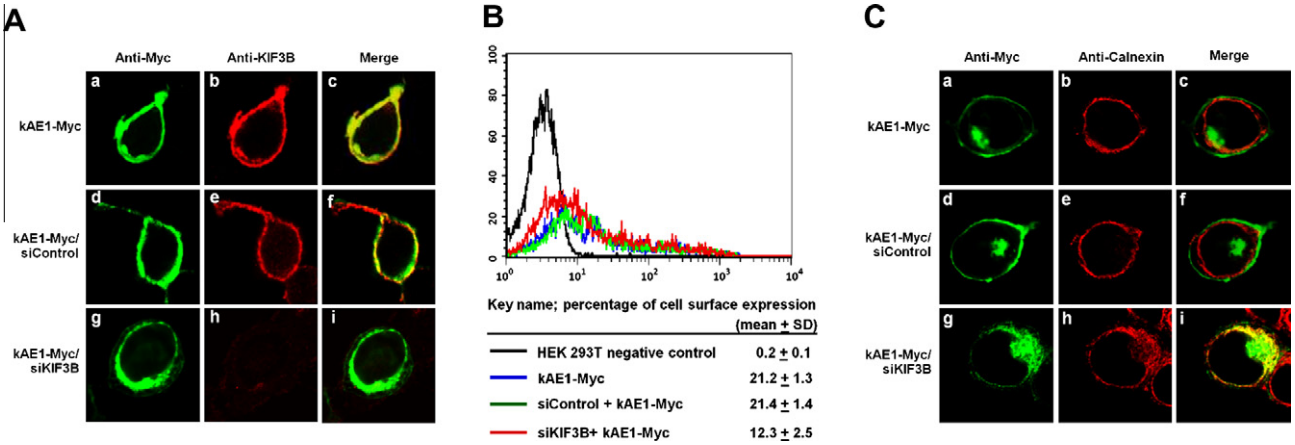

Fig. 4. KIF3B knockdown significantly reduced kAE1 on the membrane and accumulated kAE1 in ER. (A) HEK293T cells were transfected with kAE1-Myc (a–c) and co-transfected with siControl (d–f) or with siKIF3B (g–i). (B) Cell-surface expression of kAE1-Myc in transfected HEK293T cells was measured by flow cytometry. Percentages of cell surface expression of kAE1-Myc (mean ± SD) in different conditions are indicated. (C) Localizations of kAE1 and ER marker were shown in HEK293T cells with suppression of KIF3B by siRNA.

3.3. Knocking-down the expression of endogenous KIF3B by siRNA decreased cell surface kAE thereby accumulating kAE1 in the ER

To study the functional significance of KIF3B, we employed RNAi to transiently deplete the expression of endogenous KIF3B in kAE1-transfected HEK293T cells. The efficiency of the siKIF3B transfection was shown by real-time PCR (Fig. 3A) and immunoblotting (Fig. 3B), respectively. Transfection of HEK293T cells with siKIF3B reduced both KIF3B mRNA and protein >80% within 48 h. To ensure that siKIF3B did not affect kAE1 expression, kAE1 protein expression level was further determined by Western blot analysis. The expression of kAE1-Myc was not changed while that of KIF3B was markedly decreased (Fig. 2C), indicating that an off-target effect of the siKIF3B did not occur.

Sub-cellular localization of kAE1 and KIF3B in HEK293T cells was further examined by immunofluorescence stainings and confocal microscopy. HEK293T cells expressing kAE1-Myc were transfected with either siControl or siKIF3B. The results showed that, without KIF3B suppression, kAE1-Myc was located mainly at the cell surface in the parental and siControl cells (Fig. 4A, a–c and d–f). In contrast, with KIF3B suppression, kAE1-Myc was accumulated mainly in the cytoplasm of the cells (Fig. 4A, g–i).

To quantitatively measure kAE1 expression at the cell surface, the plasmid construct, which can express kAE1 containing Myc epitope at the position 557 in the third extracellular loop of kAE1, was used to allow immunological detection of the protein at the surface of intact cells by flow cytometry. The HEK293T cells individually expressing kAE1-Myc or co-expressing kAE1-Myc with siControl transfection had mean fluorescence intensities of 21.2 ± 1.3% and 21.4 ± 1.4%, respectively. However, HEK293T cells co-expressing kAE1-Myc with suppression of KIF3B showed lower levels of kAE1-Myc on the cell surface (12.3 ± 2.5%) than those of the control cells (Fig. 4B).

To focus on the location of kAE1-Myc with respect to intracellular organelles when KIF3B was suppressed, we next co-transfected kAE1-Myc with siKIF3B in HEK293T cells and stained the HEK293T cells with the antibody to calnexin, which was specific to the ER. In the parental and siControl cells, kAE1-Myc was predominantly expressed at the cell membrane and rarely co-localized with calnexin in ER (Fig. 4C, a–f). In contrast, in the cells with KIF3B suppression by siRNA, kAE1-Myc was accumulated mainly in the ER (Fig. 4C, g–i).

4. Discussion

The protein trafficking pathway is a regulated process and requires specific recognitions between cargo molecules and trafficking machinery to achieve correct targeting of cargo proteins to their destinations. Both apical and basolateral transport have common basic behaviors starting from sorting, which take place at the trans-Golgi network (TGN). Then apical and basolateral vesicles are separately transported to their final destinations thereby fusing with the apical and basolateral plasma membranes, respectively [17].

Several sorting signals for basolateral membranes are known, such as tyrosine and dileucine motifs [18]. Adaptor proteins are known to bind to these motifs and are involved in basolateral sorting. We previously reported the interaction between kAE1 and AP-1 mu1A, a subunit of AP-1A adaptor complex. AP-1 mu1A knockdown showed a marked reduction of kAE1 on the cell membrane and increased its accumulation in ER [15]. Motor proteins are also required for transportation of a cargo protein from TGN to the plasma membranes. This study additionally showed that kAE1 physically interacts with KIF3B. A dileucine motif at the C-terminal kAE1 contributes to its interaction with KIF3B. The involvements of the C-terminal kAE1 in the basolateral trafficking were previously reported [19,20]. Firstly, a 20-bp deletion in exon 20 of *SLC4A1* leading to a mutation that changes alanine to leucine (A > L) at position 888 and a premature termination codon at position 889 (A888L + 889X), which truncates the protein by 23 amino acids, were identified in two affected brothers with dRTA [21]. Secondly, R901X (band 3 Walton) mutation, which is an intragenic 13-bp duplication resulting in a deletion of the last 11 amino acids of AE1, was found to be associated with dominant dRTA in two affected brothers of one family [20–23]. Finally, tyrosine residue at position 904 (Tyr904) is crucial for polarized transport of kAE1 as Y904A or Y904A + V907A mutation caused non-polarized distribution of kAE1 in polarized MDCK cells [20,23]. Similar to the AP-1 mu1A knockdown cells, KIF3B knockdown cells significantly reduced kAE1 on the membrane and accumulated kAE1 in the cytoplasm, particularly in ER of the kidney cells. In conclusion, we characterized the interaction between human kAE1 and KIF3B and demonstrated a role for KIF3B in kAE1 trafficking to the plasma membrane.

Acknowledgments

PY is supported by Siriraj Chalermphrakiat Grant and Thailand Research Fund (TRF) – Senior Research Scholar Grant, ND by Siriraj Graduate Thesis Scholarship, MJ by TRF-Post Doctoral Research Grant, and TL by TRF Mid-Career Research Grant. We thank Duangporn Ungsupravate for technical assistance and Layne Hartsell of Sungkyunkwan University (South Korea) for editing the manuscript.

References

[1] M.J. Godinich, M.L. Jennings, Renal chloride–bicarbonate exchanger, Curr. Opin. Nephrol. Hypertens. 4 (1995) 398–401.
[2] A.E. Schofield, P.G. Martin, D. Spillett, M.J. Tanner, The structure of the human red blood cell anion exchanger (EPB3 AE1 band 3) gene, Blood 84 (1994) 2000–2012.
[3] F.C. Brosius III, S.L. Alper, A.M. Garcia, H.F. Lodish, The major kidney band 3 gene transcript predicts an amino-terminal truncated band 3 polypeptide, J. Biol. Chem. 264 (1989) 7784–7787.
[4] M.J. Tanner, The structure and function of band 3 (AE1): recent developments, Mol. Membr. Biol. 14 (1997) 155–165.
[5] X.B. Tang, J. Fujinaga, R. Kopito, et al., Topology of the region surrounding Glu681 of human AE1 protein, the erythrocyte anion exchanger, J. Biol. Chem. 273 (1998) 22545–22553.
[6] Q. Zhu, D.W. Lee, J.R. Casey, Novel topology in C-terminal region of the human plasma membrane anion exchanger, AE1, J. Biol. Chem. 278 (2003) 3112–3120.
[7] B. Bastani, S.L. Gluck, New insights into the pathogenesis of distal renal tubular acidosis, Miner. Electrol. Metab. 22 (1996) 396–409.
[8] J. Rodriguez-Soriano, New insights into the pathogenesis of renal tubular acidosis – from functional to molecular studies, Pediatr. Nephrol. 14 (2000) 1121–1136.
[9] M.J. Tanner, Band 3 anion exchanger and its involvement in erythrocyte and kidney disorders, Curr. Opin. Hematol. 9 (2002) 133–139.
[10] Y. Zhang, W.O. Hancock, The two motor domains of KIF3A/B coordinate for processive motility and move at different speeds, Biophys. J. 87 (2004) 1795–1804.
[11] N. Le Bot, C. Antony, J. White, et al., Role of xklp3, a subunit of the Xenopus kinesin II heterotrimeric complex, in membrane transport between the endoplasmic reticulum and the Golgi apparatus, J. Cell Biol. 143 (1998) 1559–1573.
[12] M.C. Tuma, A. Zill, N. Le Bot, et al., Heterotrimeric kinesin II is the microtubule motor protein responsible for pigment dispersion in Xenopus melanophores, J. Cell Biol. 143 (1998) 1547–1558.
[13] C. Wiesner, J. Faix, M. Himmel, et al., and extracellular matrix degradation in primary macrophages, Blood 116 (2010) 1559–1569.
[14] A.A. Reed, N.Y. Loh, S. Terryn, et al., CLC-5 and KIF3B interact to facilitate CLC-5 plasma membrane expression, endocytosis, and microtubular transport: relevance to pathophysiology of Dent's disease, Am. J. Physiol. Renal Physiol. 298 (2010) F369–F380.
[15] N. Sawasdee, M. Junking, P. Ngaojanlar, et al., Human kidney anion exchanger 1 interacts with adaptor-related protein complex 1 mu1A (AP-1 mu1A), Biochem. Biophys. Res. Commun. 401 (2010) 85–91.
[16] N. Sawasdee, W. Udomchaiprasertkul, S. Noisakran, et al., Trafficking defect of mutant kidney anion exchanger 1 (kAE1) proteins associated with distal renal tubular acidosis and Southeast Asian ovalocytosis, Biochem. Biophys. Res. Commun. 350 (2006) 723–730.
[17] P. Keller, D. Toomre, E. Diaz, et al., Multicolor imaging of post-Golgi sorting and trafficking in live cells, Nat. Cell Biol. 3 (2001) 140–149.
[18] H. Folsch, H. Ohno, J.S. Bonifacino, et al., A novel clathrin adaptor complex mediates basolateral targeting in polarized epithelial cells, Cell 99 (1999) 189–198.
[19] A.M. Toye, Defective kidney anion-exchanger 1 (AE1, Band 3) trafficking in dominant distal renal tubular acidosis (dRTA), Biochem. Soc. Symp. (2005) 47–63.
[20] A.M. Toye, G. Banting, M.J. Tanner, Regions of human kidney anion exchanger 1 (KAE1) required for basolateral targeting of kAE1 in polarized kidney cells: mis-targeting explains dominant renal tubular acidosis (dRTA), J. Cell Sci. 117 (2004) 1399–1410.
[21] L. Cheidde, T.C. Vieira, P.R. Lima, et al., A novel mutation in the anion exchanger 1 gene is associated with familial distal renal tubular acidosis and nephrocalcinosis, Pediatrics 112 (2003) 1361–1367.
[22] F.E. Karet, F.J. Gainza, A.Z. Gyory, et al., Mutations in the chloride–bicarbonate exchanger gene AE1 cause autosomal dominant but not autosomal recessive distal renal tubular acidosis, Proc. Natl. Acad. Sci. USA 95 (1998) 6337–6342.
[23] M.A. Devonald, A.N. Smith, J.P. Poon, et al., Non-polarized targeting of AE1 causes autosomal dominant distal renal tubular acidosis, Nat. Genet. 33 (2003) 125–127.

ผลงานตีพิมพ์อื่น ๆในระหว่างดำเนินโครงการวิจัย

Biochemical and Biophysical Research Communications 423 (2012) 398–403

Contents lists available at SciVerse ScienceDirect

Biochemical and Biophysical Research Communications

journal homepage: www.elsevier.com/locate/ybbrc

Interaction of dengue virus nonstructural protein 5 with Daxx modulates RANTES production

Sasiprapa Khunchai [a,b,1], Mutita Junking [a,1], Aroonroong Suttitheptumrong [a,b], Umpa Yasamut [a,b], Nunghathai Sawasdee [a], Janjuree Netsawang [d], Atthapan Morchang [a,b], Prapaipit Chaowalit [a], Sansanee Noisakran [e], Pa-thai Yenchitsomanus [a,*], Thawornchai Limjindaporn [a,b,c,*]

[a] Division of Molecular Medicine, Department of Research and Development, Faculty of Medicine Siriraj Hospital, Mahidol University, Bangkok, Thailand
[b] Graduate Program in Immunology, Department of Immunology, Faculty of Medicine Siriraj Hospital, Mahidol University, Bangkok, Thailand
[c] Department of Anatomy, Faculty of Medicine Siriraj Hospital, Mahidol University, Bangkok, Thailand
[d] Faculty of Medical Technology, Rangsit University, Bangkok, Thailand
[e] Medical Biotechnology Research Unit, National Center for Genetic Engineering and Biotechnology, National Science and Technology Development Agency, Bangkok, Thailand

ARTICLE INFO

Article history:
Received 8 May 2012
Available online 1 June 2012

Keywords:
Dengue virus
Nonstructural protein 5
NS5
Daxx
RANTES
CCL5

ABSTRACT

Dengue fever (DF), dengue hemorrhagic fever (DHF), and dengue shock syndrome (DSS), caused by dengue virus (DENV) infection, are important public health problems in the tropical and subtropical regions. Abnormal hemostasis and plasma leakage are the main patho-physiological changes in DHF/DSS. A remarkably increased production of cytokines, the so called 'cytokine storm', is observed in the patients with DHF/DSS. A complex interaction between DENV proteins and the host immune response contributes to cytokine production. However, the molecular mechanism(s) by which DENV nonstructural protein 5 (NS5) mediates these responses has not been fully elucidated. In the present study, yeast two-hybrid assay was performed to identify host proteins interacting with DENV NS5 and a death-domain-associate protein (Daxx) was identified. The *in vivo* relevance of this interaction was suggested by co-immunoprecipitation and nuclear co-localization of these two proteins in HEK293 cells expressing DENV NS5. HEK293 cells expressing DENV NS5-K/A, which were mutated at the nuclear localization sequences (NLS), were created to assess its functional roles in nuclear translocation, Daxx interaction, and cytokine production. In the absence of NLS, DENV NS5 could neither translocate into the nucleus nor interact with Daxx to increase the DHF-associated cytokine, RANTES (CCL5) production. This work demonstrates the interaction between DENV NS5 and Daxx and the role of the interaction on the modulation of RANTES production.

1. Introduction

Dengue virus (DENV) belongs to the *Flaviviridae* family, which contain a single positive-stranded RNA genome encoding a single polypeptide precursor. Host and viral proteases cleave this polypeptide into three structural proteins (capsid, membrane, and envelope) and seven nonstructural proteins (NS1, NS2A, NS2B, NS3, NS4A, NS4B and NS5), respectively. Clinical symptoms of DENV infection range from a predominantly febrile disease, dengue fever (DF), to dengue hemorrhagic fever (DHF) and dengue shock syndrome (DSS), which typically occurs in cases of reinfection with a different serotype of DENV. Patients with DHF present with hemorrhagic tendencies, plasma leakage, thrombocytopenia, and hemoconcentration [1]. In addition, increased levels of cytokines – so called 'cytokine storm', which relate to the pathogenesis of severe DENV infection, are observed in the patients with DHF/DSS [2].

A complex interaction between DENV proteins and the host immune response contributes to DHF/DSS [3–9]. Both inhibition of the antiviral response and stimulation of cytokine production by DENV proteins have been reported. For example, DENV NS2B3 complex, DENV NS4B and DENV NS5 contribute to the inhibition of type I IFN response [3,5,7]. DENV NS4B and DENV NS5 also enhance the production of DHF-associated cytokines [8,9].

DENV NS5 is a bi-functional enzyme containing three domains [10–12]. The N-terminus from residues 1 to 368 contains a 2′-*O*-methyltransferase while the C-terminus from residues 405 to 900 contains an RNA-dependent RNA polymerase. The interdomain region contains nuclear localization sequences (NLS), which are divided into aNLS and bNLS, respectively. Mutations in both aNLS and bNLS result in the accumulation of DENV NS5 in the cytoplasm [13].

* Corresponding authors at: Department of Anatomy, Faculty of Medicine Siriraj Hospital, Mahidol University, Bangkok, Thailand (T. Limjindaporn).
E-mail addresses: grpye@mahidol.ac.th (P.-t. Yenchitsomanus), limjindaporn@yahoo.com (T. Limjindaporn).
[1] The first two authors contributed equally to this work.

0006-291X/$ - see front matter © 2012 Elsevier Inc. All rights reserved.
http://dx.doi.org/10.1016/j.bbrc.2012.05.137

In the present study, a yeast two-hybrid assay was performed to identify host proteins interacting with DENV NS5 and a death-domain-associate protein (Daxx) which serves as transcription repressor was identified. The roles of DENV NS5 in nuclear translocation, Daxx interaction, and cytokine production were tested and DENV NS5 was demonstrated to interact with human Daxx to increase RANTES production.

2. Materials and methods

2.1. Yeast two-hybrid screening

Two-hybrid screening was performed by the interaction mating method described by Finley and Brent [14]. DENV NS5 was PCR amplified by *Pfu* DNA polymerase from a cDNA clone of DENV serotype 2 strain 16681 [15] using nucleotide primers, 5′TTG ACT GTA TCG CCG GGA ACT GGC AAC ATA3′ and 5′CCG GAA TTA GCT TGG CTG CAG CCA CAG AAC TCC TCG3′. The PCR reaction was carried out in a GeneAmp PCR System 9700 (Applied Biosystems) with an initial denaturation step of 94 °C for 5 min and followed by 35 cycles of denaturation at 94 °C for 45 s, annealing at 55 °C for 30 s, extension at 72 °C for 3 min, and one cycle of final extension at 72 °C for 10 min. Subsequently, the amplified DNA was cloned by yeast recombination [16] into the yeast expression vector pEG-NRT [17], which was derived from pEG202 [18], and contains a *HIS3* selectable marker. The constitutive ADH promoter is used to express DENV NS5 with the DNA binding domain protein LexA. Nuclear localization sequences, 5′recombination tag (5′RT), multiple cloning site (MCS) and 3′recombination tag (3′RT) were inserted between LexA and ADH terminator. The resulting bait plasmid, pEG-NS5, was verified by DNA sequencing and transformed into *Saccharomyces cerevisiae* strain RFY 206 (MATa *his3A200 leu2-3 lys2A201 ura3-52 trp1A::hisG*) containing a Lexop-*lac*Z reporter plasmid, pSH18–34 [14]. A galactose inducible HeLa cell cDNA prey library was constructed in plasmid pJZ 4–5 containing a *TRP1* selectable marker and transformed into strain RFY 231 (MATα *his3 leu2::3Lexop-LEU2 ura3 trp1 LYS2*) [14]. The bait strain then was mated with the library strains and plated on galactose drop-out medium lacking histidine, tryptophan, uracil and leucine (gal/raf -u, -h, -w, -l) to select for diploids. The production of a DENV NS5 binding protein by a prey plasmid was expected to activate the 3Lexop-*LEU*2 reporter. Putative positive clones were patched to four indicator plates: (glu/-u, -h, -w, -l), (gal/raf -u, -h, -w, -l), (glu/X-Gal-u, -h, -w), and (gal/raf/ X-Gal-u, -h, -w). Prey plasmids were rescued from clones exhibiting a galactose-inducible Leu^+ $lacZ^+$ phenotype by transformation into a Trp^- *Escherichia coli* strain KC8 [14]. Putative positive library plasmids were purified and subjected to DNA sequencing and BLAST analysis.

2.2. Generation of HEK293 cells expressing DENV NS5, or DENV NS5-K/A

DENV NS5 with a C-terminal FLAG-tag was PCR amplified by *Pfx* DNA polymerase (Invitrogen) from plasmid pET-DENV-2-NS5 using nucleotide primers, 5′ACA GGA TCC ACC ATG GGA ACT GGC AAC ATA GGA GAG ACG3′ and 5′TGT CTC GAG TTA CTT GTC ATC GTC ATC CTT GTA ATC CCA CAG AAC TCC TGC TTC TTC C3′. The PCR reaction was carried out in a GeneAmp PCR System 9700 with an initial denaturation step of 94 °C for 5 min and followed by 30 cycles of denaturation at 94 °C for 30 s, annealing at 55 °C for 30 s, extension at 68 °C for 3 min, and one cycle of final extension at 68 °C for 10 min. The PCR product was sub-cloned into plasmid pcDNA3.1/Hygro (Invitrogen) and the fidelity of the insert in the resulting plasmid, pcDNA3.1/DENV NS5, was verified by DNA sequencing.

Site-directed mutagenesis was employed to generate plasmid pcDNA3.1/DENV NS5 (K371A, K372A, K387A, K388A, K389A), namely DENV NS5-K/A. Firstly, DENV NS5 (K387A, K388A, K389A) was amplified by PCR using plasmid pcDNA3.1/DENV NS5 as a template and nucleotide primers, 5′GGA AAG AAT TAG GGG CGG CAG CGA CAC CCA GGA TGT G3′ and 5′CAC ATC CTG GGT GTC GCT GCC GCC CCT AAT TCT TTC C3′. The PCR reaction was carried out in a GeneAmp PCR System 9700 with an initial denaturation step of 94 °C for 2 min and followed by 18 cycles of denaturation at 94 °C for 30 s, annealing at 55 °C for 1 min, extension at 68 °C for 18 min. The PCR product was digested with *Dpn*I to eliminate methylated parental DNA template and transformed into competent *E.coli* strain DH5. The correct mutant clone with K387A, K388A, K389A was verified by digestion with *Fnu4*HI and DNA sequencing. Secondly, DENV NS5 (K371A, K372A, K387A, K388A, K389A), was amplified by PCR using plasmid pcDNA3.1/DENV NS5(K387A, K388A, K389A) as a template and nucleotide primers, 5′CCG AAA GAA GGC ACG GCG GCA CTA ATG AAA ATA AC3′ and 5′GTT ATT TTC ATT AGT GCC GCC GTG CCT TCT TTC GG3′. The PCR reaction and transformation is similar to those described previously. The correct mutant clone with K371A, K372A, K387A, K388A, K389A, namely DENV NS5-K/A, was verified by digestion with *Fnu4*HI and DNA sequencing.

HEK 293 cells were transiently transfected with pcDNA3.1 or pcDNA3.1/DENV NS5 or pcDNA3.1/DENV NS5-K/A by Lipofectamine® 2000 transfection (Invitrogen). Two days after transfection, the cells were collected, fixed and permeabilized with 0.1% Triton X-100 in PBS. Re-suspended cells were blocked with DMEM containing 1% BSA before incubation with mouse anti-FLAG (Sigma) antibody for 1 h. After incubation, the cells were washed twice with chilled DMEM containing 1% BSA. Then, goat anti-mouse antibody conjugated with FITC (Molecular Probes) was used as secondary antibody for 30 min. The cells were washed again and analyzed by using FACSort™ flow cytometer (Becton–Dickinson). HEK293 cells expressing either DENV NS5, or DENV NS5-K/A were also tested for the presence of DENV NS5 by Western blot analysis using anti-FLAG (Sigma).

2.3. Co-immunoprecipitation

Forty-eight h post-transfection, HEK293 cells expressing either DENV NS5 or DENV NS5-K/A were lysed in RIPA buffer containing 1% NP-40, 0.5% sodium deoxycholate, 0.1% SDS, 150 mM NaCl, 20 mM Tris–HCl; pH 7.4, 5 mM EDTA, and protease inhibitor cocktail. Five micrograms of goat anti-Daxx antibody (Santa Cruz Biotechnology) or 5 μg of mouse anti-FLAG antibody were added to lysates. The mixture was incubated with gentle rotation at 4 °C for 6 h. The incubation was continued 24 h after addition of Protein G Sepharose (Amersham Pharmacia Biosciences). Subsequently, Protein G Sepharose was collected by centrifugation at 13,000*g* for 5 min and washed twice with 0.1% Triton X-100, 150 mM NaCl, 20 mM Tris–HCl; pH 7.4, 5 mM EDTA. The bound proteins were eluted by boiling in SDS–PAGE loading buffer, separated by SDS–PAGE, and transferred to nitrocellulose membrane. After blocking with 5% skim milk, the membranes were incubated with either a mouse anti-FLAG antibody or a rabbit anti-Daxx antibody followed by probing with either a rabbit anti-mouse antibody conjugated-horseradish peroxidase (HRP) or a swine anti-rabbit antibody conjugated-HRP (DakoCytomation), respectively. Chemiluminescent signals generated by SuperSignal West Pico Chemiluminescent Substrate (Thermo Scientific) were detected using a G:BOX chemiluminescence imaging system (Syngene).

2.4. Co-localization

HEK293 cells were grown on coverslips and then transfected with plasmid expressing either DENV NS5 or DENV NS5-K/A for 48 h. The transfected cells were fixed with 0.1% formaldehyde in

PBS, rinsed, permeabilized with 0.1% Triton X-100 in PBS and blocked with 1% BSA. The cells were stained at RT for 1 h with both a mouse anti-FLAG and a rabbit anti-Daxx primary antibodies, washed and incubated at RT for 1 h with both an Alexa 488-conjugated rabbit anti-mouse Ig antibody (Molecular Probes) and a Cy3-conjugated donkey anti-rabbit Ig antibody (Jackson Immunoresearch Laboratories) as secondary antibodies. Fluorescent images were captured with a confocal microscope (model LSM 510, Carl Zeiss).

2.5. Real-time RT-PCR

Total RNA from HEK293 cells expressing either DENV NS5, or DENV NS5-K/A and cultured in the presence of 50 ng/ml TNF-α (Santa Cruz biotechnology) was isolated using Trizol reagent (Invitrogen). Cytokines were quantified by real-time RT-PCR using the following primer pairs: IL-8: 5′-TCC TGC AGA GGA TCA AGA CA-3′ and 5′-GAG CAC TTG CCA CTG GTG TA-3′, CXCL9: 5′-CAG ATT CAG CAG ATG TGA AGG A-3′ and 5′-GAA ATT CAA CTG GTG GGT GGT-3′, RANTES: 5′-CAA GGA AAA CTG GGT GCA GA-3′and 5′-TCT CCC GTG CAA TAT CTA GGA A-3′, respectively. The assay was performed using LightCycler® 480 SYBR Green I Master Mix (Roche) and a LightCycler® 480 Instrument equipped with a 96-well thermal cycler (Roche). Briefly, RNA samples were reverse-transcribed using the SuperScript^{III} First-Strand Synthesis System (Invitrogen). Then cDNA templates were subjected to a 10-min initial denaturation at 95 °C prior to 50 cycles of PCR (95 °C for 10 s, 60 °C for 10 s, and 72 °C for 20 s) in the presence of *Taq* DNA polymerase and the gene-specific primer pairs. The mRNA level was normalized with human beta-actin mRNA using the ΔΔCt method [19].

2.6. Enzyme-linked immunosorbent assay (ELISA)

Production of RANTES in HEK293 cells expressing either DENV NS5 or DENV NS5-K/A in the presence of TNF-α, was measured by Instant ELISA® (eBioscience) according to the manufacturer's instruction.

3. Results and discussion

3.1. Identification of DENV NS5 interacting proteins by a yeast two-hybrid screen

To identify human proteins that interacted with DENV NS5, we screened over 10^7 clones from a HeLa cDNA library using DENV NS5 as bait. Thirty putative positive clones were obtained. To verify the interaction, recovered prey plasmids were introduced into yeast strain RFY 231 along with the *lacZ* plasmid and bait plasmid and again tested on the indicator plates. Twelve library plasmids were purified and subjected to DNA sequencing. BLAST analysis revealed that the twelve clones corresponded to the proteins Daxx, Fas-associated factor 1 (FAF1), Calpain 2, Protein phosphatase 1 (PP-1), Splicing factor (SF3a), and Double-strand break repair protein (Mre11A).

The specificity of the interaction between DENV NS5 and Daxx, is shown in Fig. 1A wherein cells containing the DENV NS5 and Daxx, exhibited galactose-dependent leucine prototrophy and *lacZ* expression. Daxx has a strong transcriptional repression activity and can bind to several transcription factors in the nucleus [20,21]. In addition, the majority of Daxx is present in the nucleus similar to that of DENV NS5 [22,23]. Daxx is a 740 amino acid protein that contains amino-terminal amphipathic helices (PAH1, PAH2), a coiled–coiled domain (CC), an acidic domain (D/E), and a carboxyl-terminal serine/proline/threonine rich domain (S/P/T). Among them, the S/P/T domain can mediate the interaction of Daxx with numerous proteins. The region of Daxx that interacted with DEN NS5 was verified in the prey plasmid by DNA sequencing and BLAST analysis and the 211 carboxyl-terminal residues, which cover the S/P/T domain than can bind to multiple proteins including DENV capsid protein in the nucleus of DENV-infected cells, were identified [24] (Fig. 1B).

3.2. Interaction of DENV NS5 and Daxx in the nucleus of HEK293 cells expressing DENV NS5

The interaction of DENV NS5 and Daxx was confirmed in mammalian HEK293 cells. Co-immunoprecipitation of DENV NS5 and

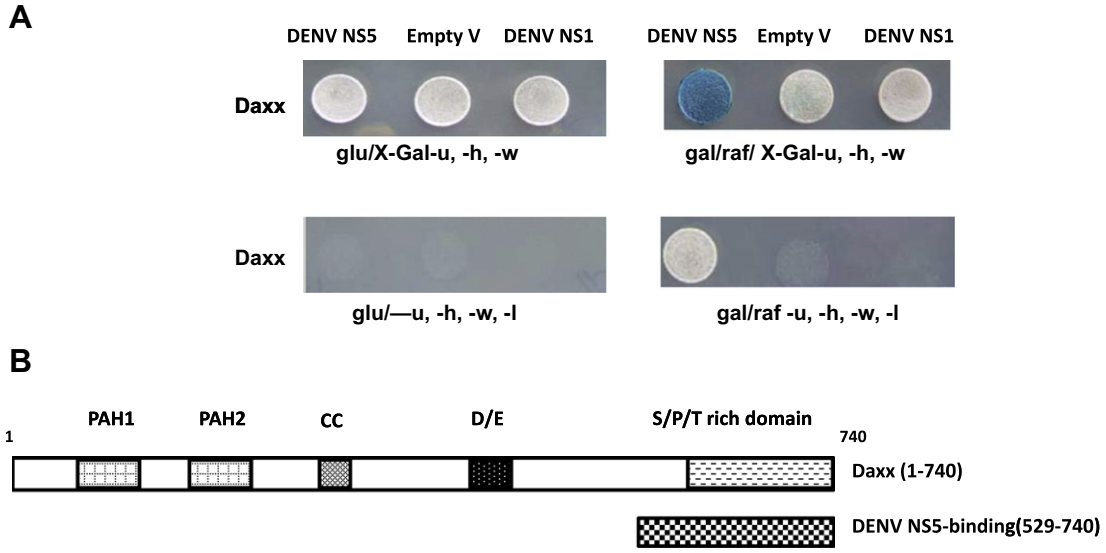

Fig. 1. DENV NS5-human Daxx interaction in a yeast two-hybrid system. (A) Yeast strain RFY231 was co-transformed with a bait plasmid, a Daxx prey plasmid and *lacZ* reporter plasmid. The bait plasmids used were pEG-NS5, expressing the lexA-DEN NS5 fusion protein, the empty bait plasmid pEG202, or an unrelated bait plasmid pEG-NS1 (DENV NS1). A specific interaction was indicated by galactose-dependent β-galactosidase expression, as evidenced by blue colonies on the galactose containing X-Gal plate and white colonies on the glucose containing X-Gal plate, and by galactose-dependent growth on the leucine deficient plate. (B) The region of Daxx that interacted with DEN NS5 was the 211 carboxyl-terminal residues, a region which binds multiple cellular proteins.

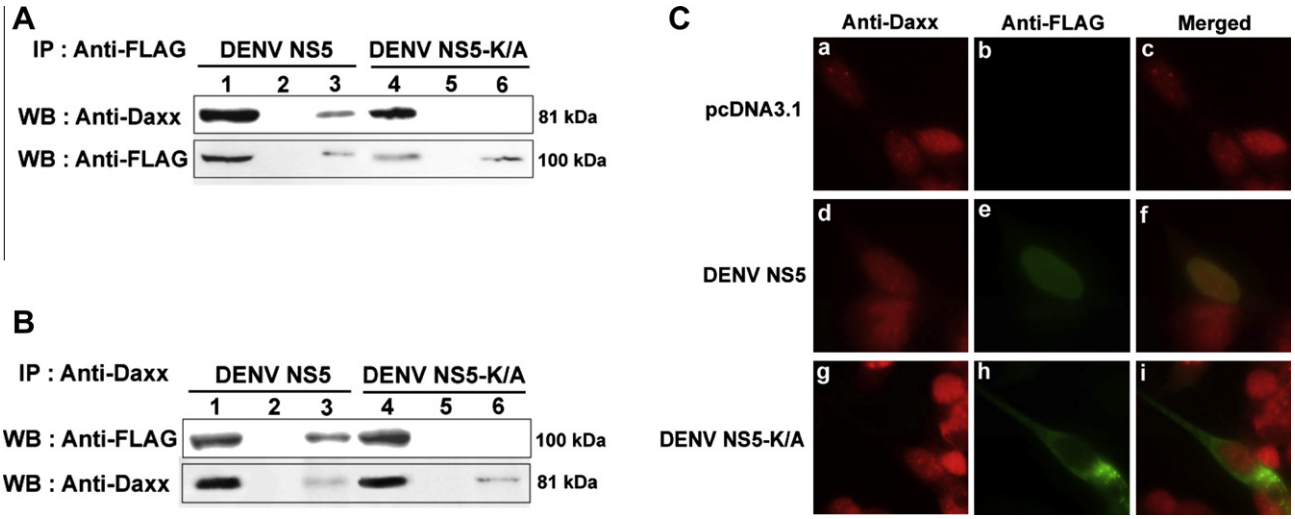

Fig. 2. Interaction between DENV NS5 and human Daxx. (A) Lysates of HEK293 cells expressing DENV NS5 or DENV NS5-K/A were immunoprecipitated with a mouse anti-FLAG antibody. Immune complexes were detected by Western blot analysis using either a mouse anti-FLAG or a rabbit anti-Daxx antibodies. Lane 1, and 4: input; Lane 2, and 5: IP with no antibody; Lane 3 and 6: IP with anti-FLAG antibody. (B) Lysates of HEK293 cells expressing DENV NS5 or DENV NS5-K/A were immunoprecipitated with a rabbit anti-Daxx antibody. Immune complexes were detected by Western blot analysis using either a mouse anti-FLAG antibody or a rabbit anti-Daxx antibody. Lane 1, and 4: input; Lane 2, and 5: IP with no antibody; Lane 3 and 6: IP with anti-Daxx antibody. (C) HEK293 cells expressing DENV NS5 or DENV NS5-K/A were fixed and immunostained with rabbit anti-Daxx antibody (panel a, d, and g) and mouse anti-FLAG antibody (panel b, e, and h). The merged image (panel c, f, and i) demonstrated co-localization between DENV NS5 and Daxx.

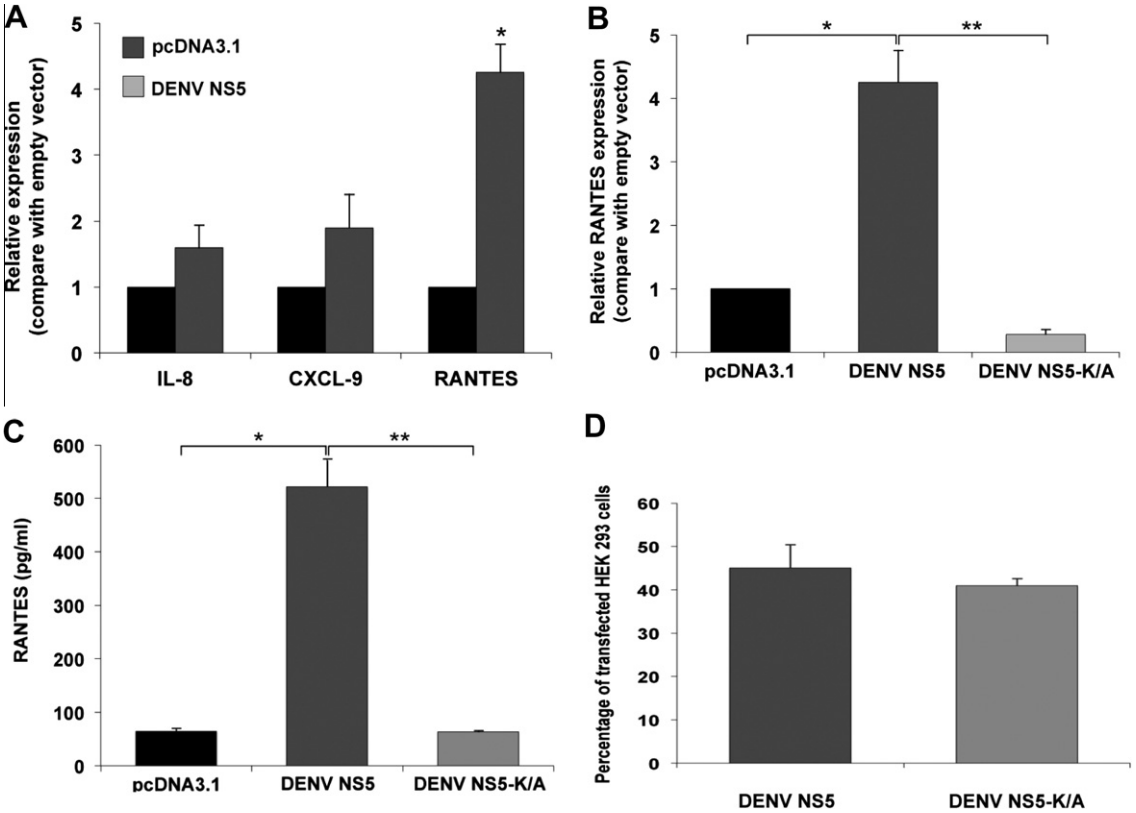

Fig. 3. Interaction between DENV NS5 and human Daxx modulates RANTES production. (A) The amount of mRNA of DHF-associated cytokines was measured in HEK293 cells expressing DENV NS5 in the presence of TNF-α. Relative gene expression (fold change) was determined by real-time PCR using primers specific to IL-8, CXCL-9 and RANTES. The results are the average of three independent experiments. The asterisks indicate statistically significant differences between HEK293 cells expressing DENV NS5 and empty vector ($^{*}p < 0.05$). (B) The mRNA expression of RANTES was measured in HEK293 cells expressing DENV NS5 in the presence of TNF-α. Relative gene expression (fold change) of RANTES was determined by real-time PCR. The results are the average of three independent experiments. The asterisks indicate statistically significant differences between HEK293 cells expressing DENV NS5 and DENV NS5-K/A ($^{*}p < 0.05$, $^{**}p < 0.01$). (C) The production of RANTES was measured by ELISA in HEK293 cells expressing DENV NS5 in the presence of TNF-α. The results are the average of three independent experiments. The asterisks indicate statistically significant differences between HEK293 cells expressing DENV NS5 and DENV NS5-K/A ($^{*}p < 0.05$, $^{**}p < 0.01$). (D) The expression of DENV NS5 or DENV NS5-K/A was determined by flow cytometry using a mouse anti-FLAG antibody.

Daxx was observed in HEK293 cells expressing DENV NS5. Anti-flag antibody co-immunoprecipitated Daxx protein and, conversely, anti-Daxx antibody co-precipitated DENV NS5 (Fig. 2A and B). Co-localization of DENV NS5 and Daxx was evident in the nucleus of HEK293 cells expressing DENV NS5 (Fig. 2C). These data supported the proposed interaction of DENV NS5 and Daxx and further suggested that association occurs mainly in the nucleus of HEK293 cells expressing DENV NS5.

3.3. Interaction DENV NS5 and Daxx modulates RANTES production

DENV NS5 was previously shown to enhance the production of IL-8 [9]. In addition, enhancement of TNF-α-stimulated NF-κB activation by DENV NS5 was reported [25]. In the present study, the level of DHF-associated cytokines including IL-8, CXCL-9 and RANTES was measured in HEK293 cells expressing DENV NS5 in the presence of TNF-α. The mRNA expression of RANTES was significantly up-regulated in HEK293 cells expressing DENV NS5 compared to empty vector-transfected HEK293 cells (Fig. 3A). RANTES is a member of the C–C chemokine family and its expression was increased both in DENV-infected cell lines and DENV-infected patients [26] and activation of RANTES production by other viral infections was reported to be regulated by NF-κB [27,28]. Therefore, enhancement of TNF-α-stimulated NF-κB activation of RANTES production may modulated by DENV NS5.

Interaction between DENV NS5 and Daxx, which normally interacts with NF-κβ [29], may modulate RANTES production. Therefore, HEK293 cells expressing either DENV NS5 or DENV NS5-K/A were created to assess in the role of NS5 nuclear translocation in Daxx interaction and RANTES production. Site-directed mutagenesis was employed to generate mutant DENV NS5 (K371A, K372A, K387A, K388A, K389A), namely DENV NS5-K/A, Whilst DENV NS5 was present in the nuclei of HEK293 cells expressing DENV NS5, HEK293 cells expressing DENV NS5-K/A had no detectable DENV NS5 protein in the nucleus (Fig. 2C). Secondly, co-immunoprecipitation and co-localization of DENV NS5-K/A and Daxx was examined. Co-immunoprecipitation of DENV NS5 and Daxx was observed only in HEK293 cells expressing DENV NS5, but not in HEK293 cells expressing DENV NS5-K/A. Anti-flag antibody co-immunoprecipitates Daxx protein and, conversely, anti-Daxx antibody co-precipitated DENV NS5 in HEK293 cells expressing DENV NS5 but not in HEK293 cells expressing DENV NS5-K/A. (Fig. 2A and B). Furthermore, co-localization of DENV NS5 and Daxx was evident in the nucleus of HEK293 cells expressing DENV NS5 but not in HEK293 cells expressing DENV NS5-K/A. (Fig. 2C). Finally, the RANTES production in either HEK293 cells expressing DENV NS5 or DENV NS5-K/A. was measured by real-time RT-PCR and ELISA, respectively. As expected, both mRNA expression and RANTES production were significantly higher in HEK293 cells expressing DENV NS5 than those in HEK293 cells expressing DENV NS5-K/A (Fig. 3B and C). This difference was not due to differences in transfection efficiency or protein expression since DENV NS5 and DENV NS5-K/A were expressed at similar levels as determined by immunofluorescence staining (Fig. 3D). Thus, in the absence of a functional NLS, DENV NS5 could neither translocate into the nucleus nor interact with Daxx to increase RANTES secretion.

As TNF-α signaling activates NF-κB and RANTES production during DENV infection [2,30] and NF-κB is known to activate the RANTES promoter [28], DENV NS5 may increase the amount of NF-κB available to activate RANTES expression through its interaction with Daxx, which normally interacts with NF-κB [29] (Fig. 4). The molecular mechanisms that control the competitive binding of DENV NS5, Daxx, and NF-κB require further investigation. However, this work is the first to demonstrate the *in vivo* interaction between DENV NS5 and Daxx and its role in modulating RANTES production.

Acknowledgments

TL is supported by Mid-Career Thailand Research Fund–Commission of Higher Education (TRF-CHE) Research Grant, Mahidol University Grant, and Siriraj Chalearmprakiat Fund, SK by CHE Ph.D. Program, MJ by TRF-Post Doctoral Research Grant, AM and UM by TRF-Royal Golden Jubilee Ph.D. Program. PY is a TRF-Senior Research Scholar. We are grateful to Dr. William A Fonzi, Georgetown University, USA, for helpful discussion and continuous support, Dr. Russell L Finley Jr., Wayne State University, USA, for

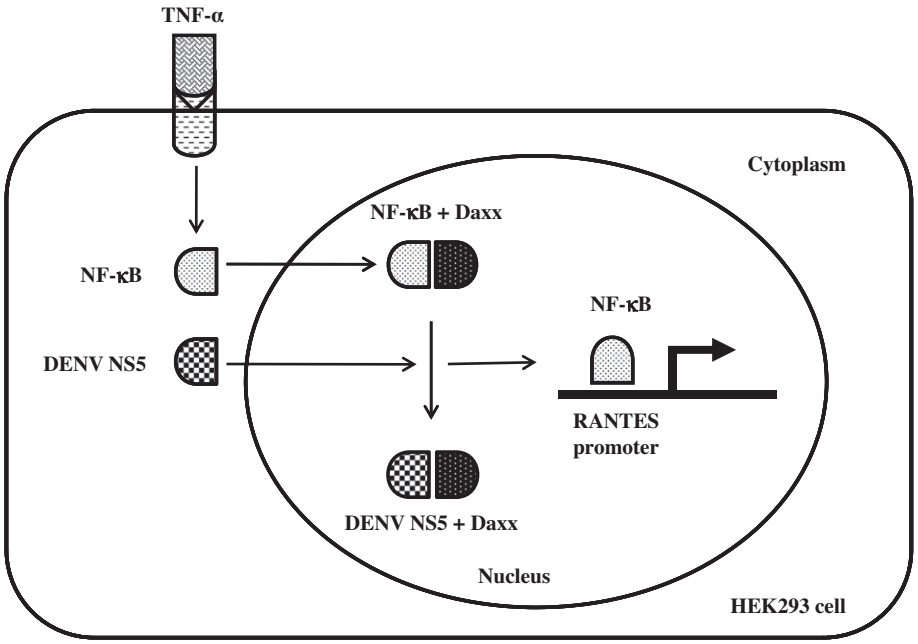

Fig. 4. Proposed model for modulation of Rantes production by DENV NS5. TNF-α signaling activates NF-κB and the competitive binding between DENV NS5 and Daxx limits the interaction between Daxx and NF-κB thereby releasing NF-κB to activate RANTES production.

reagents of yeast two-hybrid system, and Dr. Nopporn Sitthisombut, Chiang Mai University, for pBluescript II KS containing cDNA of DENV serotype 2 strain 16681.

References

[1] S.B. Halstead, Pathogenesis of dengue: challenges to molecular biology, Science 239 (1988) 476–481.
[2] P. Avirutnan, P. Malasit, B. Seliger, S. Bhakdi, M. Husmann, Dengue virus infection of human endothelial cells leads to chemokine production, complement activation, and apoptosis, J. Immunol. 161 (1998) 6338–6346.
[3] J. Ashour, M. Laurent-Rolle, P.Y. Shi, A. Garcia-Sastre, NS5 of dengue virus mediates STAT2 binding and degradation, J. Virol. 83 (2009) 5408–5418.
[4] J. Ashour, J. Morrison, M. Laurent-Rolle, A. Belicha-Villanueva, C.R. Plumlee, D. Bernal-Rubio, K.L. Williams, E. Harris, A. Fernandez-Sesma, C. Schindler, A. Garcia-Sastre, Mouse STAT2 restricts early dengue virus replication, Cell Host Microbe 8 (2010) 410–421.
[5] J.R. Rodriguez-Madoz, A. Belicha-Villanueva, D. Bernal-Rubio, J. Ashour, J. Ayllon, A. Fernandez-Sesma, Inhibition of the type I interferon response in human dendritic cells by dengue virus infection requires a catalytically active NS2B3 complex, J. Virol. 84 (2010) 9760–9774.
[6] M. Mazzon, M. Jones, A. Davidson, B. Chain, M. Jacobs, Dengue virus NS5 inhibits interferon-alpha signaling by blocking signal transducer and activator of transcription 2 phosphorylation, J. Infect. Dis. 200 (2009) 1261–1270.
[7] J.L. Munoz-Jordan, M. Laurent-Rolle, J. Ashour, L. Martinez-Sobrido, M. Ashok, W.I. Lipkin, A. Garcia-Sastre, Inhibition of alpha/beta interferon signaling by the NS4B protein of flaviviruses, J. Virol. 79 (2005) 8004–8013.
[8] J.F. Kelley, P.H. Kaufusi, E.M. Volper, V.R. Nerurkar, Maturation of dengue virus nonstructural protein 4B in monocytes enhances production of dengue hemorrhagic fever-associated chemokines and cytokines, Virology 418 (2011) 27–39.
[9] C.L. Medin, K.A. Fitzgerald, A.L. Rothman, Dengue virus nonstructural protein NS5 induces interleukin-8 transcription and secretion, J. Virol. 79 (2005) 11053–11061.
[10] M.P. Egloff, D. Benarroch, B. Selisko, J.L. Romette, B. Canard, An RNA cap (nucleoside-2′-*O*-)-methyltransferase in the flavivirus RNA polymerase NS5: crystal structure and functional characterization, EMBO J. 21 (2002) 2757–2768.
[11] J.K. Forwood, A. Brooks, L.J. Briggs, C.Y. Xiao, D.A. Jans, S.G. Vasudevan, The 37-amino-acid interdomain of dengue virus NS5 protein contains a functional NLS and inhibitory CK2 site, Biochem. Biophys. Res. Commun. 257 (1999) 731–737.
[12] T.L. Yap, T. Xu, Y.L. Chen, H. Malet, M.P. Egloff, B. Canard, S.G. Vasudevan, J. Lescar, Crystal structure of the dengue virus RNA-dependent RNA polymerase catalytic domain at 1.85-angstrom resolution, J. Virol. 81 (2007) 4753–4765.
[13] M.J. Pryor, S.M. Rawlinson, R.E. Butcher, C.L. Barton, T.A. Waterhouse, S.G. Vasudevan, P.G. Bardin, P.J. Wright, D.A. Jans, A.D. Davidson, Nuclear localization of dengue virus nonstructural protein 5 through its importin alpha/beta-recognized nuclear localization sequences is integral to viral infection, Traffic 8 (2007) 795–807.
[14] R. Brent, R.L. Finley Jr., Understanding gene and allele function with two-hybrid methods, Annu. Rev. Genet. 31 (1997) 663–704.
[15] R. Sriburi, P. Keelapang, T. Duangchinda, S. Pruksakorn, N. Maneekarn, P. Malasit, N. Sittisombut, Construction of infectious dengue 2 virus cDNA clones using high copy number plasmid, J. Virol. Methods 92 (2001) 71–82.
[16] T.L. Orr-Weaver, J.W. Szostak, Yeast recombination: the association between double-strand gap repair and crossing-over, Proc. Natl. Acad. Sci. USA 80 (1983) 4417–4421.
[17] T. Limjindaporn, D. Mairiang, S. Khunchai, W. Wongwiwat, A novel yeast two hybrid vector, pEG-NRT, for protein protein interaction studies, Siriraj Med. J. 59 (2007) 175–177.
[18] J. Gyuris, E. Golemis, H. Chertkov, R. Brent, Cdi1, a human G1 and S phase protein phosphatase that associates with Cdk2, Cell 75 (1993) 791–803.
[19] K.J. Livak, T.D. Schmittgen, Analysis of relative gene expression data using real-time quantitative PCR and the 2(-Delta Delta C(T)) method, Methods 25 (2001) 402–408.
[20] J.S. Michaelson, D. Bader, F. Kuo, C. Kozak, P. Leder, Loss of Daxx, a promiscuously interacting protein, results in extensive apoptosis in early mouse development, Genes Dev. 13 (1999) 1918–1923.
[21] S. Torii, D.A. Egan, R.A. Evans, J.C. Reed, Human Daxx regulates Fas-induced apoptosis from nuclear PML oncogenic domains (PODs), EMBO J. 18 (1999) 6037–6049.
[22] X. Yang, R. Khosravi-Far, H.Y. Chang, D. Baltimore, Daxx, a novel Fas-binding protein that activates JNK and apoptosis, Cell 89 (1997) 1067–1076.
[23] H.Y. Chang, H. Nishitoh, X. Yang, H. Ichijo, D. Baltimore, Activation of apoptosis signal-regulating kinase 1 (ASK1) by the adapter protein Daxx, Science 281 (1998) 1860–1863.
[24] T. Limjindaporn, J. Netsawang, S. Noisakran, S. Thiemmeca, W. Wongwiwat, S. Sudsaward, P. Avirutnan, C. Puttikhunt, W. Kasinrerk, R. Sriburi, N. Sittisombut, P.T. Yenchitsomanus, P. Malasit, Sensitization to Fas-mediated apoptosis by dengue virus capsid protein, Biochem. Biophys. Res. Commun. 362 (2007) 334–339.
[25] S. Wati, S.M. Rawlinson, R.A. Ivanov, L. Dorstyn, M.R. Beard, D.A. Jans, S.M. Pitson, C.J. Burrell, P. Li, J.M. Carr, Tumour necrosis factor alpha (TNF-{alpha}) stimulation of cells with established dengue virus type 2 infection induces cell death that is accompanied by a reduced ability of TNF-{alpha} to activate nuclear factor {kappa}B and reduced sphingosine kinase-1 activity, J. Gen. Virol. 92 (2011) 807–818.
[26] Y.L. Lin, C.C. Liu, J.I. Chuang, H.Y. Lei, T.M. Yeh, Y.S. Lin, Y.H. Huang, H.S. Liu, Involvement of oxidative stress, NF-IL-6, and RANTES expression in dengue-2-virus-infected human liver cells, Virology 276 (2000) 114–126.
[27] P. Genin, M. Algarte, P. Roof, R. Lin, J. Hiscott, Regulation of RANTES chemokine gene expression requires cooperativity between NF-kappa B and IFN-regulatory factor transcription factors, J. Immunol. 164 (2000) 5352–5361.
[28] H. Moriuchi, M. Moriuchi, A.S. Fauci, Nuclear factor-kappa B potently up-regulates the promoter activity of RANTES, a chemokine that blocks HIV infection, J. Immunol. 158 (1997) 3483–3491.
[29] J. Park, J.H. Lee, M. La, M.J. Jang, G.W. Chae, S.B. Kim, H. Tak, Y. Jung, B. Byun, J.K. Ahn, C.O. Joe, Inhibition of NF-kappaB acetylation and its transcriptional activity by Daxx, J. Mol. Biol. 368 (2007) 388–397.
[30] D. Hober, L. Poli, B. Roblin, P. Gestas, E. Chungue, G. Granic, P. Imbert, J.L. Pecarere, R. Vergez-Pascal, P. Wattre, et al., Serum levels of tumor necrosis factor-alpha (TNF-alpha), interleukin-6 (IL-6), and interleukin-1 beta (IL-1 beta) in dengue-infected patients, Am. J. Trop. Med. Hyg. 48 (1993) 324–331.